

# Cost-Efficient Operation of Heat Pump Pools

Optimisation and operation from the perspective of a German aggregator

Master's Thesis

Marc-André Triebel

External Organisation: Fraunhofer Institute for Solar Energy Systems ISE

4<sup>th</sup> Semester: M.Sc. Energy Engineering - Thermal Energy and Process Engineering

June 2017

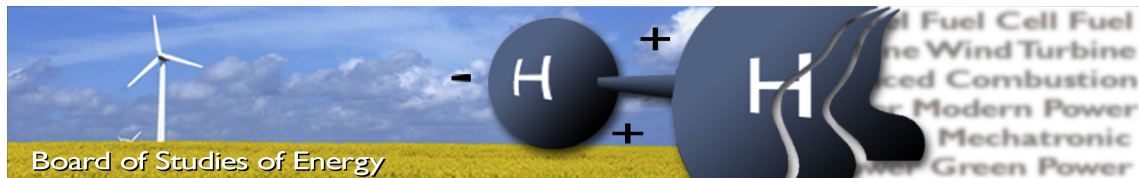
Department of Energy Technology



AALBORG UNIVERSITET







<b>Title:</b>	Cost-efficient Operation of Heat Pump Pools Optimisation and operation from the perspective of a German aggregator
<b>Author:</b>	Marc-André Triebel
<b>Semester:</b>	4 <sup>th</sup> Semester, Spring 2017
<b>Study Programme:</b>	Master of Science, Energy Engineering Thermal Energy and Process Engineering
<b>Semester Theme:</b>	Master's Thesis
<b>External Organisation:</b>	Fraunhofer Institute for Solar Energy Systems ISE
<b>Time Period:</b>	01.02.2017 to 01.06.2017
<b>ECTS:</b>	30
<b>Supervisors University:</b>	Kim Sørensen (kso@et.aau.dk), Mads Pagh Nielsen (mpn@et.aau.dk)
<b>Supervisor Fraunhofer ISE:</b>	David Fischer (David.Fischer@fraunhofer.ise.de)
<b>Project group:</b>	TEPE4-1007

*M.-A. Triebel*

Marc-André Triebel

Submission form:	Electronic submission
Pages, total:	102
Content pages, total (including abstract):	75
Supplements:	Load profile set of curves for heat pumps from the <i>Stromnetz Berlin GmbH</i>

By signing this document, each member of the group confirms that all group members have participated in the project work, and thereby all members are collectively liable for the contents of the report. Furthermore, all group members confirm that the report does not include plagiarism.



# Abstract

## **Cost-Efficient Operation of Heat Pump Pools - Optimisation and operation from the perspective of a German aggregator**

by Marc-André Triebel

The mitigation of Climate Change and the associated decrease in the greenhouse gas emissions originating from the building sector requires an increase of the installation rates of heat pumps in Germany. One way to give the necessary incentives to achieve this would be to reduce the heat pumps' electricity consumption costs. With the aid of simulations, this master's thesis analyses the potential to conduct a more cost-efficient operation of a heat pump pool. The scenario investigated comprises a centrally acting aggregator, which is responsible for the operation of 284 heat pumps operating in Germany. In order to reduce the electricity consumption costs, the aggregator conducts a *Linear Programming*-optimisation each day and purchases the obtained optimised electricity consumption trajectory on the *EPEX* day-ahead spot market. The optimisation problem is based on a storage model and is constrained by the available flexibility of the heat pump pool. The achieved optimised operation of the pool shows a characteristic load shifting pattern which is similar to the ones presented in related research. Through the optimisation, the pool's electricity consumption is partly shifted to times having a lower electricity price while accounting for the load shifting efficiency. In order to match the actual pool operation with the one purchased, the aggregator uses a pool controller which influences the individual heat pump operation by sending *SG-Ready* trigger signals. By using the different trigger signals, the pool controller is able to operate the pool according to the optimised trajectory. The achieved accuracy of trajectory shows an error in the relative annual energy consumption of around 1 %.



# Preface

This report is the master's thesis for the Master of Science study programme *Energy Engineering - Thermal Energy and Process Engineering* at *Aalborg University* in Denmark. This project work has been conducted at and in cooperation with the *Fraunhofer Institute for Solar Energy Systems ISE* in Freiburg, Germany. The student's work was associated with the research project *WPsmart im Bestand* led by the *Fraunhofer ISE*.

This report is dealing with the cost-efficient operation of a pool of heat pumps in order to use its flexibility and thereby optimise and conduct its operation. Several heat pump and simulations models developed by the *Fraunhofer ISE* have been used. The student's work was mostly carried out in the programming language *Python* used within the integrated development environment *Eclipse*. Moreover, for a good understanding of the scientific content presented within this report, a basic knowledge in thermodynamics, heat pumps, optimisation and control theory is recommended.

## Reader's guide

At the beginning of this report the abstract is given, followed by this preface, the table on contents, the nomenclature, the list of abbreviations, the list of figures and the list of tables. The table of contents lists all chapters and sections of this thesis. The bibliography is presented at the end of the report.

Within this report the *Harvard Method* is used as the literary reference style. The sources are presented as [Author, Year]. In case it helps to find the respective cited information, the page number of the respective source is provided as well. Throughout the whole report, the references are given directly at the end of the sentence carrying the respective statement cited. Direct citations are given in italic font within quotation marks with the reference being mentioned at the end of the sentence. Moreover, when references are given at the end of a paragraph, the whole paragraph is based on the source. Furthermore, in case a reference is given before bullet points, all the bullet points are based on the reference if not stated otherwise. The same applies for enumerations and formulas. Additionally, all the figures and tables within this report are numbered according to the section in which they are given. Within one section, their number is ascending with the number of figures/tables given in this section. When the figure is originating from a reference, the source is stated in the caption of the figure. The same applies for tables. Within this report abbreviations are used after they have been introduced once. All abbreviations are listed in the list of abbreviations, presented on Page xiv. The load profile set of curves being used for the generation of the standard load profile of the heat pump pool investigated is submitted together with this report electronically.

## Acknowledgements

I would like to address acknowledgements and thanks to the supervisors of my master's thesis:

- Kim Sørensen, main supervisor and associate professor at *Aalborg University*.
- Mads Pagh Nielsen, co-supervisor and associate professor at *Aalborg University*.
- David Fischer, supervisor, researcher and doctoral student at the *Fraunhofer Institute for Solar Energy Systems ISE*.

I would like to thank them for all their help and advise and the interesting discussions.

Moreover, I would like to sincerely thank Oliver Lutz for his helpful advise and the fruitful discussions. Furthermore, thanks are addressed to Arne Groß for his help programming matters. Moreover, I would like to thank Alexander Harbrecht, Josef Michael Olaf Bernhardt, Marvin Raabe, Florian Kaufmann, Agustin Motte Cortès, René Klaus Garcia Rosas, Sabine Klupp and Carina Hock, which I have shared the office with for the instructive and enriching time. Furthermore, thanks are addressed to the choir *Twäng!* for the lovely and enriching rehearsals, concerts and times spent together during the process of this thesis.

The figure on the front cover of this report is a photography showing the headquarter of the *Fraunhofer Institute for Solar Energy Systems ISE* in Freiburg. The photography has the caption "Haupteingang des Fraunhofer ISE ©Fraunhofer ISE" and was taken by *Guido Kirsch*. The copyright belongs to *Fraunhofer Institute for Solar Energy Systems ISE* and the photography is free for editorial use ("frei für redaktionelle Zwecke"). Acknowledgements are given to *Anne Kovach-Hebling* from the PR-department of the *Fraunhofer ISE* for the provision of the picture and the permission to use it for this thesis.

# Contents

<b>Abstract</b>	<b>v</b>
<b>Preface</b>	<b>vii</b>
Reader's guide . . . . .	vii
Acknowledgements . . . . .	viii
<b>Nomenclature</b>	<b>xi</b>
<b>List of Figures</b>	<b>xv</b>
<b>List of Tables</b>	<b>xviii</b>
<b>1 Introduction</b>	<b>1</b>
1.1 Motivation . . . . .	1
1.2 Problem analysis . . . . .	4
1.3 State of the art . . . . .	6
1.4 Problem definition . . . . .	17
1.5 General methodology and general limitations . . . . .	19
<b>2 The heat pump models</b>	<b>21</b>
2.1 Layout of the system in the models . . . . .	21
2.2 Thermal load profiles . . . . .	22
2.3 Decision about heat distribution system . . . . .	23
2.4 Heat pump models . . . . .	24
2.5 Sizing of the heat pump systems . . . . .	24
2.6 Thermal storage models . . . . .	25
2.7 Sizing of the thermal storages . . . . .	26
2.8 Controls of the single heat pump . . . . .	26
2.9 External signals . . . . .	26
2.10 Validation of the heat pump models . . . . .	27
<b>3 The heat pump pool</b>	<b>29</b>
<b>4 Analysis of the uninfluenced heat pump pool operation</b>	<b>33</b>
4.1 Thermally driven operation . . . . .	33
4.2 Standard load profile . . . . .	36
4.3 Difference between both operations . . . . .	39
4.4 Costs of operation . . . . .	41
4.5 Load shifting potential . . . . .	45
<b>5 Optimisation of the heat pump pool operation</b>	<b>49</b>
5.1 Methodology of the optimisation . . . . .	49

---

5.2	Analysis of the optimised operation trajectory . . . . .	53
<b>6</b>	<b>Controlling the heat pump pool operation</b>	<b>61</b>
6.1	Framework of the pool controller . . . . .	61
6.2	Proof of concept . . . . .	67
6.3	Analysis of the controlled cost-efficient operation . . . . .	71
<b>7</b>	<b>Conclusion and perspectives</b>	<b>77</b>
7.1	Conclusion . . . . .	77
7.2	Perspectives . . . . .	79
	<b>Bibliography</b>	<b>80</b>

# Nomenclature

Symbol	Description	Unit
$a$	Coefficient	-
$a_i$	Coefficients	Various
$b$	Coefficient	K/W
$C$	Thermal capacity	J/K
$COP$	Coefficient Of Performance	-
$C_{sto}$	Heat capacity of the building	J/K
$D$	Differential value of the PID-controller	s
$d$	Day	
$E_{flex}$	Shiftable energy	kWh
$f$	Factor for blocking hours	-
$H$	Number of hours spot price is known in advance	-
$h$	hour	h
$I$	Integral value of the PID-controller	1/s
$J^*$	Cost function to be optimised	DKK or Euro
$J_{el}$	Electricity costs	DKK
$k$	Discrete timestep	min
$kA$	Heat loss coefficient	J/(Ks)
$k_{\dagger}$	Trade-off parameter	DKK/K <sup>2</sup>
$N$	Number of timesteps within the day	-
$n_{pers}$	Number of occupants in the building	-
$P$	Proportional value of the PID-controller	-
$P_{max,th}$	Maximum available electricity consumption of the pool	kW
$P_{max,std}$	Maximum electricity consumption of the pool	kW
$p_{el}^*$	Optimised electricity consumption of the pool	kW
$p_{el}^+$	Power charging the storage	kW
$p_{el}^-$	Power discharging the storage	kW
$R$	Thermal resistance	K/W
$S$	Safety margin for the sizing of the DHW storage	l
$s$	Scaling factor for standard load profile	kWh/K
$TMZ$	Temperaturmaßzahl (temperature characteristic number)	K

Symbol	Description	Unit
$T_{\text{amb}}$	Ambient temperature	K
$T_{\text{biv}}$	Bivalence temperature	K
$T_{\text{room}}$	Temperature of the room	K
$T_{\text{m}}$	Mean ambient temperature	K
$T_{\text{m,eq}}$	Equivalent ambient temperature	K
$T_{\text{nom}}$	Nominal temperature	K
$T_{\text{ref}}$	Reference temperature	K
$T_{\text{sink}}$	Temperature of the sink	K
$T_{\text{source}}$	Temperature of the source	K
$T_{\text{sp}}$	Setpoint temperature	K
$T_{\text{sto}}$	Temperature of the storage	K
$t$	Time	s
$u$	Load of the heat pump pool	MWh
$u_k$	Control variable in timestep $k$	kW
$u_{\text{act}}$	Regulating power volume	MWh
$u_{\text{sch}}$	Scheduled power volume day-ahead	MWh
$u_{\text{spot}}$	Purchased power volume day-ahead	MWh
$V_{\text{DHW}}$	Volume of the storage for domestic hot water	l
$V_{\text{SH}}$	Volume of the storage for space heating	l
$v$	Daily load pattern of the buildings	kWh
$w$	Exogenous disturbances	kWh
$x$	Energy stored in the storage	kWh
$\overline{ASHC}$	Mean annual specific heat consumption	kWh/(m <sup>2</sup> a)
$\tilde{c}$	Predicted day-ahead price for electricity	Euro/TWh
$\dot{T}$	Derivative of the temperature	K/s
$\dot{Q}_{\text{BH}}$	Heat production of the back-up heater	W
$\dot{Q}_{\text{demand}}$	Heat demand	W
$\dot{Q}_{\text{DHW,nom}}$	Nominal heat load for DHW	W
$\dot{q}_{\text{DHW}}$	Nominal heat load for DHW per person	W
$\dot{Q}_{\text{HL,nom}}$	Nominal heat load of the heat pump	W
$\dot{Q}_{\text{HP}}$	Heat production of the heat pump	W
$\dot{Q}_{\text{HP,nom}}$	Nominal capacity of the heat pump	W
$\dot{Q}_{\text{SH}}$	Space heating load	W
$\tilde{p}_{\text{el}}$	Predicted electricity consumption of heat pump pool	kW
$\tilde{T}$	Prediction of the temperature	K
$\tilde{T}_{\text{a}}$	Prediction of the ambient temperature	K
$\tilde{\bar{T}}_{\text{amb}}$	Predicted mean ambient temperature	K
$\tilde{x}$	Prediction of the integrated temperature error	K

---

<b>Symbol</b>	<b>Description</b>	<b>Unit</b>
$\alpha$	Duration of the heat pump pool	min
$\beta$	Regeneration of the heat pump pool	min
$\gamma$	Relative annual absolute error	-
$\eta$	Load shifting efficiency	-
$\Delta t$	Change in time	s
$\Delta T$	Temperature diff. between sink and source	K
$\kappa$	Discrete timestep	s
$\chi$	Integrated temperature error	K
$\pi$	Power price	DKK/MWh
$\pi_{\text{bid}}$	Price bid	DKK/MWh
$\pi_{\text{RP}}$	Regulating power price	DKK/MWh
$\Omega$	Units in the pool	-
$\Omega^+$	Active units in the pool	-
$\Omega^-$	Non-active units in the pool	-
$\tilde{\pi}$	Power price prediction	DKK/MWh
$\tilde{\pi}_{\text{avg}}$	Average predicted spot price	DKK/MWh
$ \omega $	Number of units to trigger	-
$ \Omega $	Number of units in the pool	-
$ \Omega^+ $	Number of active units in the pool	-
$ \Omega^- $	Number of non-active units in the pool	-
$\mathcal{H}$	Discrete intra-day time space	h
$\mathcal{K}$	Discrete day-ahead time space	h
$\mathcal{T}$	Range of indoor temperatures	T
$\mathcal{U}$	Range of power volume	MWh

---

<b>Abbreviation</b>	<b>Description</b>
ASHP	Air-sourced heat pump
BH	Back-up heater
BWP	Bundesverband Wärmepumpen e.V.
CHP	Combined heat and power
COIN-OR	Computational Infrastructure for Operations research
COP	Coefficient of performance
DHW	Domestic hot water
DLC	Direct load control
DSM	Demand-side management
DSO	Distribution system operator
DWD	Deutscher Wetterdienst
EPEX	European power exchange
Fraunhofer ISE	Fraunhofer Institute for Solar Energy Systems ISE
GHG	Greenhouse Gas
GSHP	Ground-sourced heat pump
HC	Heating curve
HP	Heat pump
KPI	Key parameter of interest
LP	Linear programming
MILP	Mixed integer linear programming
MPC	Model predictive controls
OTC	Over the counter
PuLP	Python linear programming
SFH	Single family house
SH	Space heating
SLP	Standardlastprofil (standard load profile)
SOC	State of charge
SPF	Seasonal performance factor
TH	Terraced house
TMZ	Temperaturmaßzahl (temperature characteristic number)
TRY	Test reference year

# List of Figures

1.1	Annual renewable shares of electricity production in Germany. In recent years, the share of renewable sources has reached a value of around one third of the German electricity production. Source: Burger and Fraunhofer Institute for Solar Energy Systems ISE [2017b] (figure edited). Cited: 2017-04-20. . . . .	1
1.2	Electricity production and spot prices in Germany in March 2017. Daily and weekly pattern can be seen for the prices (right axis, red and blue line), the electricity production (left axis, grey, yellow and green shapes) and the load (left axes, black line). The share of solar (yellow shape) and wind (green shape) are fluctuating over the course of time, partly balanced by the conventional production (grey shape). The import balance (purple shape) is changing over time, but is mostly negative (electricity export). Source: Burger and Fraunhofer Institute for Solar Energy Systems ISE [2017a] (figure edited). Cited: 2017-04-05.	2
1.3	Heat pump sales (blue bars) and ratio between electricity and gas prices (green line) in Germany for the case of renovation of buildings. Source: Koch et al. [2015, p. 11] (figure edited). . . . .	3
1.4	Results of the spot price optimisation. Source: [Biegel et al., 2013] (figure edited).	12
1.5	Results of the spot price and regulating power market optimisation. Source: [Biegel et al., 2013] (figure edited). . . . .	14
1.6	Electricity consumption of the simulated heat pump pool (blue) compared to the consumption purchased on the day-ahead spot market (red). Source: [Pedersen et al., 2014] (figure edited). . . . .	15
1.7	Comparison between the heat pump pool operation (blue) with fixed and dynamic indoor temperature boundaries. The electricity consumption has to match the purchased consumption (red). Source: [Pedersen et al., 2014] (figures edited). . . . .	16
1.8	Explanation of the general interaction between central aggregator and individual heat pump unit for the case of an air-sourced heat pump system. Copyright of the figure and single elements at <i>Fraunhofer ISE</i> . . . . .	18
1.9	General methodology of this master's thesis. . . . .	19
2.1	Simplified hydraulic layout of the system of a single heat pump as being used in the models. Source: [Fischer et al., 2016b, p. 855] (figure edited). . . . .	22
2.2	Regressions models used based on manufacturer's data in order to determine the coefficient of performance and the thermal heat pump capacity for air-sourced and ground-sourced heat pumps. Source: [Fischer et al., 2016b, p. 856] (figures edited). . . . .	24
3.1	General steps taken in order to obtain the pool of heat pumps for the analysis of its operation. . . . .	29
3.2	Ambient temperature of the test reference year 2015 for Potsdam, Germany. . .	31

4.1	Electricity consumption of the pool of heat pumps in the thermally driven operation. . . . .	34
4.2	Electricity consumption of the pool of heat pumps in the thermally driven operation. The operation is depicted for a representative winter day and a representative summer day. . . . .	35
4.3	Average electricity consumption of the heat pump pool for the thermally driven operation in winter (December, January, February). The mean progress over the day is represented by the yellow line. The petrol-green shapes indicate ranges of the quantiles within the mean day (q0-q100, q10-q90, q20-q80, q30-q70, q40-q60). . . . .	35
4.4	Average electricity consumption of the heat pump pool for the thermally driven operation in summer (June, July, August). The mean progress over the day is represented by the yellow line. The petrol-green shapes indicate ranges of the quantiles within the mean day (q0-q100, q10-q90, q20-q80, q30-q70, q40-q60). . . . .	36
4.5	Electricity consumption of the pool of heat pumps for the standard load profile. . . . .	39
4.6	Annual duration curves of the electricity consumption of the heat pump pool for the thermally driven operation and for the standard load profile. . . . .	39
4.7	Deviation of the thermally driven operation from the standard load profile illustrated by the deviation of the heat pump pool’s electricity consumption. . . . .	40
4.8	Average electricity consumption of the heat pump pool for the thermally driven operation and the for standard load profile operation for the whole year. The mean progress over the day is represented by the yellow (thermally driven operation) and grey (standard load profile) lines. The petrol-green (thermally driven operation) and orange (standard load profile) shapes indicate ranges of the quantiles within the mean day (q0-q100, q10-q90, q20-q80, q30-q70, q40-q60). . . . .	41
4.9	Day-ahead <i>EPEX</i> spot market price for electricity in 2015. . . . .	42
4.10	Average <i>EPEX</i> day-ahead spot market price for electricity in Germany for the whole year. The mean progress over the day is represented by the yellow line. The petrol-green shapes indicate ranges of the quantiles within the mean day (q0-q100, q10-q90, q20-q80, q30-q70, q40-q60). . . . .	42
4.11	Average electricity consumption costs of the heat pump pool for the thermally driven operation and for the standard load profile operation for the whole year. The values are shown as costs in Euro per hour. The mean progress over the day is represented by the yellow (thermally driven operation) and grey (standard load profile) lines. The petrol-green (thermally driven operation) and orange (standard load profile) shapes indicate ranges of the quantiles within the mean day (q0-q100, q10-q90, q20-q80, q30-q70, q40-q60). . . . .	43
4.12	Cumulated costs of electricity consumption for the thermally driven and the standard load profile operation. . . . .	44
4.13	Electricity consumption costs for the deviation between the thermally driven and the SLP operation. Note, that the values represents the deviation in costs per minute. . . . .	44
4.14	Available flexible energy and maximum power versus ambient temperature for the different <i>SG-Ready</i> signals. Mean values are indicated by a thick line, while the shapes represent the q25-q75 quartile range. Source: [Fischer et al., 2016b, p. 861]. . . . .	46

4.15	Characteristic response of a heat pump pool's electricity consumption to a short activation trigger signal. Source: [Fischer et al., 2016b, p. 860] (figure edited).	46
4.16	Times of duration and regeneration versus ambient temperature for the different <i>SG-Ready</i> signals. Mean values are indicated by a thick line, while the shapes represent the q25-q75 quartile range. Source: [Fischer et al., 2016b, p. 862].	47
4.17	Characteristic response of a heat pump pool's electricity consumption to a long activation trigger signal. Source: [Fischer et al., 2017] (figure edited).	47
5.1	Model developed for and used in the optimisation.	49
5.2	Results of the <i>LP</i> optimisation obtained for the 1 <sup>st</sup> of February.	54
5.3	Results of the <i>LP</i> optimisation obtained for the 26 <sup>th</sup> of December.	55
5.4	Difference between the optimised pool operation and the predicted pool operation.	56
5.5	Cumulated costs of electricity consumption for the thermally driven operation, the standard load profile operation and the optimised operation.	57
5.6	Daily savings in electricity consumption costs for the optimised operation compared to the thermally driven operation and to the standard load profile.	58
6.1	Schematic depiction of the pool operation and how the operation of the individual unit is influenced by the pool controller.	62
6.2	Degrees of freedom for the conversion of the error into direct load control signals for a centrally acting aggregator, which is triggering the units in the pool directly.	62
6.3	Algorithm for the "specific triggering of units" approach dependent on the control variable $u$ in the timestep $k$ . The algorithm transfers the number of units to trigger $ \omega $ into respective <i>SG-Ready</i> signals to be sent to specific units. $\Omega$ represents the units in the pool and $ \Omega $ the size of the pool.	65
6.4	Algorithm for the "random triggering of units" approach dependent on the control variable $u$ in the timestep $k$ . The algorithm transfers the number of units to trigger $ \omega $ into respective <i>SG-Ready</i> signals to be sent to the units. $\Omega$ represents the units in the pool and $ \Omega $ the size of the pool. $\Omega^+$ are the active units in the pool, $\Omega^-$ represent the non-active units in the pool and the respective norms stand for the sizes of the respective group.	65
6.5	Operation of the pool controller at the 16 <sup>th</sup> of February.	68
6.6	Operation of the pool controller at the 12 <sup>th</sup> of February.	70
6.7	Operation of the heat pump pool at the 1 <sup>st</sup> of February. The figure compares different configurations of the pool controller and their ability to operate the pool according to the setpoint. The setpoint is represented by the optimised operation trajectory purchased.	71
6.8	Hourly error of the operation influenced by the pool controller with intermittent PI-controller. The values represent the difference in the energy purchased and the energy consumed by the pool operation in the respective hour.	72
6.9	Relative error of the operation influenced by the pool controller with intermittent PI-controller versus relative setpoint. The relation is calculated with regard to the thermally driven operation at the respective hour.	74
6.10	Hourly relative error of the operation influenced by the pool controller with intermittent PI-controller. The values represent the difference in the energy purchased and the energy consumed by the pool operation in the respective hour. The values are normalised to the setpoint in the respective hour.	75

---

7.1	Results of the <i>LP</i> optimisation obtained for the 1 <sup>st</sup> of February. . . . .	78
-----	---------------------------------------------------------------------------------------------	----

## List of Tables

2.1	<i>SG-Ready</i> signals and their implementation in the heat pump models. . . . .	28
2.2	Validation results for the simulated (Sim.) and the measured (Meas.) heat pump pool. The key performance indicators are: Seasonal performance factor (SPF), operation hours and on-off cycles per day. Source: [Fischer et al., 2016b, p. 858] (table edited). . . . .	28
3.1	Composition of the heat pump pool by age and type of building. Composition of the houses is taken from <i>Wolf [2016]</i> . . . . .	30

# 1 Introduction

## 1.1 Motivation

In 2015, the nations of the world have agreed on the *United Nations Climate Change Conference, COP21* in Paris to keep the rise in global temperature below 2 K compared to pre-industrial level. This level of global warming corresponds to a concentration of greenhouse gases (GHG) in the atmosphere of around 450 ppm in 2100 as a majority of studies claim [Intergovernmental Panel on Climate Change, 2014, p. 10]. Moreover, it is suggested, that the global annual emissions of around 49 GtCO<sub>2</sub>eq [Intergovernmental Panel on Climate Change, 2014, p. 6] have to decline in order to stabilise the GHG concentration in the atmosphere below the limit of 450 ppm in 2100. Thus, a reduction of the global annual GHG emissions of 41 % to 72 % has to be achieved in 2050 associated with a sustained decline until 2100 [Intergovernmental Panel on Climate Change, 2014, p. 13]. In 2010, Germany was responsible for 2 % of the global GHG emissions [Kahlenborn and Brünig, 2014, p. 34]. In order to take its responsibility for climate change mitigation and to account for the shutdown of atomic power plants, Germany has passed the *Erneuerbare-Energien-Gesetz (German Renewable Energy Sources Act)* in 2000. With the aid of the associated subsidies, this law has led to an increasing share of renewable electricity production in Germany. Figure 1.1 shows the trend over the last years and highlights, that at present, around a third of the total German electricity production is originating from renewable sources.

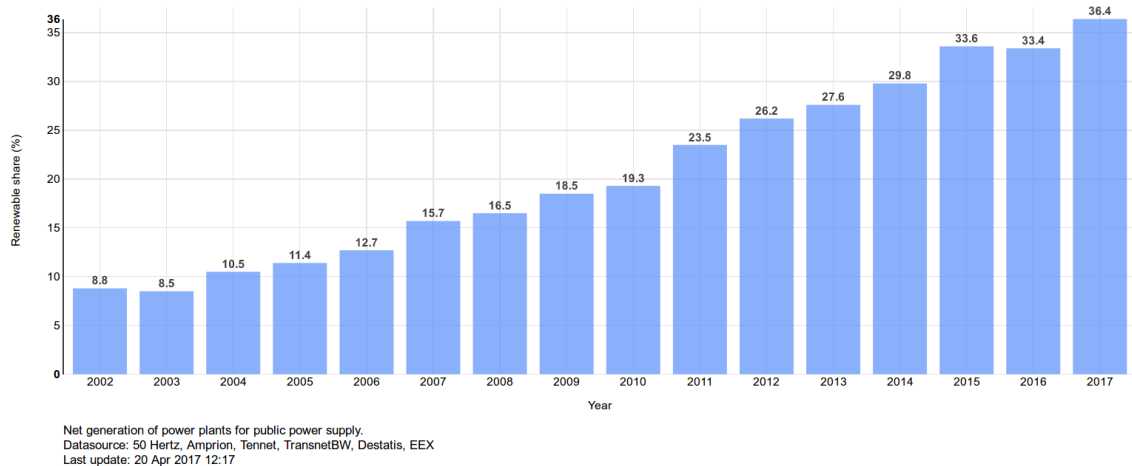


Figure 1.1: Annual renewable shares of electricity production in Germany. In recent years, the share of renewable sources has reached a value of around one third of the German electricity production. Source: Burger and Fraunhofer Institute for Solar Energy Systems ISE [2017b] (figure edited). Cited: 2017-04-20.

Due to its volatility, the share of renewable energy sources in the German electricity production is changing over time. Figure 1.2 presents the electricity production and spot market prices in Germany in March 2017. Note that the difference between the load and the sum of electricity production and import balance is caused by the fact, that conventional power plants producing less than 100 MW are not depicted here. Figure 1.2 shows high daily variabilities in the share of renewable energies and the spot market prices. Moreover, periodical patterns over days and weeks can be observed.

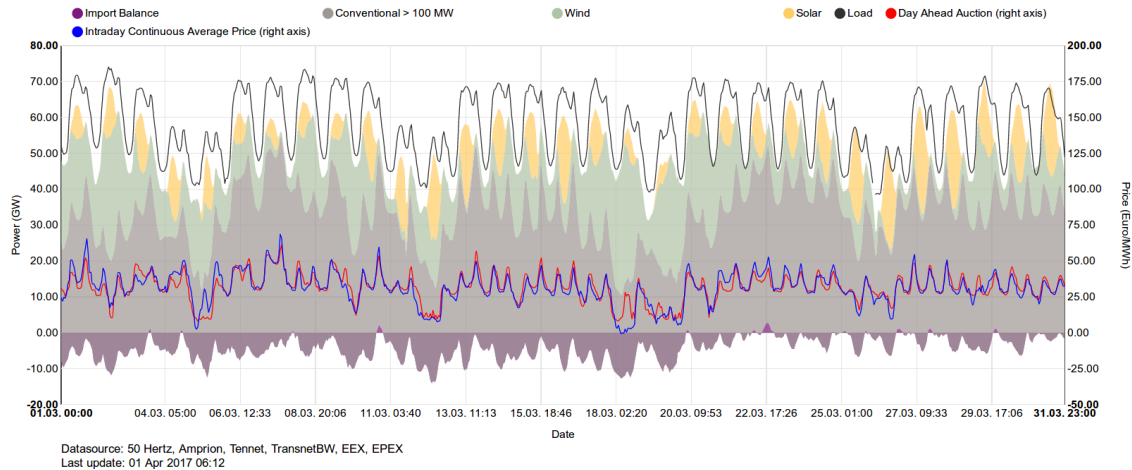


Figure 1.2: Electricity production and spot prices in Germany in March 2017. Daily and weekly pattern can be seen for the prices (right axis, red and blue line), the electricity production (left axis, grey, yellow and green shapes) and the load (left axes, black line). The share of solar (yellow shape) and wind (green shape) are fluctuating over the course of time, partly balanced by the conventional production (grey shape). The import balance (purple shape) is changing over time, but is mostly negative (electricity export). Source: Burger and Fraunhofer Institute for Solar Energy Systems ISE [2017a] (figure edited). Cited: 2017-04-05.

In addition to the *Erneuerbare-Energien-Gesetz*, Germany has decided to mitigate climate change by reducing its GHG emissions by 80 % to 95 % in 2050 compared to the level of 1990 [BMUB, 2016, p. 2]. In order to achieve this goal, several milestones for 2030 have been defined, aiming to assess and adjust the transition path towards a high level of GHG neutrality [BMUB, 2016, p. 9]. The plan of the German Government intends to reduce the GHG emissions of the building sector from 119 GtCO<sub>2</sub>eq in 2014 to 70 to 72 GtCO<sub>2</sub>eq in 2030 [BMUB, 2016, p. 26]. This reduction corresponds to a decline of the emissions of two third compared to the level of 1990 [BMUB, 2016, p. 26]. When considering the GHG emissions of households, space heating (SH) and domestic hot water (DHW) accounts for 68.5 % respectively 15.2 % of the final energy consumption [Arbeitsgemeinschaft Energiebilanzen e.V., 2013, p. 22] and therefore, they are responsible for a high share of the GHG emitted by households.

Heat pumps (HP) represent one technique to provide SH and DHW. By using the heat of the environment as a source, HPs usually provide a multiple amount of heat compared to the amount of energy invested. This is reflected by their high coefficient of performance (COP), which normally ranges between 1.5 and 4 [Cengel et al., 2003, p. 401]. Hence,

accompanied by the expansion of renewable electricity production, electrically driven HPs represent a suitable technique to achieve the German climate change mitigation goals. Moreover, HPs can be used for the realisation of a *smart grid* by using their thermal storages for demand side management (DSM) applications [Fischer and Madani, 2017, p. 344]. Moreover, volatile energy production from renewable sources can be balanced by the usage of HPs.

In 2013, over 700,000 HPs have been installed in Germany [Nowak and Westring, 2015, p. 88]. Figure 1.3 presents the German HP sales in renovated buildings and shows the ratio between electricity and gas prices in recent years. Figure 1.3 illustrates, that annual HP sales have decreased to a level of 20,000. Moreover, the figure shows a correlation between the ratio of electricity to gas price and the level of HP sales when renovating a house. By analysing Figure 1.3, it can be concluded, that the costs for electricity consumption of HPs are playing a major role for the attractiveness to install a HP.

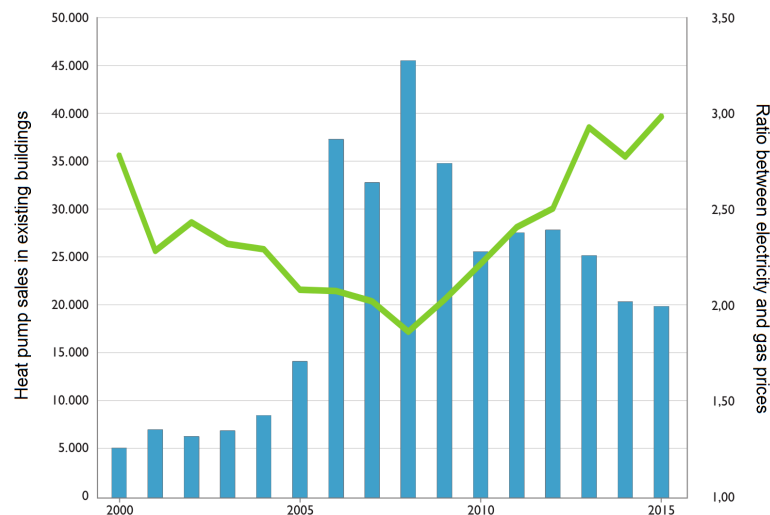


Figure 1.3: Heat pump sales (blue bars) and ratio between electricity and gas prices (green line) in Germany for the case of renovation of buildings. Source: Koch et al. [2015, p. 11] (figure edited).

In order to fulfil the GHG mitigation goals imposed, it is predicted that Germany needs to have a portfolio of around 5 to 6 million HPs installed in 2030 [Fraunhofer IWES/IBP, 2017, pp. 10-11]. Thus, the sales of HPs have to increase by 60 % to 5 times in the future [Fraunhofer IWES/IBP, 2017, pp. 10-11]. The installation of HPs should focus on existing buildings, due to the low share of around 2 % of HPs in existing buildings [Fraunhofer IWES/IBP, 2017, p. 11] and the continually high share of existing buildings' energy consumption in the total buildings' energy consumption in the future [Fraunhofer IWES/IBP, 2017, p. 88]. In order to fulfil the necessary GHG mitigation, it is important to give incentives for the further installation of HPs in residential buildings. As illustrated by Figure 1.3, relatively low energy consumption costs for the operation of HPs are a major incentive for the installation of HPs. Since HPs are usually equipped with thermal storages, their load can be shifted [Fischer et al., 2016b] and thus, HP operation can benefit from the variability of the electricity prices. Consequently, it is important to investigate, how the operation of HPs in residential buildings can be optimised economically.

## 1.2 Problem analysis

This master's thesis is contributing to the project *WPsmart im Bestand* (<https://wp-monitoring.ise.fraunhofer.de>) led by the *Fraunhofer Institute for Solar Energy Systems ISE* and conducted in cooperation with several HP manufacturers and energy utilities. This project is dealing with HPs installed in existing buildings with various levels of refurbishment. These HPs' operation is monitored and analysed within a fieldtest and simulations. Moreover, the HPs' load shifting potential is investigated in order to reveal the potential for load shifting applications by using the HPs' flexibility. Within the project *WPsmart im Bestand* (smart operation of HPs in existing buildings), some HPs are equipped with an infrastructure in order to enable them to receive direct load control (DLC) signals. The development of an approach to control and operate these "smart" HPs in the fieldtest optimally by using DLC is aimed. As a consequence, the approaches developed within this master's thesis are designed with regard to their applicability in the fieldtest and the project *WPsmart im Bestand*.

As shown in Section 1.1, it is necessary to investigate, how the operation of HPs can be conducted more cost-efficiently. Hence, this master's thesis is investigating, how HPs can be operated in a way, that decreases the costs for electricity consumption. Due to the project associated and the legal framework given, the considerations conducted are focussing on the case of Germany, but can be transferred to other countries when altering the associated assumptions and boundary conditions accordingly. In order to investigate, how the operation of HPs can be improved economically, it is necessary to know the legal framework determining the costs for the operation of the HPs. In Germany, it is currently possible to operate HPs in two different ways:

- Operating the individual HP in its normal energy efficient mode. According to §12 of the *Stromnetzzugangsverordnung*, the distribution system operator (DSO) has to assume, that end-consumers with a annual electricity consumption below 100,000 kWh (the individual HPs) are operating according to standard load profiles (SLP) [Deutscher Bundestag, 2016]. The costs for electricity are determined by local tariffs. Different tariff models exist, but highly variable tariffs are missing. Hence, the usage of the load shifting potential of the HP is not rewarded monetarily. Thus, the deviation from the expectable SLP operation is not adequately beneficial for the HP operator.
- The HP operator is purchasing its electricity consumption by himself and can therefore benefit from variable prices. By using the flexibility of the HP's electricity consumption, monetary benefits can be generated by shifting the load to more favourable times. In order to avoid financial penalties, the HP's energy consumption should match with the energy purchased.

Concluding these considerations, benefiting monetarily from the usage of the HP's flexible electricity consumption is only possible, when purchasing the electricity directly. For this work, which is considering the case of Germany, the *EPEX* spot market (<http://www.epexspot.com/en/>) is the suitable place for purchasing electricity. Due to simplicity of the investigated approaches, *over the counter (OTC)* trading is not considered here. Due to the diversity in existing tariff-models, this work is making the following

assumption: The tariffs offered for the SLP-like operation of the HPs are calculated by matching the consumption declared by the SLP operation with the related day-ahead price. The costs calculated by this consideration are taken as one of the reference costs for the operation of the HPs within this work. All further investigations of the electricity consumption costs are calculated by using the same day-ahead prices for electricity and are compared to these costs.

In order to decrease the costs of operation, the costs for the HP's electricity consumption have to be lowered. Consequently, the operation of the HPs has to be altered from the normal thermally driven behaviour towards an operation, which accounts for the variability of the electricity prices. Hence, the operation of the HPs needs to be optimised economically with regard to the variable electricity prices. By changing the electricity consumption of the HPs, demand side management (DSM) is conducted. It is shown in *Carmo et al. [2014]*, that DSM is possible to be conducted with HPs, while *Fischer et al. [2016b]* has shown, that the available load shifting potential, the so-called flexibility, is limited. As a consequence, the economic optimisation of the HP operation is constrained by end-user requirements and the available flexibility of the HPs.

When influencing the operation of a pool of HPs, it is important to consider on which hierarchy level the decision about the influence of the HP operation is taken. Hence, different approaches regarding the localisation of the intelligence determining the HP operation are possible. *Rohbogner et al. [2012]* divided the flow of information within an energy management system into the categories "*Central-hierarchical Control Structure*", "*Distributed-hierarchical Control Structure*" and "*Decentralized Control Structure*" [Rohbogner et al., 2012, pp. 1302-1303]. Based on this classification, *Fischer and Madani [2017]* inferred a classification for the operation of HP units, which distinguishes between: [Fischer and Madani, 2017, p. 351]

- Direct Control: Passive systems receive direct set values transmitted from a higher control level.
- Indirect Control: Passive intelligent systems optimise their own operation according to a cost signal.
- Agent Based Control: Active systems are acting individually and therefore negotiate between each other in order to implement a control action with regard to the individual and common optimisations of the operations.

Hence, the operation determination infrastructure of the HPs can be divided into centralised (Direct Control), decentralised (Agent Based Control) and hybrid (Indirect Control) approaches. The approach to alter and determine the HP operation taken within this work shall be scalable to a large number of HP units in order to be able to maximise the financial profits related. When realising the operation determination infrastructure, decentralised approaches require a higher number of intelligences determining the operations. Moreover, local intelligences require local measurement infrastructure for the determination of operation as well. Consequently, the more decentralised the approach, the higher the total costs for its implementation.

In order to keep the threshold for the implementation of the approach considered within this work as low as possible, it is decided to consider a centrally acting pool aggregator.

This aggregator is deciding on the operation of the particular HP unit. Additionally, the aggregator has to make a contract with the owner of the HP and make compensation payments to him for altering his HP's operation. Therefore, the aggregator is acting as a legal entity. For the occupation of the role of the aggregator, many realisations are possible including various possible business-models. The exact definition of the business-model and the role of the aggregator is spared here and a general consideration is taken. Furthermore, the central aggregator wants to maximise its profits. Thus, his portfolio of systems controlled has to be as large as possible. As a consequence, this work is assuming, that the central aggregator is responsible for the operation of a pool of HPs, rather than controlling only single units. By pooling, the aggregator is able to maximise his profits by benefiting from the larger amount of shifted electricity consumption and thereby higher electricity costs avoided. Furthermore, the aggregator is deciding on the operation of each HP unit in the pool and is aiming to shift and influence the HPs' operation according to the economic optimum. Additionally, it is important to define, how the aggregator is influencing the HPs' operation. Thus, a communication infrastructure between individual HP and aggregator is required.

When implementing the infrastructure for the realisation of the central aggregator approach, it is preferable to use already existing and well-established frameworks in order to keep the costs of implementation and the amount of modification requisites low. The *SG-Ready* interface offers such a standardised interface and is already established among the German HP manufacturers. Consequently, the *SG-Ready* standard is used for the influence on the operation of the HP operation by the central aggregator. In general, *SG-Ready* is offering a range of trigger signals in order to affect the operation of the HPs. Due to the impact on the HP's operation, these *SG-Ready* signals can be seen as direct load control (DLC) (see Section 2.9 for more details). The trigger signals are processed by the internal controller of each individual HP. Thus, by using *SG-Ready*, the individual HP has the possibility to ignore the signal transmitted via the *SG-Ready* interface. This is the case, when the operation according to the trigger signal would violate the operation conditions of the individual HP (see Section 2.9). Consequently, the central aggregator approach of this work is classified as an *Indirect Control* infrastructure, where trigger signals (incentives) are sent from the aggregator to the individual HPs and the individual HP's operation is optimised accordingly, when being approved locally.

### 1.3 State of the art

Within a literature study, several scientific papers have been studied. The review-paper *Fischer and Madani [2017]* provides a good overview about the topic "heat pumps in smart grids". The authors concluded, that a majority of the scientific papers dealing with a cost-optimised operation of HPs are rather focussing on decentralised optimisation approaches than on centralised optimisation [Fischer and Madani, 2017, p. 10]. Moreover, price focussed operation of HPs was often using the day-ahead spot market prices [Fischer and Madani, 2017, p. 9]. In the following, several scientific studies are presented. The first papers presented are dealing with the general investigation of the load shifting potential of HPs as being flexible consumers. The papers presented subsequently are rather focusing on the realisation of an optimum operation regarding a superior goal. After this, two studies

are presented in detail, due to their focus on a central acting HP pool aggregator as it is the focus of this thesis. The sources of the information presented in the following are stated in the respective paragraph. This section closes with the analysis of the models and findings of the various studies and the value added by this master's thesis.

In *Biegel et al. [2014]*, a pool of flexible consumers was analysed with regard to their ability to participate in the ancillary service market for the case of providing primary or secondary control reserve. When providing control reserve, the issues of limited energy capacity of the flexible consumption units and the prediction of their baseline consumption are essential. The behaviour of the pool was modelled by using a lumped model representing the electricity demand of the pool and its current energy capacity. The operation of the consumers interacted with the provision of reserve power and therefore, the energy capacity of the pool is directly affected by the provision of reserve power. Within this study, the aggregator of the pool units was able to continuously adjust its operational schedule, while also ensuring, that the transmission system operator has enough time to react to these adjustments. Consequently, the flexibility of the individual flexible consumption devices could be restored at any time. Hence, the pool was able to overcome the issues of limited energy capacities and inaccurate predictions of the baseline consumption. Thus, *Biegel et al. [2014]* concluded, that a pool of flexible consumers could participate in the ancillary service markets. This was highlighted by two investigated cases, one case of very low energy capacity and one case of inaccurately predicted baseline consumption. In both cases, the participation in the ancillary service markets was assessed to be possible.

*Pedersen et al. [2013]* analysed the ability of a pool of HPs to balance the electrical grid. For this purpose, a central aggregator used model predictive controls (MPC) in order to optimise the HP pool operation with regard to the energy prices. The thermal capacity of the houses was represented by a lumped model. The controller utilised this thermal capacity in order to stabilise the grid by switching the HPs on or off. Moreover, beside the objective to stabilise the grid, the controller had to ensure that the indoor temperatures of the houses were kept within the comfort range. Tests of the approach developed showed good results, since a better grid stabilisation was obtained by shifting the HP pools' energy consumption time-wise.

The studies *Fischer et al. [2016b]*, *Wolf [2016]* and *Fischer et al. [2017]* investigated the flexibility of an aggregated German HP pool. The pool consisted of 284 HPs representing the distribution and variety of the stock of German houses equipped with HPs [Wolf, 2016] (see also Section 3 within this thesis). The flexibility of this pool was analysed by triggering the HPs with *SG-Ready* signals (for more information about *SG-Ready*, see Section 2.9 or *Koch [2013]*). These three sources are the only ones found, which are directly utilising the *SG-Ready* interface. *Fischer et al. [2016b]* and *Wolf [2016]* triggered an uninfluenced pool every hour of the year. Subsequently, the obtained large database about the flexibility was analysed with regard to the ambient temperature. It was found, that the HP pool's flexibility is highly dependent on the ambient temperature. *Fischer et al. [2017]* focused on the load shifting potential and the efficiency when shifting load. Here, the pool was triggered every 19 hours over the course of the year. The results showed a strong seasonal dependency of the load shifting potential, being the lowest in the warm summer months.

*Fink and Leeuwen [2016]* investigated the optimal control of a pool consisting of one combined heat and power (CHP) unit and 102 HPs. Since the central CHP provided the electricity for the HPs and both, HPs and CHP, provided the thermal demand of the buildings in the pool, the HP units and the CHP and their controls interacted. Within this paper, the operation of the CHP was optimised in order to provide as much of the electricity demand by the HPs as possible. At the same time, the heat produced by the CHP was used for district heating. The pool of houses in *Fink and Leeuwen [2016]* comprised of at least 280 houses connected to the district heating system and thereby their thermal demand was supplied by the CHP. Additionally, the pool of houses included 104 houses equipped with HPs and thermal storages. In order to obtain the operation of the CHP, the schedules of the HP operations were ordered using an *Earliest Deadline First*-like algorithm, thus prioritising the HPs' electricity demands by the time they become due. In order to determine their priority, the individual HPs were performing model predictions and only communicate an upper and a lower boundary for their respective electricity demand to the CHP. Hence, the amount of transmitted information was kept low, so privacy issues (transmission of the houses' thermal demand) were handled. The *Earliest Deadline First* control approach yielded better results compared to a *Mixed Integer Linear Programming (MILP)* approach, since *MILP* was not able to treat the privacy issues sufficiently and the number of On/Off-switches of the units was reduced by using *Earliest Deadline First*. Moreover, the operation of the CHP was more steady when considering the priority of the HPs' electricity demand. *Fink and Leeuwen [2016]* concluded, that the *Earliest Deadline First* approach was a good alternative to cost-based or auction-based control approaches.

Summarising the findings of the papers presented above, it can be stated, that HPs are offering flexibility, that can be utilised for various applications, and that a pool of HPs can be operated according to certain objectives (for instance cost reductions). Within the literature study, two papers have been identified to be the most relevant for the topics covered by this thesis, because they have investigated the economic optimisation and the operation of an aggregated HP pool. Both papers are dealing with a central HP pool aggregator and are presented in the following. The paper *Electricity Market Optimization of Heat Pump Portfolio* written by *Biegel et al.* deals with the optimal purchase of the HP pool's electricity consumption on the day-ahead and on the intra-day spot market and used a lumped HP pool model for its investigations. This paper is presented in detail with a focus on the optimisation of the HP pool operation with regard to the electricity costs. By using a lumped model in order to represent the HP pool behaviour, the actual dispatch of energy between the units in the pool is not treated in detail within this paper. Hence, the paper *Maximizing Storage Flexibility in an Aggregated Heat Pump Portfolio* written by *Pedersen et al.* is presented within this section as well. This paper optimised the operation of an aggregated HP pool economically too, but analysed the dispatch of energy between the individual HP unit of the pool in detail as well. The purpose of the detailed dispatch analysis was, to adequately realise the scheduled HP pool operation obtained by the economic optimisation. Since *Biegel et al. [2013]* have not covered this important aspect sufficiently, *Pedersen et al. [2014]* is presented additionally with a focus on the dispatch algorithm only.

### 1.3.1 *Biegel et al. [2013]*

In this paper, the economic optimisation of the operation of a pool of domestic HPs was presented. The pool was operated from the perspective of an aggregator. The aggregator purchased the optimised predicted electricity consumption on the day-ahead spot market. The flexibility of the HP pool was used in order to allow the aggregator to place bids on the intra-day regulating power market. This study was conducted by simulations. For the simulations, the experiences and data from the project *Styr din varmepumpe* (control your HP) were used for parameter setting and comparison. The simulations were conducted for a pool of 10,000 HPs operating in the Nordic market. The paper's methodology and findings are presented in detail in the following passages. [Biegel et al., 2013]

The focus of the scenario drawn in this study was on Denmark with its high shares of renewable energy sources and its aim to turn off fossil-based power plants. In order to account for the thereby missing balancing services, an aggregator should operate a pool of HPs in order to use their flexibility for the purpose of grid stabilisation. The aggregator was defined as a legal entity able to use the consumer's flexible consumption via entering into contracts. In order to earn the consumer's contractual compensation, the operation of this pool was optimised economically. [Biegel et al., 2013]

Due to reasons of complexity of both, the optimisation and the prediction of the behaviour of a pool of HPs operating individually, this study was using a lumped model. This lumped model represented the cumulated HP pool behaviour. The authors concluded that unpredictable disturbances and the deviations between individual HP and mean pool behaviour would smooth out through the pooling. Since it was not aim of the study to describe the HPs accurately on individual level, this aggregated model was found to be sufficient. The HP pool was described with a first order model. This model did not account for the dispatch of electricity to the individual HPs and neither for the control algorithms on individual level. Equation 1.1 presents the equation used in order to describe and optimise the HP pool behaviour by modelling the change in the mean indoor temperature of the pool. [Biegel et al., 2013]

$$\dot{T}(t) = \frac{1}{RC} (T_a(t) - T(t)) + \frac{1}{C} (u(t) + v(t) + w(t)) \quad (1.1)$$

In Equation 1.1,  $R$  represented the thermal resistance of the pool and  $C$  its thermal capacity. The indoor temperature of the pool  $T$  got subtracted from the ambient temperature  $T_a$  for each time  $t$ .  $u(t)$  was the electricity consumption of the HP pool,  $v(t)$  the daily load profile of the houses and  $w(t)$  the exogenous disturbances. Due to the pooling,  $v(t)$  and  $w(t)$  would smooth out. By the aid of measurements, the indoor temperature and the electricity consumption of the pool could be limited within boundaries. Since the energy in the Nordic market is traded on an hourly base, Equation 1.1 was discretised in order to obtain  $T(k+1)$ , the mean indoor temperature of the pool corresponding to each hour  $k$ . For the conducted quadratic fitting for the identification of the discretised parameters, one year's data of 130 HPs was used. [Biegel et al., 2013]

In this study, the predicted energy to be consumed by the HP pool was purchased at the day-ahead spot market using accurate estimations of the actual prices. Equation 1.2 shows the total costs of electricity for the pool operation  $J_{\text{el}}(k)$ , in each hour  $k$ . Since the energy was traded for every hour, the consumption of the pool in each hour had to match with the electricity purchased for this hour for the price  $\pi(k)$ . In cases when the pool consumption purchased,  $u_{\text{spot}}(k)$ , did not match with the actual one,  $u(k)$ , the difference in energy had to be bought as balancing power from the transmission system operator. This balancing power had the regulating power price,  $\pi_{\text{RP}}(k)$ . By this consideration, Equation 1.2 is obtained. [Biegel et al., 2013]

$$J_{\text{el}}(k) = u_{\text{spot}}(k)\pi(k) + (u(k) - u_{\text{spot}}(k))\pi_{\text{RP}}(k) \quad (1.2)$$

In their work, *Biegel et al. [2013]* divided the optimisation into two parts. First, the flexibility of the HP pool was optimised regarding the spot prices. Then in a second optimisation scenario, the regulating power market was included into considerations as well. [Biegel et al., 2013]

### Spot Price Optimisation

In this optimisation, the overall electricity costs should be decreased by shifting the electricity consumption to times with lower prices. The optimisation was subdivided into two parts, a day-ahead part and an intra-day part. Day-ahead, the predicted energy consumption was optimally bought on the spot market based on day-ahead price predictions. The purchased consumption determined the operation for each hour, which was then optimised intra-day, taking into account the costs for violations as well. [Biegel et al., 2013]

For the day-ahead optimisation, it was decided, that the indoor temperature should converge around a steady-state setpoint  $T_{\text{sp}}$  instead of reaching to the temperature boundaries. This was achieved by minimising the integrated temperature error around the setpoint, called  $\chi$ , in the Optimisation Problem 1.3. The Optimisation Problem 1.3 was formulated for the purchase of electricity between 11 o'clock and 12 o'clock for the following day, hence the variable space  $\mathcal{K}=\{k+13, \dots, k+36\}$ : [Biegel et al., 2013]

$$\begin{aligned} & \text{minimise: } \sum_{\kappa \in \mathcal{K}} (\tilde{\pi}(\kappa)u(\kappa) + k_I \chi^2(\kappa)) \\ & \text{subject to: } T(\kappa + 1) = aT(\kappa) + (1 - a)\tilde{T}_a(\kappa) + b(u(\kappa) + v(\kappa)), \kappa \in \mathcal{K} \\ & \quad x(\kappa + 1) = x(\kappa) + T(\kappa) - T_{\text{sp}}, \kappa \in \mathcal{K} \\ & \quad u(\kappa) \in \mathcal{U}, T(\kappa) \in \mathcal{T}, \kappa \in \mathcal{K} \\ & \quad T(k+13) = \tilde{T}(k+13) \\ & \quad x(k+13) = \tilde{x}(k+13) \end{aligned} \quad (1.3)$$

In this formulation,  $a$  and  $b$  represented the parameters defined through the quadratic fitting in the discretisation procedure.  $\mathcal{T}$  described the acceptable indoor temperature

range,  $\mathcal{U}$  is the power range,  $k_I$  represented a trade-off parameter. Since the temperatures, integrated temperature tracking error and spot prices are unknown day-ahead, the Formulation 1.3 calculated with the predictions  $\tilde{T}$ ,  $\tilde{u}$  and  $\tilde{\chi}$ . The daily load profile  $v(\kappa), \kappa \in \mathcal{K}$  was known from measurements within the project. By the aid of Formulation 1.3, the electricity to be purchased at the day-ahead spot market  $u_{\text{spot}}^*(\kappa), \kappa \in \mathcal{K}$  was obtained. [Biegel et al., 2013]

Through the intra-day optimisation, the actual operation of the HP pool was determined. Here, the spot prices were assumed to be known for  $H$  hours into the future. The variable space was now  $\mathcal{H} = \{k, \dots, k + H - 1\}$ . For the resultant Optimisation Problem 1.4, the actual indoor temperatures  $T$  and their integrated temperature tracking error  $\chi$  had to be collected. [Biegel et al., 2013]

$$\begin{aligned}
 & \text{minmise: } \sum_{\kappa \in \mathcal{H}} (\pi(\kappa)u(\kappa) + k_I x^2(\kappa)) \\
 & \text{subject to: } T(\kappa + 1) = aT(\kappa) + (1-a)\tilde{T}_a(\kappa) + b(u(\kappa) + v(\kappa)), \kappa \in \mathcal{H} \\
 & \quad x(\kappa + 1) = x(\kappa) + T(\kappa) - T_{\text{sp}}, \kappa \in \mathcal{H} \\
 & \quad u(\kappa) \in \mathcal{U}, T(\kappa) \in \mathcal{T}, \kappa \in \mathcal{H}
 \end{aligned} \tag{1.4}$$

This formulation yielded the solution  $u_{\text{spot}}^*(k)$ , determining how the aggregator had to operate the HP pool. The applied algorithm consisted of the Formulation 1.4 which was repeated for each hour of the day and therefore determining the operation of the pool. Each day between 11 o'clock and 12 o'clock, the Formulation 1.3 was used to determine the day-ahead planning of the operation to be purchased at the spot market. For the simulation, a liquid market was assumed, meaning, that the market prices would not be affected by the operation and bidding of the aggregator. The simulation of 10,000 HPs yielded the results, presented in Figure 1.4. In the upper plot, the day-ahead price (blue) and its prediction (red) are shown. The middle part of the figure presented the actual operation monitored in the project *Styr din varmepumpe* (green), which was scaled up to the simulation pool size, and the operation determined by the controller (purple). Moreover, the lower plot of Figure 1.4 showed the monitored indoor temperature (green) and the one yielded by the optimisation (purple). The plots presented, that the consumption of the pool was shifted towards time of lower electricity prices while still keeping the indoor temperatures within the boundaries. This shifting of consumption led to savings of 18 %. [Biegel et al., 2013]

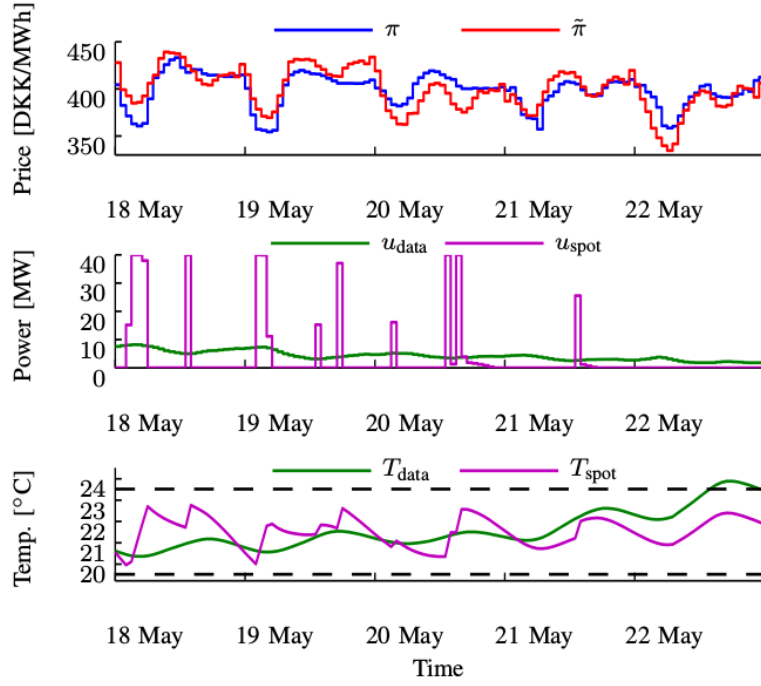


Figure 1.4: Results of the spot price optimisation. Source: [Biegel et al., 2013] (figure edited).

### Spot Price and Regulating Power Market Optimisation

In this part of the work, the optimisation of the operation was added by the possibility to place bids on the regulating power market. Therefore, the algorithm of the spot price optimisation was extended. Due to regulative constraints, the operation schedule of the pool had to be determined 45 min in advance. Hence, the scheduled power consumption  $u_{\text{sch}}(k)$  had to be determined until the hour  $k-1$ . Furthermore, the volume of regulating power, which the aggregator had to deliver, is denoted  $u_{\text{act}}(k)$ . In summary, the aggregator had to control the pool in order to consume  $u_{\text{reg}}(k) = u_{\text{sch}}(k) + u_{\text{act}}(k)$ . The bidding for regulating power was chosen to be only conducted when it would have been favourable, otherwise  $u_{\text{act}}(k) = 0$ . The authors chose to examine the marginal costs for delivering regulating power instead of predicting the price for the regulating power. In order to determine the optimised operation, the Formulation 1.5 was introduced. [Biegel et al., 2013]

$$\begin{aligned}
 & \text{minmise: } \sum_{\kappa \in \mathcal{H}} (\pi(\kappa)u(\kappa) + k_I \chi^2(\kappa)) - T(H) \frac{\tilde{\pi}_{\text{avg}}}{b} \\
 & \text{subject to: } T(\kappa + 1) = aT(\kappa) + (1 - a)\tilde{T}_a(\kappa) + b(u(\kappa) + v(\kappa)), \kappa \in \mathcal{H} \\
 & \quad x(\kappa + 1) = x(\kappa) + T(\kappa) - T_{\text{sp}}, \kappa \in \mathcal{H} \\
 & \quad u(\kappa) \in \mathcal{U}, T(\kappa) \in \mathcal{T}, \kappa \in \mathcal{H} \\
 & \quad u(k) = u_{\text{sch}}(k) + u_{\text{act}}(k)
 \end{aligned} \tag{1.5}$$

In this formulation,  $\tilde{\pi}_{\text{avg}}$  was the average predicted spot price and  $T(H) \frac{\tilde{\pi}_{\text{avg}}}{b}$  represented the

energy stored in the portfolio at the end of the horizon, where the spot prices are known,  $H$ . Moreover, the costs for participating and bidding in the regulating market were described by Equation 1.6. In this equation,  $J^*(0)$  represented the costs, when not providing regulating power. These costs were accounted with the costs for delivering regulating power  $J^*(u_{\text{act}})$  of the volume  $u_{\text{act}}(k)$  and the pool's cost for imbalance  $u_{\text{act}}(\pi_{\text{bid}}(u_{\text{act}}(k)) - \pi(k))$ . The bidding price  $\pi_{\text{bid}}$  was chosen to be the break-even point of Equation 1.6. Since the regulating price was determined by merit-order, the aggregator normally profited when being activated for regulating power. [Biegel et al., 2013]

$$J^*(0) = J^*(u_{\text{act}}) + u_{\text{act}}(\pi_{\text{bid}}(u_{\text{act}}(k)) - \pi(k)) \quad (1.6)$$

The algorithm in the simulations was still using the intra-day optimisation of the Formulation 1.4, but with the Formulations 1.5 and 1.6, the bidding in the regulating market was included and optimised as well. Here bids were placed for every multiple of 10 MW with a minimum bidding volume of 10 MW. Moreover, the aggregator steered the operation according to the purchased electricity consumption, thus the aggregator accounted for provided regulating power if applicable. Again, the algorithm optimised the purchase of energy at the day-ahead market in the hour between 11 o'clock and 12 o'clock. The results of this second optimisation and simulation scenario were presented in Figure 1.5. The upper part of this figure showed the realised spot price (blue) and the regulating power price (red). In the seconds subplot, the measured operation in the field (green) was presented, as well as the activation of regulating power (yellow) and the resulting pool consumption (purple). The lower part of Figure 1.5 showed the measured indoor temperature and the one obtained through the optimisation. Again, the temperature was within the boundaries. Furthermore, the figure presents, that the pool was activated for upward regulation ( $u_{\text{act}} < 0$ ) when the regulating power price was high. Consequently, the actual power consumption  $u_{\text{reg}}$  was lower than the purchased power consumption at the day-ahead market  $u_{\text{sch}}$  in these times, since the decrease in power consumption was traded as upward regulating power. The savings realised by this optimisation were 20 %. Thus, the savings increased by the further intra-day optimisation from 18 % to 20 %. [Biegel et al., 2013]

### Summary of the findings

The authors highlighted, that they have been using an idealised model and therefore, the savings when implementing this approach in reality would be lower. Moreover, when dealing with perfect predictions of the spot prices, the savings increased further by 5 %. *Biegel et al.* concluded, that it is possible to operate a pool of heat pumps according to spot prices and optimise its operation in terms shifting its consumption to more favourable times. However, since the savings per heat pump were around 500 DKK per year (around 70 Euro per year), the installation costs would have to be small in order to implement such an aggregator approach [Biegel et al., 2013]

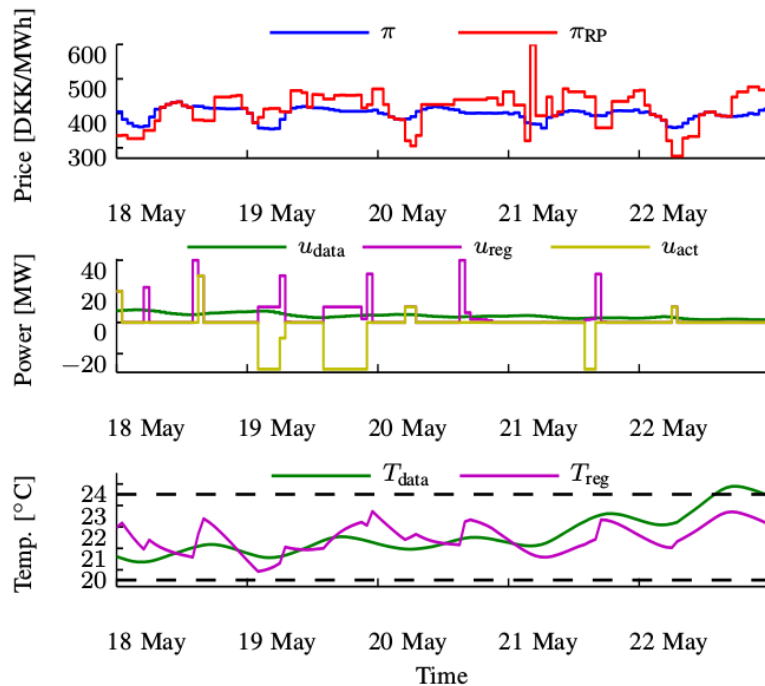


Figure 1.5: Results of the spot price and regulating power market optimisation. Source: [Biegel et al., 2013] (figure edited).

### 1.3.2 Pedersen et al. [2014]

This paper investigated the storage possibilities of HP pools in order to stabilise the grid when having a high share of fluctuating renewable energies. An aggregated model of the HP pool was used in order to purchase energy on the day-ahead market optimally. Based on this purchase, the energy was distributed between the buildings in the pool by a model-free scheduling algorithm. Moreover, trading possibilities on the intra-day market have been analysed. Hence, this paper dealt with the dispatch of energy between the individual HP units in the pool in order to operate the pool according to the optimised, scheduled and purchased operation trajectory. The model-free approach for the dispatch was detailed enough in order to depict the behaviour of single HP units (in comparison, Biegel et al. [2013] was using a lumped model for the description of the whole pool behaviour). [Pedersen et al., 2014]

This paper was associated with the project *Styr din varmepumpe* too. It was using a pool of 100 real inhabited houses, which were equipped with HPs. Moreover, measurement devices were installed in each houses in order to monitor the outdoor temperature, the indoor temperature, the heat power of the HP and the electrical power of the HP. Furthermore, the HPs were able to be switched on and off externally. The behaviour of the HP pool was modelled using the measurement data of the real houses. Then, the operation of the HP pool was optimised economically with regard to the day-ahead prices. The optimisation was conducted one day advance to the actual operation of the pool over the course of the year for each day. [Pedersen et al., 2014]

In the investigated scenario of the paper, the optimised operation trajectory obtained would have been purchased on the *NORD POOL Elspot market*. Within the simulations,

the operation of the HP pool had to match the operation bought. For this purpose, a model-free approach was used. The HPs were divided into six groups representing six possible states of the HPs ("On and may switch off", "On and must stay on", "On and must switch off", "Off and may switch on", "Off and must stay off", "Off and must switch on"). The grouping was motivated by the minimum times between On/Off switches of 25 min and the indoor temperatures of the individual houses with respect to the indoor temperature boundaries. The switches from one state to another are motivated by these parameters as well. [Pedersen et al., 2014]

In a simulation comprising of 100 houses and using outdoor temperature variations, the operation according to the optimised operation trajectory purchased was analysed. The individual houses were describes as first order systems with their parameters being normally distributed. Besides the electricity consumption of each house, its indoor temperatures, as well as the run time status, time since last change in run time status, outdoor temperature, minimum HP on-time, minimum HP off-time, upper indoor temperature boundary, lower indoor temperature boundary and reference indoor temperature were monitored. In order to match the operation trajectory purchased with the actual HP pool operation, the HPs have been switched on or off. Within the six different groups reflecting their state, the HPs were ordered by their margin between indoor temperature and temperature boundary. Based on the required power of the pool, the individual HPs have been activated with respect to their state. Thus, the HPs with the states "On and must stay on" and "Off and must switch on" have been activated first. If necessary, more HPs have been activated, until the required power of the pool has been matched. The order of the states for the activation has been chosen to be: "On and must stay on", "Off and must switch on", "On and may switch off", "Off and may switch on", "On and must switch off" and "Off and must stay off". When necessary (*e.g.* too many HPs were active compared to the target), HPs' states have been switched, although their run time constraints would have contradicted to this. The results of the simulation with this dispatch algorithm was presented in Figure 1.6. [Pedersen et al., 2014]

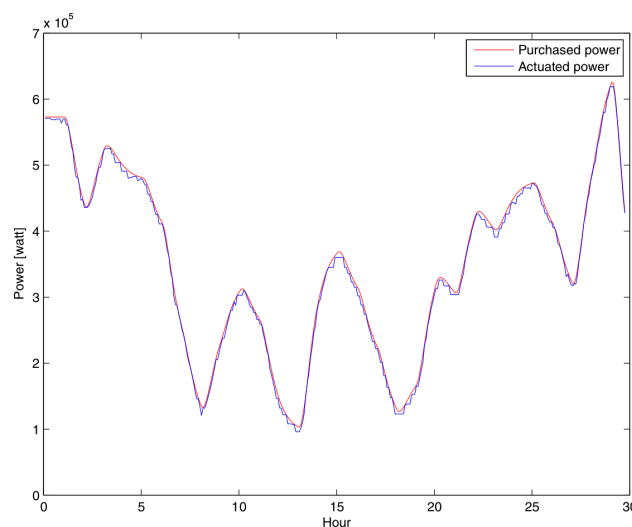


Figure 1.6: Electricity consumption of the simulated heat pump pool (blue) compared to the consumption purchased on the day-ahead spot market (red). Source: [Pedersen et al., 2014] (figure edited).

Figure 1.6 showed, that the HP pool operation was matching with the operation trajectory purchased. Moreover, the indoor temperatures in the individual houses have been kept within the temperature boundaries. In a subsequent analysis, the possibility to provide regulating power with the HP pool was analysed, in order to enable economic intra-day optimisation of the pool operation. For this purpose, the indoor temperature boundaries have been determined dynamically. Thereby, the flexibility of the pool could have increased by adjusting the temperature boundaries dynamically (squeezing the range of the temperature boundaries). Thus, the pool was able to follow a target operation trajectory as required for the provision of regulating power. This was illustrated by the pool's response to a pulse as presented in Figure 1.7, where Figure 1.7a showed the operation of the HP pool for fixed temperature boundaries and Figure 1.7b presented the pool operation with adjusted indoor temperature boundaries. It can be seen, that adjusted temperature boundaries led to a better match between demanded pool operation and the actual one. [Pedersen et al., 2014]

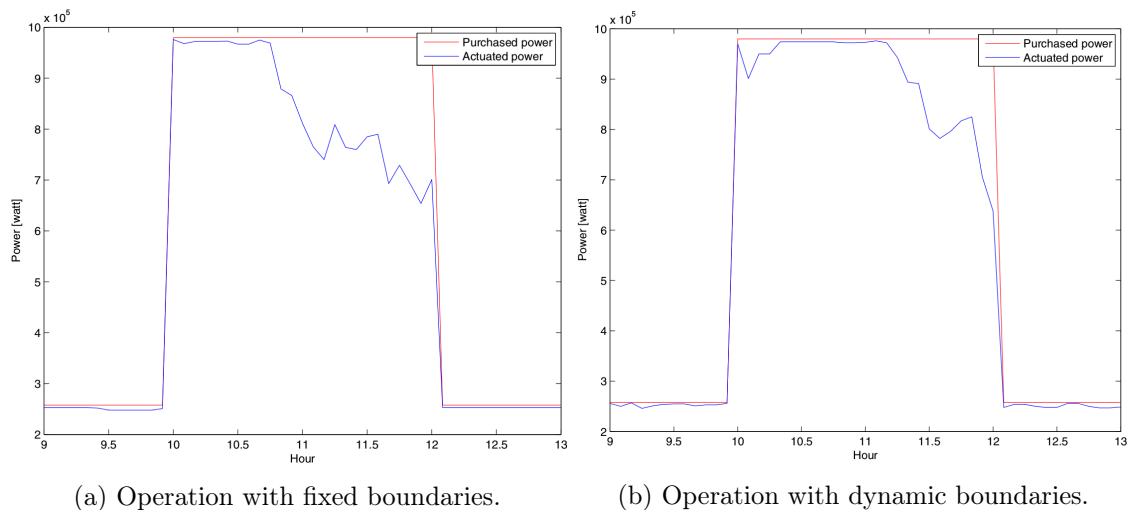


Figure 1.7: Comparison between the heat pump pool operation (blue) with fixed and dynamic indoor temperature boundaries. The electricity consumption has to match the purchased consumption (red). Source: [Pedersen et al., 2014] (figures edited).

### 1.3.3 Discussion about the models and findings of the literature study and the value added by this work

Most studies presented have been using a lumped model in order to represent the behaviour of the pool of HPs. It is queried by the author of this master's thesis, whether a lumped model is able to sufficiently represent the behaviour of the whole pool. Since the relatively extreme operation of single HP units might affect the overall flexibility of the whole pool, it is decided, that the individual HP operation should be represented in the models used for this thesis rather than using a lumped model for the whole pool. Moreover, DLC is mostly realised in the literature by switching the HPs on or off. Furthermore, extensive information about the operation of the individual HP units are required by some studies in order to determine the operation of the HP pool. This information often includes the indoor temperatures, which comes with the necessity for further measurement devices in order to determine the representative indoor temperature of the respective house. When using

individual HP models and the *SG-Ready* specifications for the determination of the DLC signals, the comfort of the individual houses is ensured automatically (see Section 2.9). As a consequence of these considerations, the value added by this master's thesis is as follows: This thesis adds further value to the scientific field of the cost-efficient operation of HP pools by:

- investigating the economic optimisation potential of the operation of a HP pool, when using models representing the individual unit behaviour and the associated available HP pool flexibility for a day-ahead optimisation.
- heading for the realisation of the optimum purchased consumption trajectory by only having limited information about the individual HP's operation (electricity consumption) and by using the refined and market-available DLC signals of *SG-Ready* and as a consequence being able to adjust the pool's operation more sensitively.

## 1.4 Problem definition

As being motivated and described by Section 1.1 and 1.2, it is of interest, to optimise the operation of a pool of HPs economically. In order to alter the HP pool's operation towards a more cost-efficient state, the available flexibility of the HP pool has to be taken into account. Moreover, the usage of a market-available and standardised interface for DLC is important in order to ease the implementation of the approach investigated. As a consequence, this master's thesis is dealing with the following two research questions: What are the saving rates for the optimisation of the electricity consumption costs of a pool of HPs with regard to the available flexibility of the pool? Which accuracy of trajectory is achievable, when operating the pool according to the optimised operation trajectory by using market-available DLC signals? In order to treat these two questions, this work is divided into several parts. The main content of this work can be divided into the following subject areas investigated:

- Analysis of the the thermally driven operation and the standard load profile of a heat pump pool with a subsequent investigation of the associated costs for electricity consumption.
- Optimisation of the heat pump pool's electricity consumption costs with regard to the available flexibility of the pool.
- Development of a control framework for the successful heat pump pool operation according to a target by using the *SG-Ready* trigger signals for direct load control.
- Analysis of the controlled heat pump pool operation and evaluation of the accuracy of trajectory of the control approach, when operating the pool according to the economically optimised electricity consumption trajectory.

In order to explain and illustrate the framework and approach developed and used within this thesis, Figure 1.8 is presenting the interdependence of the various components. Figure 1.8 shows the interaction between individual HP and aggregator for the case of an air-sourced heat pump (ASHP). Note that the pool used within this work is generally considering electrically driven HPs and consists of ASHP and ground-sourced heat pumps (GSHP) (see Section 3 for more details about the HP pool composition).

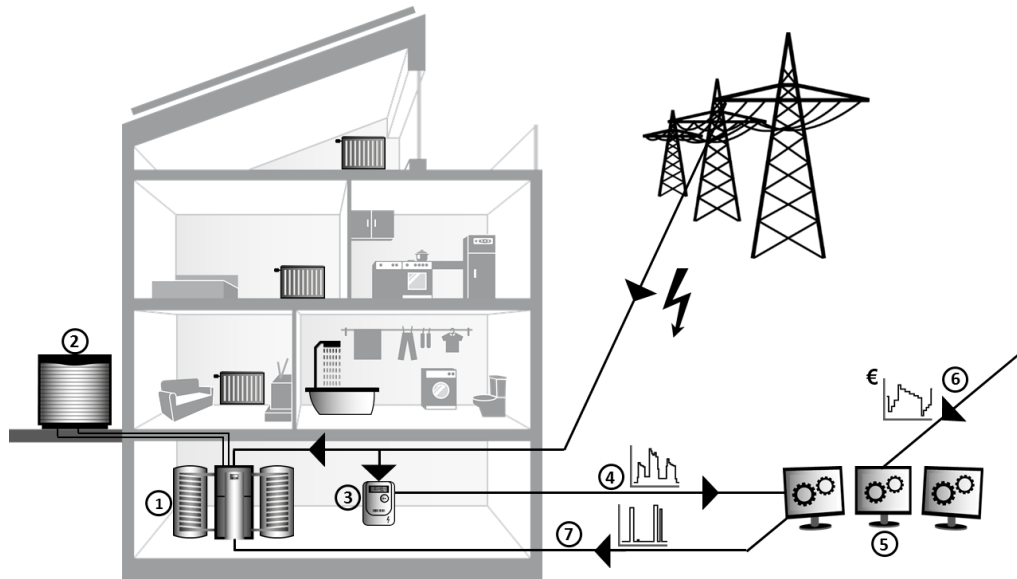


Figure 1.8: Explanation of the general interaction between central aggregator and individual heat pump unit for the case of an air-sourced heat pump system. Copyright of the figure and single elements at *Fraunhofer ISE*.

In Figure 1.8, ① is representing the HP with ② being its outdoor-unit. For its operation, the HP is taking electricity from the electricity grid and is supplying the house with SH and DHW. A smart meter ③ is monitoring the electricity consumption of the HP and sends this information ④ to the aggregator ⑤. The aggregator gathers the operation information (electricity consumption) of all HP units in the pool and receives information from the *EPEX* spot market ⑥ (for the analysis of the HP operation and the spot market prices, see Section 4). The aggregator uses the entirety of the information in order to derive an optimised operation (see Section 5). For this, the aggregator predicts the HP pool operation and optimises it economically. While doing that, the aggregator takes into account the available load shifting potential. Thus, the aggregator knows, how much the optimised HP operation may deviate from the predicted HP operation. The optimised pool operation can be seen as a schedule to be fulfilled by the actual HP pool operation. In this work, it is assumed, that the aggregator is purchasing the optimised operation trajectory on the *EPEX* day-ahead spot market at 12:00 o'clock on the day before. Thus, the aggregator has to predict the day-ahead prices in advance in order to conduct the optimisation. The purchase of electricity at the spot market is not treated in detail within this work. After that, the aggregator is sending *SG-Ready* trigger signals to the individual HPs ⑦ (see Figure 1.8) in order to guarantee, that the HP pool is operating according to the optimised operation trajectory purchased. Hence, the aggregator is deriving DLC decisions for individual HPs based on the operation of the whole HP pool. The deviation of the actual HP pool operation from the scheduled operation purchased is aimed to be equal to zero in order to avoid compensatory payments at all times.

In order to keep the costs for the implementation of the approach developed and used within this work as low as possible, the smart meter ③ is only monitoring the electricity consumption ④ of the HPs ① (see Figure 1.8). This assumption is taken, in order to avoid costly further measurement infrastructure, which would have to be installed in every

house of the pool. However, by only knowing the electricity consumption of each HP, the aggregator has to deal with a limited amount of information in order to predict, optimise and influence the operation of the HP pool. As explained in Section 1.2, this work is using the *SG-Ready* interface for the DLC of the individual HPs in the pool. Thus, the HPs' operation can be influenced by four different trigger signals ("Off", "On", "Superheat (HP)" and "Superheat (HP+BH)", see Section 2.9).

## 1.5 General methodology and general limitations

This section gives a short overview about the general methodology used within this work and the limitations associated. In order to summarise the sections above and illustrate the general proceeding taken within this thesis, Figure 1.9 presents the general methodology.



Figure 1.9: General methodology of this master's thesis.

The investigations and analyses carried out within this master's thesis have been conducted using the programming language *Python* within the integrated development environment *Eclipse*. Moreover, the HP models and the simulation framework used have already been developed and used in previous works (see for instance *Fischer et al. [2016a]*, *Wolf [2016]*, *Fischer et al. [2016b]* and *Fischer et al. [2017]*). Within this work, the existing simulation framework has been extended. By using the existing HP models, the limitations of these models are implicitly applied for the considerations of this work. Since the HP models have been validated (see Section 2.10), the results yielded and analysed by using this simulation framework are considered to be valid as well. In this work, the considered pool of houses, in which the HPs are installed, was already composed in previous work (see for instance *Wolf [2016]*, *Fischer et al. [2016b]*). After thorough checks, it has been decided, that the pool composition is still valid for the investigations of this work. Due to randomisation of HP parameters, the HP sizing is different to the ones used in *Wolf [2016]* and *Fischer et al. [2016b]* (see Section 3). Additionally, the economic considerations of this work are only dealing with the costs for the electricity consumption. Investment costs and other maintenance and operational costs are excluded from the considerations. Moreover, the calculations of costs carried out in this thesis are using the *EPEX* spot market's day-ahead prices for electricity in Germany. Intra-day optimisation of the HP pool operation is excluded as well as the detailed consideration of electricity tariff structures.



## 2 The heat pump models

Within this section, the HP models used are explained. The fundamental theory on Thermodynamics and HPs is not given here. If necessary, it can be found in the standard literature like *Cengel et al. [2003]*.

In the following, the load profile models and HP models used for the master's thesis are explained. The models have been developed in the department of the *Fraunhofer ISE*, where this master's thesis has taken place. Taken together, these models form a framework, which simulates the operation of HPs according to German standards. This simulation framework has several inputs and can be applied to any pool. The models are the basis for the further investigations carried out and descriptions about them can be found in the literature mentioned below.

Since the models were not developed by the author of this work, it is not main focus of this work to describe the models and their function in detail. Nevertheless, the following passages will give a sufficient overview about how the models are working. When referring to knowledge presented by a source, the reference, where this information was taken from, is given for the respective sentence or passage. If no reference is given, the statements presented are based on the analyses and configurations of the models made by the author of this thesis himself.

In order to easily find the references for the deep understanding of the models, they shall be given here. Literature about the models dealing with the generation of thermal load profiles for the houses can exemplary be found in *Fischer et al. [2016a]* and *Wolf [2016]*. The sources *Wolf [2016]*, *Fischer et al. [2016b]* and *Fischer et al. [2017]* are dealing with the models to describe the HP sizing and operation according to the thermal load profile of the respective house. The order of the sources mentioned is representing (in descending order) the level of detail in describing the respective content.

The following sections firstly explain the layout of the houses and HPs included in the models. After that, an explanation about how the thermal load profiles of the individual houses have been generated is given. This is followed by the explanation about how the HP models are working. The latter is split into the decision about the heat distribution system of the house, the function of the HP models, the sizing of the HPs, the internal controls of the HPs, the treatment of external signals and the validation of the HP models.

### 2.1 Layout of the system in the models

Within this work, only air-sourced heat pumps (ASHP) and ground-sourced heat pumps (GSHP) are considered, as they are the most relevant technologies on the German market (see Section 3 and *Gorris and Jacob [2013, p. 35]*) and their operation has already been modelled in the validated HP models available for this work. Hence, the other HP technologies available on the market are neglected in this work. The modelled ASHPs

and GSHPs are on-off HPs meaning, that the compressor speed is not variable. The HP models used are built up on a system layout for the single HP pool member as depicted in Figure 2.1. In the models, the physical behaviour of two thermal storages, the HP, the backup-heater (BH) and the controller are described. The operation of one system is presenting the operation of one HP unit implemented in one house, and thereby one member of the pool investigated. The demands for SH and DHW are determined by thermal load profiles (see Section 2.2). These demands are supplied by the respective storages. The overall HP system (see Section 2.4) has to adjust its operation to the demand subtracted from the thermal storages (see Section 2.6). The operation of HP and BH are determined by the controller of the HP unit (see Section 2.8). While operating, the HP system (HP and BH) is consuming electricity. The operation of the HP can be influenced by external signals (see Section 2.9). The electricity consumption of every single HP system coping with its very own load profiles can be cumulated to the overall pool operation and electricity consumption.

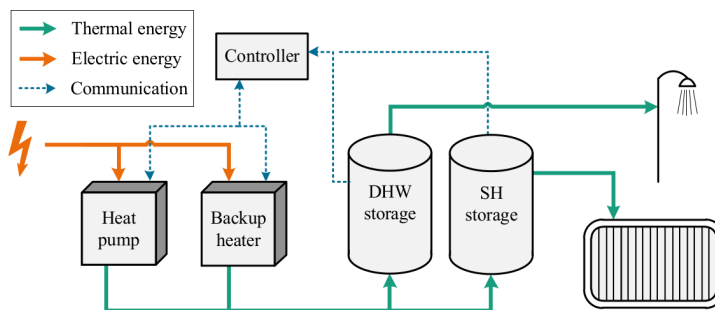


Figure 2.1: Simplified hydraulic layout of the system of a single heat pump as being used in the models. Source: [Fischer et al., 2016b, p. 855] (figure edited).

## 2.2 Thermal load profiles

In order to simulate the operation of a pool of HPs, it is necessary to know the thermal load the individual HP unit has to supply. For this purpose, the thermal load profiles of the buildings need to be generated. In the following, the functions of the models to generate these load profiles are outlined. Since it is not focus of this work to generate thermal load profiles, the ones generated and used for *Fischer et al. [2016b]* and *Wolf [2016]* are used for the further simulations and investigations conducted in this thesis. The definition and description of the pool used in the investigations of this work is presented in Section 3. The validation of the models can be found in *Fischer et al. [2016a]* and in *Wolf [2016, Section 3]*.

The thermal load profiles are generated using a stochastic bottom-up approach and are divided into DHW demand and SH demand. The load profile generation tool is called *SynPRO* and was developed in the department of the *Fraunhofer ISE*, where this master's thesis has taken place. According to the definition of the pools, these load profiles are generated and account for different properties of the individual house: climate data, type of building, level of refurbishment of the building and number of occupants and their type of employment. Due to the stochastic approach of this model, each house gets allocated

its own unique load profiles even in cases when several house have the same properties. [Fischer et al., 2016b, p. 855]

The DHW load profiles are calculated by using a combination of a behavioural model and a physical model. Based on data, the probability distributions for the duration, start and frequency of each DHW consumption have been modelled. Through a stochastic bottom-up approach, these probability distributions are used in order to generate a daily varying schedule of the DHW demand. This DHW demand is then converted into the related thermal DHW demand. [Fischer et al., 2016b, p. 855]

The thermal load profiles for SH are generated out of a combination of a physical and a behavioural model. The underlying models for SH load profiles account for different building physics by using *DIN EN ISO 13790 [2008]* with a 5R1C building model (the 5R1C building model reflects the thermal behaviour of a house by using 1 thermal capacity and 5 thermal resistances, see *DIN EN ISO 13790 [2008]* and especially its page 35 for further information). User behaviour, as well as solar gains, heat losses, ventilation and internal gains, are included in the models for the generation of SH load profiles. [Fischer et al., 2016b, p. 855]

## 2.3 Decision about heat distribution system

The heat distribution system of the building has a major impact on the required supply water temperatures of the HP system and consequently on the HP operation. The HP models can chose between a radiator system and a floor heating system. The heating curve (HC), which determines the required supply water temperature based on the ambient temperature, is different for each of the two heat distribution systems. In general, radiators require a higher supply water temperature. The HP models allocate a heating curve to each building based on its specific annual energy demand per square meter calculated from the thermal SH load profiles. After that, the heating curves are shifted upwards and downwards due a randomisation factor in order to depict the reality found in buildings. Moreover, the higher the specific annual energy demand per square meter, the higher the possibility that a radiator system and thus higher supply water temperatures are chosen by the HP model. The setpoint temperature for the supply water temperature for SH is determined by Equation 2.1, where the ambient temperature  $T_{\text{amb}}$  is used, as well as the coefficients  $a_i$ , which are different for each heating curve (the values for the coefficients  $a_i$  can be found in *Table 1* in *Fischer et al. [2016b, p. 855]*). [Fischer et al., 2016b, p. 856 & p. 858]

$$T_{\text{set}} = a_0 + a_1 T_{\text{amb}} + a_2 T_{\text{amb}}^2 \quad (2.1)$$

Equation 2.1 is only valid for ambient temperatures below 15°C. Furthermore, the specific annual energy demand is determining a threshold for the ambient temperature. If the three day averaged ambient temperature is below this threshold, SH for the house is activated. In comparison to older buildings, newer buildings activate SH at lower ambient temperatures due to their better insulation. [Fischer et al., 2016b, p. 858]

## 2.4 Heat pump models

The HP models distinguish between air-sourced heat pumps (ASHP) and ground-sourced heat pumps (GSHP). For each type of technology, the coefficient of performance (COP) is modelled by the quadratic Equation 2.2 and the thermal capacity of the HPs  $\dot{Q}_{\text{HP}}$  by the linear Equation 2.3. [Wolf, 2016, pp. 16-18]

$$COP = a_0 + a_1\Delta T + a_2\Delta T^2 \quad (2.2)$$

$$\dot{Q}_{\text{HP}} = a_3 + a_4T_{\text{source}} \quad (2.3)$$

The temperature difference  $\Delta T$  is calculated by subtracting the temperature of the HP source  $T_{\text{source}}$  from the temperature of the HP sink  $T_{\text{sink}}$ . The parameters  $a_i$  have been determined by regressions applied on manufacturer's data sheets. The regressions are presented in Figure 2.2.  $\Delta T$  and  $T_{\text{source}}$  are limited to the ranges depicted in this figure. [Wolf, 2016, pp. 16-18]

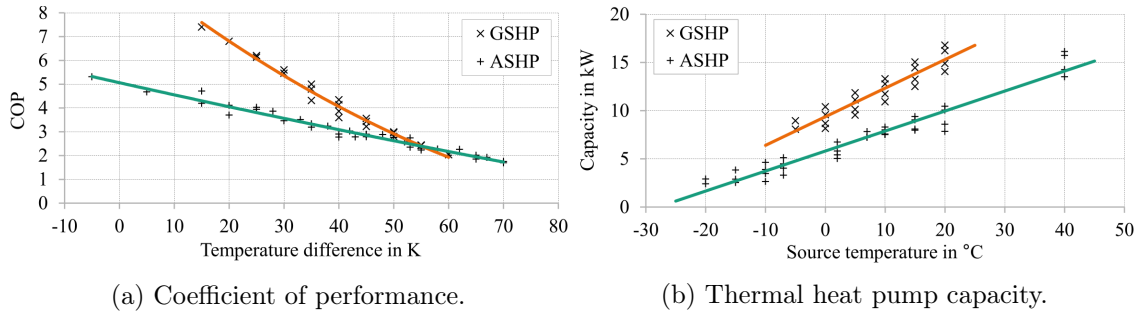


Figure 2.2: Regressions models used based on manufacturer's data in order to determine the coefficient of performance and the thermal heat pump capacity for air-sourced and ground-sourced heat pumps. Source: [Fischer et al., 2016b, p. 856] (figures edited).

The obtained  $COP$  of each HP unit is randomised in order to represent different performances of the HP units found in real data. The heat produced by the BH  $\dot{Q}_{\text{BH}}$  is modelled as the product of the electricity consumed by the BH and the fixed conversion efficiency equal to 0.99. [Fischer et al., 2016b, pp. 856-858]

## 2.5 Sizing of the heat pump systems

The HP capacity has to account for the thermal load required to be supplied at the lowest consulted temperature of the system, the bivalence/nominal temperature  $T_{\text{biv}}/T_{\text{nom}}$ . For ASHP, which are equipped with a BH, the bivalence temperature is used referring to the lowest temperature, at which the BH is not activated yet. For GSHP, which do not have a BH, the nominal temperature is used. The maximum SH demand is therefore called bivalence/nominal space heating load  $\dot{Q}_{\text{SH}}$ . Additionally, the HP has to supply the nominal DHW heat load,  $\dot{Q}_{\text{DHW,nom}}$ , which is calculated as the product of  $\dot{q}_{\text{DHW}}$  and  $n_{\text{pers}}$ .

$\dot{Q}_{\text{DHW}}$  was chosen based on recommendations to be 0.20 kW and  $n_{\text{pers}}$  is the number of occupants in the building. The nominal heating load  $\dot{Q}_{\text{HL,nom}}$  for GSHP is then calculated by Equation 2.4. For the calculation of the bivalence heating load for ASHP  $\dot{Q}_{\text{HL,biv}}$ , the same formula is used while  $T_{\text{nom}}$  is exchanged by  $T_{\text{biv}}$ . [Wolf, 2016, pp. 20-22]

$$\dot{Q}_{\text{HL,nom}} = f_{\text{block}} \left( \dot{Q}_{\text{SH}}(T_{\text{nom}}) + \dot{Q}_{\text{DHW,nom}} \right) \quad (2.4)$$

With this equation, the maximum capacity of the HP  $\dot{Q}_{\text{HP,nom}}$  is determined as being  $\dot{Q}_{\text{HL,nom}}$  for GSHP and  $\dot{Q}_{\text{HL,biv}}$  for ASHP.  $\dot{Q}_{\text{HP,nom}}$  is then randomised in order to account for over- and under-sizing as it has been found in real data (see *Figure 4* in *Fischer et al. [2016b]*). The factor  $f_{\text{block}}$  refers to the *blocking hours*. In Germany, lower electricity tariffs for HPs are offered, when the HP owner accepts that the electricity utility is able to switch his HP off (for instance in order to stabilise the local electricity grid). This can be done up to three times a day for a maximum of two hours each. The factor  $f_{\text{block}}$  is calculated with the aid of Equation 2.5, where  $n_{\text{block}} \in [0, 6]$  represents the number of blocking hours per day. [Wolf, 2016, pp. 20-22]

$$f_{\text{block}} = \frac{24 \text{ h}}{24 \text{ h} - n_{\text{block}}} \quad (2.5)$$

The sizing of the BH for ASHP systems is performed in the HP models according to Equation 2.6. The capacity of the BH has to account for the thermal load, that can be supplied by the HP alone no longer. Thus, the nominal load of the BH is calculated with the aid of the nominal heat load  $\dot{Q}_{\text{HL,nom}}$  and the HP power at the nominal temperature  $\dot{Q}_{\text{HP}}(T_{\text{nom}})$ . [Wolf, 2016, p. 22]

$$\dot{Q}_{\text{BH,nom}} = \dot{Q}_{\text{HL,nom}} - \dot{Q}_{\text{HP}}(T_{\text{nom}}) \quad (2.6)$$

## 2.6 Thermal storage models

The thermal storages for DHW and SH are represented by mixing tank models. They are modelled under the assumption, that the temperature inside the storage is homogeneous. The change in the storage temperature  $\Delta T_{\text{sto}}$  per timestep  $\Delta t$  is calculated with the aid of Equation 2.7, which is representing the energy balance of the respective storage. Here,  $C_{\text{sto}}$  represents the heat capacity of the building,  $kA$  is the total heat loss coefficient, the heat supply of the HP is  $\dot{Q}_{\text{HP}}$ , the heat supply of the BH is  $\dot{Q}_{\text{BH}}$  and the thermal demand is represented by  $\dot{Q}_{\text{demand}}$ . [Fischer et al., 2016b, p. 856]

$$C_{\text{sto}} \frac{\Delta T_{\text{sto}}}{\Delta t} = kA(T_{\text{room}} - T_{\text{sto}}) + \dot{Q}_{\text{HP}} + \dot{Q}_{\text{BH}} - \dot{Q}_{\text{demand}} \quad (2.7)$$

## 2.7 Sizing of the thermal storages

The sizing of the thermal storages is based on guidelines. The volume of the DHW storage  $V_{\text{DHW}}$  is defined by Equation 2.8, where  $n_{\text{pers}}$  is the number of occupants in the building and  $S$  represents a safety margin ranging from 1.0 l to 1.25 l. The value of  $S$  is increasing with a lower number of occupants, starting at  $S=1.0$  for 200 occupants. [Wolf, 2016, p. 23]

$$V_{\text{DHW}} = S \cdot 65.0 \cdot n_{\text{pers}}^{0.72} \quad (2.8)$$

The volume of the SH storage  $V_{\text{SH}}$  is based on the nominal heat pump power  $\dot{Q}_{\text{HP,nom}}$  and coefficients  $a_i$ , which were obtained from manufacturers' sizing recommendations. Equation 2.9 represents the formula used for the calculation of  $V_{\text{SH}}$ . [Fischer et al., 2016b, p. 857]

$$V_{\text{SH}} = a_0 + a_1 \dot{Q}_{\text{HP,nom}} \quad (2.9)$$

The storage sizes are randomised in order to account for over- and under-sizing found in real data [Fischer et al., 2016b, p. 858]. Moreover, the state of charge (SOC) of all storages is randomised for the start of the simulations as well.

## 2.8 Controls of the single heat pump

The single HPs are controlled by an on-off controller, as presented in Figure 2.1. The controller's aim is to keep the storage temperatures within the allowed temperature limits. The exact temperature limits per storage type within this work can be found in Table 2.1 in Section 2.9. The controller switches the HP on, when the thermal storage temperature reaches the lower boundary. The controller switches the HP off, when the thermal storage temperature reaches the upper boundary. Since the dynamic of the compressor of the HP is limited due to reliability issues, a minimum run-time of the compressor of 6 min and a minimum pause time of 3 min are guaranteed by the controller. In general, the demand from the DHW storage is prioritised. Moreover, the BH is switched on in times, when the thermal capacity of the HP is not sufficient. Depending on the exact states of the two storages, the controller supplies them differently and switches the BH on based on these states. For the detailed descriptions and conditions, it is referred to *Wolf [2016, pp. 19-20 & App. B]*. [Wolf, 2016, pp. 19-20]

## 2.9 External signals

The simulations carried out with the HP models described above are tailored for HPs operating in Germany. The *Bundesverband Wärmepumpen e.V. (BWP)* (German Heat Pump Association) has established a standardised interface for the purpose of triggering the individual HP externally. With this interface it is possible to send specified signals to

the individual HP and thereby alter the operation of the triggered HP. This approach of DLC can be used by (for instance) a central aggregator and is implemented into the HP models used within this work. This trigger-interface was established by the *BWP* as a label, called *SG-Ready*. The *SG-Ready* label is given to HPs fulfilling its specifications and having the standardised interface for external *SG-Ready* trigger signals. The regulations of *SG-Ready* demand, that the HP operation has to have four different modes. The HP has to alter its operation according to these modes. The four *SG-Ready* modes are: [Koch, 2013]

1. The HP is switched off. This can be done for a maximum duration of 2 hours and is related to the *blocking hours*.
2. The HP is running in its normal thermally driven mode.
3. The HP gets the recommendation to switch on. This is accompanied by increased operation of the HP for DHW and SH supply.
4. The HP has to switch on. This mode can be interpreted by the manufacturers in two different ways:
  - a) The HP is switched on actively.
  - b) The HP and its BH are switched on. The elevation of the setpoint temperatures of the thermal storages is optional.

As it can be seen, the *SG-Ready* labels leaves some degree of freedom about how to implement the trigger signals in detail. Within the HP models, the different *SG-Ready* signals are implemented as presented in Table 2.1. In the normal mode, the HPs are operating with the temperature boundaries [45.0°C, 52.5°C] for the DHW storage and [HC, HC + 5°C] for the SH storage, thus 5°C around the set temperatures determined by the building's heating curve (HC) for the current ambient temperature [Fischer et al., 2017]. An "Off" trigger signal switches the HPs off. The "On" signal switches the HPs on and is increasing the storage temperature boundaries by 5°C. The "Superheat" signals increase the storage temperature boundaries to maximum and switch the HPs on ("Superheat (HP)") or switches the HPs and the BHs on ("Superheat (HP+BH)"). It is implemented in the HP models, that the HP systems are following the trigger signals and change their storage temperature boundaries accordingly. For the case, that an activation/deactivation initiated by the trigger signal would force the HP to operate outside its current storage temperature boundaries, the trigger signal is ignored until the operation according to the signal can be performed within the current storage temperature boundaries. The interpretation of the *SG-Ready* signals as presented in Table 2.1 and used within this thesis is the same as used in *Fischer et al. [2017]*.

## 2.10 Validation of the heat pump models

The HP models used within this thesis have been validated. A detailed validation can be found in *Wolf [2016, pp. 25-32]*. The results of the validation are summarised in the following while the detailed reproduction of the validation process is spared here. The HP models have been validated with real data from over 100 HPs gathered in a field test. A randomisation of the sizing of the systems was required in order to obtain more valid results. The key performance indicators (KPI) for the validation have been chosen to be: Seasonal performance factor (SPF) (annual thermal energy demand of the building

SG-Ready name	Corresponding name in this thesis	Implementation in models	SH storage set temperatures in models	DHW storage set temperatures in models
Off (1)	Off	HP switches off.	[HC, HC + 5°C]	[45.0°C, 52.5°C]
Normal (2)	Normal	HP operates with normal set-points.	[HC, HC + 5°C]	[45.0°C, 52.5°C]
Recommended on (3)	On	HP switches on, hystereses are increased.	[HC + 5°C, HC + 10°C]	[50.0°C, 57.5°C]
Forced on (4a)	Superheat (HP)	HP switches on, temperatures increased to max.	[55°C, 60°C]	[52.5°C, 60.0°C]
Forced on with BH (4b)	Superheat (BH+HP)	HP and BH switches on, temperatures increased to max.	[55°C, 60°C]	[52.5°C, 60°C]

 Table 2.1: *SG-Ready* signals and their implementation in the heat pump models.

divided by the annual energy consumption of the HP system), operation hours of the HP and number of HP cycles. The results of this validation are presented in Table 2.2. The errors yielded in the mean values of the KPIs have been up to 5 %. Moreover, the ranges of the values of the KPIs were in the same ranges for the simulations and the field test data. Based on this investigation of the validation results, the HP models have been assessed to be valid. [Fischer et al., 2016b, pp. 857-858]

HP	Dataset	SPF			Operation hours			Cycles		
		Mean	Min	Max	Mean	Min	Max	Mean	Min	Max
ASHP	Meas.	3.2	2.3	4.3	2242	1298	4629	13.0	4.0	29.0
ASHP	Sim.	3.2	2.5	3.9	2240	1461	3626	13.5	6.4	25.9
GSHP	Meas.	4.1	3.0	5.4	2002	795	4044	11.0	3.0	26.0
GSHP	Sim.	4.2	3.2	5.2	2012	1468	3086	11.4	6.5	19.0

Table 2.2: Validation results for the simulated (Sim.) and the measured (Meas.) heat pump pool. The key performance indicators are: Seasonal performance factor (SPF), operation hours and on-off cycles per day. Source: [Fischer et al., 2016b, p. 858] (table edited).

### 3 The heat pump pool

This chapter is defining the HP pool as it is used within this master’s thesis. The pool composition is divided into two parts. First, the houses within the pool are defined. Secondly, based on the thermal load profiles of the houses in the pool, the HPs are sized (details about the thermal load profiles and the sizing procedure can be found in Section 2). The result is a pool, consisting of HPs operating according to the thermal load profiles of the respective houses and the external signals (see Section 2.9). Figure 3.1 illustrates the single steps taken in order to obtain HP pool and be able to analyse the operation of the HP pool. Note, that the HP operation can be altered by triggering and thereby deviate from the standard thermally driven operation, while using the same HP pool with the same sizing parameters.

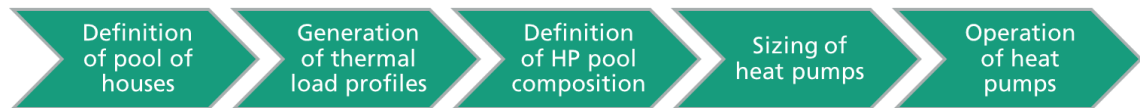


Figure 3.1: General steps taken in order to obtain the pool of heat pumps for the analysis of its operation.

Regarding the houses in the pool, this work is using the same composition as used in *Fischer et al. [2016b]*, *Fischer et al. [2017]* and *Wolf [2016]*. Based on this composition, thermal load profiles for the respective houses have been generated and used in the sources. This thesis is using the same thermal load profiles in order to determine the thermal demand of the buildings for SH and DHW.

In the following, the methodology for the houses’ pool composition as presented in detail in *Wolf [2016, Section 2.1 and 5.1]* is given. The pool of houses is representing the distribution of German houses equipped with HPs. As presented in Section 1.1, it is important to consider the operation of HPs in a representative pool, which also has to compromise of existing buildings. According to Platt et al. [2010, p. 41], 88 % of the German HPs were installed in single family houses (SFH), 10 % in terraced houses (TH) and 2 % in multifamily houses in 2010. Moreover, it was predicted for 2016, that 75 % to 85 % of the German HPs would be installed in new buildings and 15 % to 25 % in existing buildings [Gorris and Jacob, 2013, p. 42]. Furthermore, the share of ASHP in the German HP sales is increasing in recent years and reaches around 70 % for 2015, while GSHP has a share of around 23 % and ground water sourced HPs have a share of 7 % [Gorris and Jacob, 2013, p. 35].

Based on this information, *Wolf [2016]* derived the detailed composition of houses in the pool by age and level of refurbishment as presented in Table 3.1. In total, it was chosen to compose the pool out of 284 houses in order to allow analyses with representative subpools [Wolf, 2016, p. 33]. Due to their small share, multifamily houses have been neglected by

*Wolf [2016]*. Thus, the pool of houses consists of 88 % SFH and 12 % TH [Wolf, 2016, p. 34]. For the level of refurbishment, the classification "existing building" was chosen to be represented by thermal load profiles reflecting the thermal load of buildings built before 1978 or built between 1978 and 2002 [Wolf, 2016, pp. 33-34]. "New buildings" have been represented by thermal load profiles for buildings built after 2002 or with an advanced level of refurbishment (similar to a *passive house*) [Wolf, 2016, pp. 33-34]. The detailed number of houses as derived and defined by *Wolf [2016]* is given in Table 3.1 per building type (SFH or TH) and level of refurbishment. This composition of houses results in a share of 21 % existing buildings and 79 % new buildings [Wolf, 2016, p. 34]. Hence, the current distribution of HPs in German houses is reflected by this pool. Table 3.1 is also giving the mean annual specific energy demand per square meter  $\overline{ASHC}$  of the houses of the respective group as presented in [Wolf, 2016, p. 34]. It can be seen, that SFH have a higher thermal load per m<sup>2</sup> due to their higher area of walls adjacent to the ambient.

Type	Age	Number	Building			
			$\overline{ASHC}$ [ $\frac{\text{kWh}}{\text{m}^2\text{a}}$ ] <sup>1</sup>	SH demand range [kWh]	DHW demand range [kWh]	HP electricity consumption range [kWh]
SFH	before 1978	25	233	[27835, 39954]	[2516, 4062]	[7851, 17019]
	1978-2002	25	144	[17770, 26339]	[2511, 4171]	[6013, 10323]
	after 2002	100	81	[10791, 17968]	[2511, 4171]	[3956, 8196]
	advanced	100	55	[7347, 12530]	[2467, 4203]	[3065, 6296]
TH	before 1978	5	166	[21545, 23332]	[2804, 3231]	[6002, 9548]
	1978-2002	5	108	[12833, 17914]	[2237, 3941]	[4446, 7423]
	after 2002	12	74	[8650, 11759]	[2844, 3930]	[3498, 5738]
	advanced	12	51	[6052, 9345]	[2257, 3939]	[2642, 4495]

<sup>1</sup> values taken from *Wolf [2016, p. 34]*

Table 3.1: Composition of the heat pump pool by age and type of building. Composition of the houses is taken from *Wolf [2016]*.

Based on this composition of houses, thermal load profiles for each house of the pool have been generated by *Wolf [2016]*. The generation is conducted via the stochastic bottom-up model *SynPRO* as describes in Section 2.2. The generation of the thermal load profiles used the representative weather data given by the test reference year (TRY) 2015 for Potsdam, Germany, as provided by the *Deutscher Wetterdienst (DWD)* [Wolf, 2016, p. 36]. The ambient temperature in this data is presented in Figure 3.2. The x-axis of this figure shows the day of the year, the y-axis presents the respective hour of the day. The colourbar on the right side of Figure 3.2 indicates the temperature associated with the respective colour. Figure 3.2 presents cold temperatures in winter, high temperatures in summer and a wide range of temperature within single days in the changing season. The thermal load profiles generated by *Wolf [2016]* are used within this work. The thermal demands for SH and DHW as found in the range of thermal load profiles are presented in Table 3.1. It can be seen, that the building type and the level of refurbishment have a high impact on the SH demand. Thus, newer buildings adjacent to other houses (TH) show lower SH demands. The amount of DHW demand is not as affected by the level of

refurbishments, since it is mostly determined by the number of occupants in the houses and their behaviour. The ranges in the values presented in Table 3.1 represent the ranges determined by the minimum and the maximum values found in the pool for the respective building type and age.

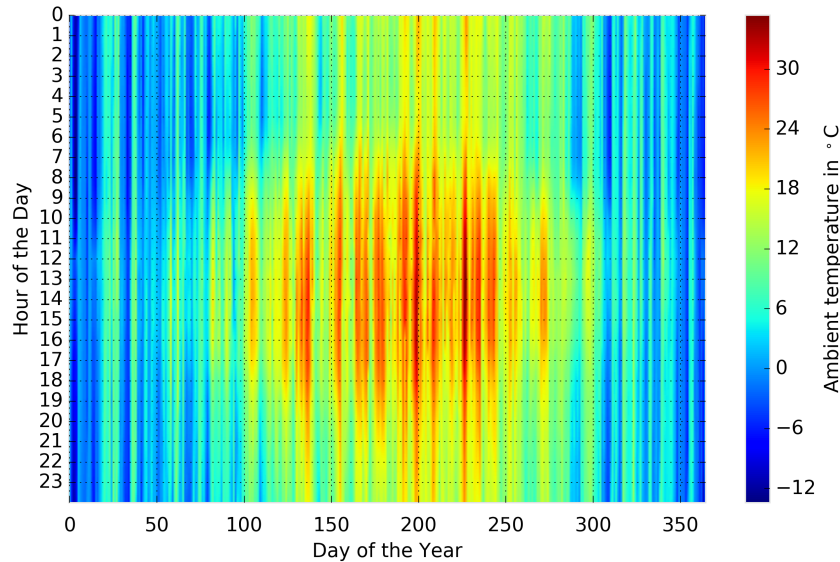


Figure 3.2: Ambient temperature of the test reference year 2015 for Potsdam, Germany.

Based on these thermal load profiles for SH and DHW demand created by *Wolf [2016]*, the electrically driven HPs and their storages are sized as described in Section 2. While sizing the individual HPs based on their respective thermal load profiles, several parameters are randomised. Within this master's thesis, the simulation framework for the HPs has been extended in order to enable the saving of the HPs' sizing parameters. Thus, it is possible to simulate different scenarios with the exact same HP pool, since the sizing procedure with its associated randomisation is not conducted each time again. When sizing the HPs, the simulation framework decides randomly whether an ASHP or a GSHP is chosen in order to cover the associated SH and DHW profiles. This decision is taken via a uniform distribution. Here, the same distribution of 75 % ASHP and 25 % GSHP as defined in *Wolf [2016, p. 34]* is chosen. The share of ground water source in the German HPs was neglected [*Wolf, 2016, p. 33*]. The ranges for the electricity consumption of the HPs for the thermally driven operation are presented in Table 3.1. It can be seen, that the age and the type of the building is affecting the thermal demand of the houses and thereby the electricity demand of the respective HPs as well. Thus, older buildings with more walls adjacent to the ambient show a higher electricity consumption in order to provide the required heat by using their HPs.



# 4 Analysis of the uninfluenced heat pump pool operation

This chapter investigates the standard operation of the HP pool. All simulations are conducted with a resolution of 1 min. Section 4.1 investigates the thermally driven operation of the pool of HPs. Based on this investigation, the standard load profile (SLP) of the pool is derived in Section 4.2. The SLP is taken as one of the references for the assessment of the subsequent optimisation (see Section 5). The deviation of the thermally driven operation from the SLP is analysed in Section 4.3. After that, the day-ahead spot market price is analysed together with the costs of electricity consumption when operating the HP pool (see Section 4.4). Moreover, the load shifting potential of the pool is presented in Section 4.5. For all investigations carried out, the HP pool as defined and composed in Section 3 is used.

## 4.1 Thermally driven operation

This Section is analysing the thermally driven operation as determined by the provision of the thermal demand of the buildings in the pool. For the determination thermal demand, the SH and DHW load profiles as described in Section 3 are used. The HPs in the pool are sized and operate according to these profiles. The pool operation investigated here is not influenced by any external signals. Thus, the internal controller of the individual HPs are not triggered externally and maintain the thermal storages within their boundaries of  $[HC, HC + 5^{\circ}\text{C}]$  for SH and  $[45.0^{\circ}\text{C}, 52.5^{\circ}\text{C}]$  for DHW (note that the temperatures of the individual SH storages are dependent on the respective heating curve, see Section 2.9). As described in Section 2.9, the internal controller activates the HP only, when one of the temperatures of the two thermal storages reach the lower boundary. When activated, the HP heats the respective storage, until the temperature reaches the upper boundary. Within this work, the controller will always heat the thermal storages from their lower to their upper temperature boundaries. Thus, the thermally driven operation reflects the most energy-efficient operation possible within this work. Less energy can only be consumed, if operating the storages at lower temperatures (for instance: lower storage temperature boundaries, not conducting a full heating cycle from the lower to the upper temperature boundary, *etc.*), which is not considered within this thesis.

In the following the analysis of the thermally driven operation is given. Figure 4.1 presents the electricity consumption of the HP pool over the course of the year. The highest level of electricity consumption can be found in the coldest winter days. Moreover, it can be seen, that the electricity consumption is very small in summer compared to the amount reached in winter. In the changing season, the level of electricity consumption shows the highest variety over the course of the day. In winter, the consumption decreases during midday. Moreover, the consumption is increased during the morning hours in summer. It

can be concluded, that due to high ambient temperatures, the consumption in summer is only caused by DHW, while the consumption in winter is mostly dominated by the SH demand.

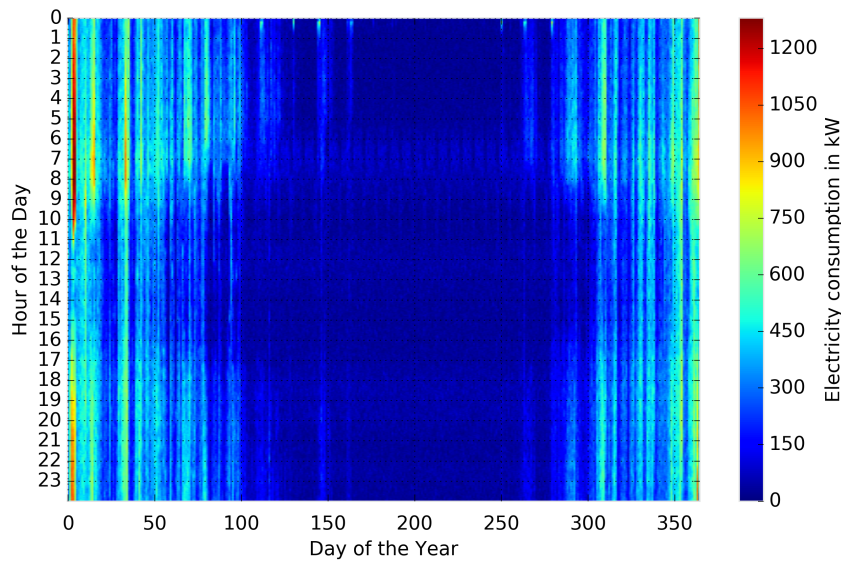


Figure 4.1: Electricity consumption of the pool of heat pumps in the thermally driven operation.

When analysing the thermally driven operation further, it is found, that the maximum amount load of the HP pool is 1280.69 kW. This value is reached at 08:13 o'clock at the 4<sup>th</sup> of January. Within this minute the highest energy demand of 21.34 kWh is consumed by the HP pool. This high consumption is caused by the high thermal demand due to the low ambient temperatures. At this point, 279 of the 284 HPs are active, while some are even using their BH in order to provide the required thermal demand. The highest dynamic of the pool operation is found at 01:00 o'clock at the 11<sup>th</sup> of May. At this timestep, the absolute change in the electricity consumption is the highest observed. Here, the electricity consumption increases by 456.65 kW within one timestep of 1 min. This increase corresponds to an increase of 36.4 % compared to the maximum electricity consumption of the pool in 2015. The HP pool consumes an amount of 1,703,132.3 kWh in total over the whole year. Figure 4.2 presents the electricity consumption of the HP pool for both, a representative winter day (20<sup>th</sup> of January) and a representative summer day (19<sup>th</sup> of July). It can be seen, that especially in winter, a high dynamic in the pool's electricity consumption can be observed. Thus, the level of electricity consumption can change remarkably within a single timestep of 1 min. In Figure 4.2, the electricity consumption in the winter day drops from around 400 kW before 09:00 o'clock to around 215 kW within one hour.

The analysis is now focussing on the average progress of the electricity consumption of the HP pool over the course of the day. The following two figures show, how the electricity consumption is changing within a day in average. The data is obtained by grouping the HP pool load by the minute of the day for the respective season. Thus, Figure 4.3 and 4.4 show the typical daily electricity consumption pattern in winter (December, January,

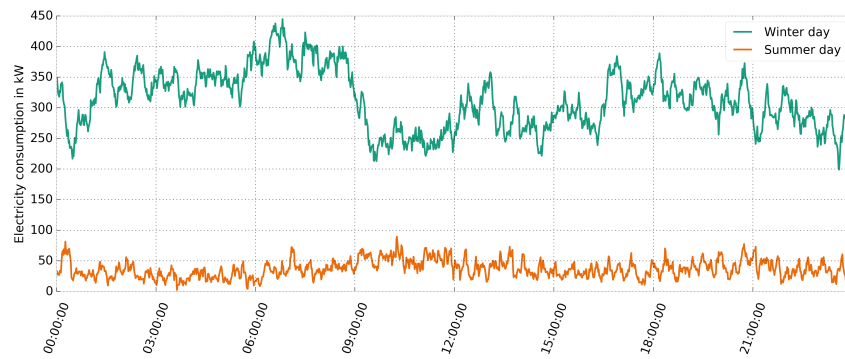


Figure 4.2: Electricity consumption of the pool of heat pumps in the thermally driven operation. The operation is depicted for a representative winter day and a representative summer day.

February) and summer (June, July, August), respectively. The yellow line indicates the mean electricity consumption. Hence, the yellow line in Figure 4.3 is presenting the mean course of the electricity consumption in winter days. The petrol-green shapes indicate the different ranges in quantiles (q0-q100, q10-q90, q20-q80, q30-q70, q40-q60). The darker colour of the shape, the smaller is range of quantiles, thus the smaller is the number of days included in this shape. Figure 4.3 shows, that the mean ranges from around 300 kW to 500 kW. The mean consumption is the highest in the morning hours around 7 o'clock (around 500 kW) and the lowest in the afternoon (around 300 kW). This is caused by the fact, that the ambient temperatures are the highest in the afternoon in winter as presented in Figure 3.2. Therefore the SH demand of the buildings is lower in the afternoon compared to the morning. Moreover, it can be seen in Figure 4.3, that the variety of electricity consumption is high in winter. Thus, the amount of consumption covered by the q0-q100 quantile ranges from close to 0 kW to around 1250 kW and shows a less steady course over the day compared to the mean consumption line. Moreover, the narrower quantile ranges (q10-q90, q20-q80, q30-q70, q40-q60) deviate less from the mean consumption as the q0-q100 range. This indicates, that only a small number of days are deviating much from the mean, while 80 % of the days cover a range of consumption which is similar to

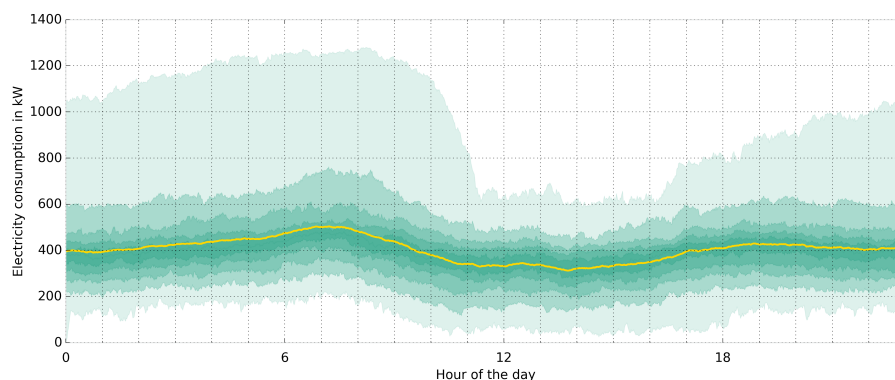


Figure 4.3: Average electricity consumption of the heat pump pool for the thermally driven operation in winter (December, January, February). The mean progress over the day is represented by the yellow line. The petrol-green shapes indicate ranges of the quantiles within the mean day (q0-q100, q10-q90, q20-q80, q30-q70, q40-q60).

the mean consumption. The majority of the winter days (q30-q70) shows a consumption curve, that differs little from the mean consumption and is represented by a small band around the mean line in Figure 4.3.

Regarding the average electricity consumption of the HP pool in summer, as presented in Figure 4.4, the electricity consumption shows values ranging from 0 kW to around 420 kW. The mean consumption line ranges from around 30 kW to around 70 kW. The highest values are observed in the morning hours around 8 o'clock. Compared to a typical winter day (see Figure 4.3), Figure 4.4 presents a lower electricity consumption in summer, which is mainly caused by the DHW demand. Thus, the highest amount can be seen in the morning, when DHW demand for taking a shower and other hot water applications is the highest. 80 % of the summer days (q10-q90) differ sparsely from the mean consumption line. Thus, the daily DHW demand in summer is following a certain pattern. Only 20 % of the days show a wider range in the electricity consumption that is mainly occurring in the early hours of the day. This is caused by the SH demand to be covered in some of the summer days by some of the HPs. This SH demand leads to the high amount of electricity demand at night as observed in Figure 4.4.

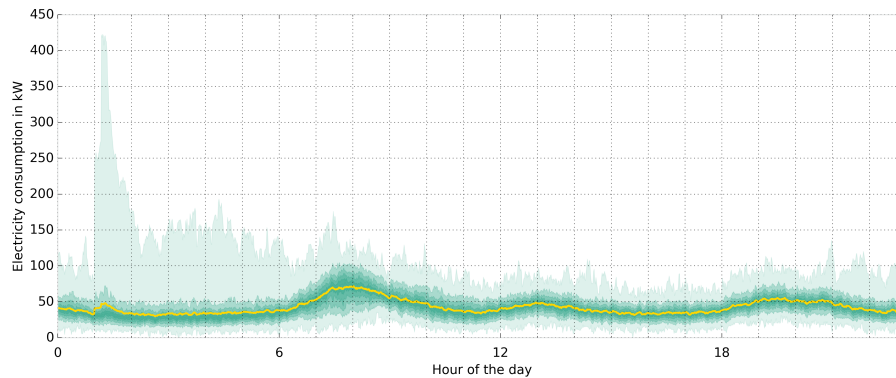


Figure 4.4: Average electricity consumption of the heat pump pool for the thermally driven operation in summer (June, July, August). The mean progress over the day is represented by the yellow line. The petrol-green shapes indicate ranges of the quantiles within the mean day (q0-q100, q10-q90, q20-q80, q30-q70, q40-q60).

## 4.2 Standard load profile

The standard load profile (SLP) (German word: Standardlastprofil) is a profile representing the expected operation of units. For HPs, the SLP is representing the thermal demand of a certain number of HPs. By using SLPs, grid operators are able to predict the grid load originating from different consumers. Moreover, the electricity consumption for the HPs is purchased according to the SLP [Hartmann et al., 2003, p. 1]. The SLPs are varying locally due to changes in ambient temperature and local HP system compositions and distributions. This section is deriving the SLP for the HP pool considered and is analysing its operation.

### 4.2.1 Derivation of the standard load profile

The methodology to derive SLPs has been described in the *Lastprofilen für unterbrechbare Verbrauchseinrichtungen - Praxisleitfaden* published by the *Verband der Netzbetreiber e.V. (VDN)* as referred by *Hartmann et al. [2003]* (Note that this association and its works can now be found under the name *Forum Netztechnik/Netzbetrieb (FNN)* in the *Verband der Elektrotechnik, Elektronik und Informationstechnik (VDE)* and the *Bundesverband der Energie- und Wasserwirtschaft (BDEW)*). Based on this regulation, the local distribution system operator (DSO) has to publish a temperature-dependent load profile set of curves for his area [Hartmann et al., 2003, p. 2]. Since the thermal load profiles for the HP pool of this work are generated by using the TRY weather data for Potsdam in 2015, the corresponding load profile set of curves has to be taken in order to derive the SLP for this HP pool. Since no suitable data was available from the DSO of Potsdam during the conduction of this thesis, the HP load profile set of curves for Berlin is chosen. By using the data for Berlin, it is assumed, that Berlin and Potsdam are sharing the same course of temperatures and that the local composition and distribution of HP systems is the same. This assumption is propped by the facts, that Berlin and Potsdam are located close to each other and are sharing the same climate zone (see the map of the German climate zones in *Bundesamt für Bauwesen und Raumordnung (BBR) in Zusammenarbeit mit der Climate and Environment Consulting Potsdam GmbH und dem Deutschen Wetterdienst [2012, p. 18]*). The data for the determination of the SLP of the HPs is found on the website *Stromnetz Berlin GmbH [2016a]* and can directly be assessed over the link in *Stromnetz Berlin GmbH [2016b]*. The data is valid for the operation of HPs in Berlin since 2013 and the associated *Excel*-file is submitted together with this thesis. In the following, the procedure in order to obtain the SLP based on the load profile set of curves is described.

Since the load profile set of curves is a temperature dependent set of scaled curves describing the load profile for the course of one day, the set of curves needs to be derived for the respective weather data and HP pool. In the first step, the daily mean ambient temperature  $T_m$  has to be calculated for each day [Hartmann et al., 2003, p. 4]. This calculation is performed for the weather data used for the generation of the buildings' thermal load profiles as presented in Section 3. By the aid of the mean ambient temperature of the day  $T_m(d)$ , the equivalent daily ambient temperature  $T_{m,eq}$  is calculated by using Equation 4.1. [Verband der Netzbetreiber, 2004, p. 7]

$$T_{m,eq}(d) = 0.5 \cdot T_m(d) + 0.3 \cdot T_m(d-1) + 0.15 \cdot T_m(d-2) + 0.05 \cdot T_m(d-3) \quad (4.1)$$

The calculation of  $T_{m,eq}$  for each day  $d$  is using the mean temperatures of the previous days, weighted based on their currentness respectively. By this, the impact of the weather of the previous days on the thermal capacity of the building is taken into account as well. After calculating the daily equivalent ambient temperatures, the *Temperaturmaßzahl TMZ* (temperature characteristic number) is determined. By doing this, the equivalent daily temperature is normed to a reference temperature  $T_{ref}$ . The calculation of the *TMZ* is presented in Equation 4.2. [Hartmann et al., 2003, p. 4]

$$TMZ = \max(T_{\text{ref}} - T_{\text{m,eq}}; 1 \text{ K}) \quad (4.2)$$

By the aid of this equation, the  $TMZ$  is calculated for each day, by taking the maximum of the difference between the reference temperature and the equivalent ambient temperature of the respective day and 1 K.  $T_{\text{ref}}$  is a constant and for the data used defined to be  $T_{\text{ref}} = +17^\circ\text{C}$  [Stromnetz Berlin GmbH, 2016a]. The load profile set of curves used is valid for an ambient temperature of at least  $-15^\circ\text{C}$  [Stromnetz Berlin GmbH, 2016a]. For ambient temperatures above  $17^\circ\text{C}$ , the  $TMZ$  has to be used [Stromnetz Berlin GmbH, 2016a], as defined by Equation 4.2. *Stromnetz Berlin GmbH [2016b]* provides a time series of the HP load for the respective  $TMZ$  values. This data has a resolution of 15 min representing the average HP load over the course of 15 min. After obtaining the time series of the SLP for the whole year, the data needs to be scaled in order to represent the actual HP. In the case of this thesis, the consumption of the whole HP pool is used for the scaling. The scaling is conducted via a scaling factor  $s$  as described in Equation 4.3. [Hartmann et al., 2003, p. 5]

$$s = \frac{\sum(p_{\text{el}})}{\sum(TMZ)} \quad (4.3)$$

This equation uses the annual energy consumption of the HP pool  $\sum(p_{\text{el}})$  and the sum of the  $TMZ$ . For  $\sum(p_{\text{el}})$ , the annual electricity consumption of the thermally driven operation of 1,703,132.3 kWh is used. Then, this value is divided by the sum of  $TMZ$  calculated to be 3120 K. The yielded scaling factor is then multiplied with the time series for the SLP. The obtained SLP of the HP pool is analysed in the following section. Its annual electricity consumption amounts to 1,645,436.3 kWh. The deviation from the consumption of the thermally driven operation of around 3.4 % is assessed to be small enough in order to accept the obtained SLP.

#### 4.2.2 Analysis of the standard load profile

When analysing the SLP for the HP pool yielded by the calculations described in Section 4.2.1, the profile shows a steady operation over the course of the day. This is illustrated in Figure 4.5. It can be seen, that the load is constant during one day and only changing from day to day. Thus, *Stromnetz Berlin GmbH [2016a]* is assuming, that fluctuations in the electricity consumption of the HP pool are not occurring during the day. The SLP shows the highest electricity consumption in winter, while still varying during winter. A moderate load can be seen for the changing season. In summer, the electricity consumption remains on a low level. Over the course of the year, a range between around 34 kW and around 665 kW is observed for the load of the HP pool.

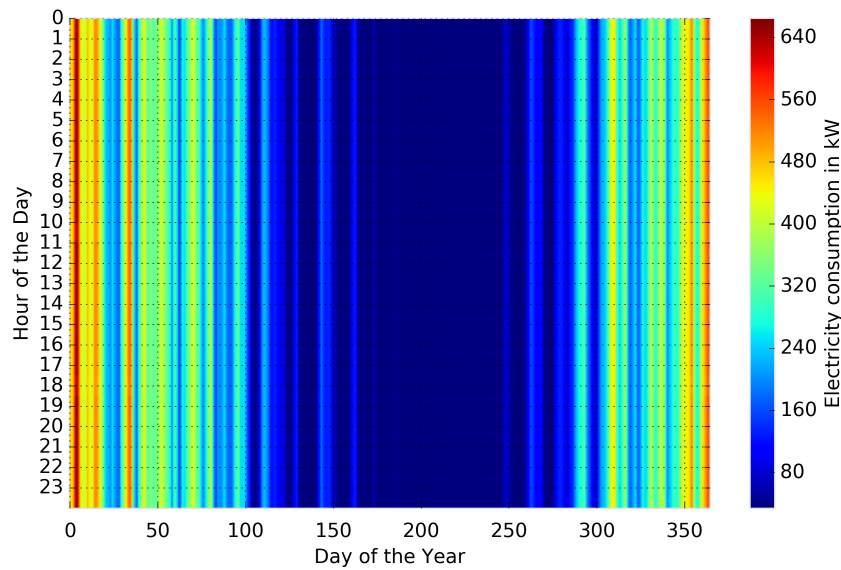


Figure 4.5: Electricity consumption of the pool of heat pumps for the standard load profile.

### 4.3 Difference between both operations

This Section analyses the differences between the thermally driven HP pool operation (see Section 4.1) and the pool operation represented by the SLP (see Section 4.2). The analyses have shown that the SLP operation is steady over the course of the day, while the thermally driven operation is changing, as presented in Figure 4.1 and 4.5. The annual duration curve (see Figure 4.6) is analysing the HP pool load over the course of the year by presenting the loads in descending order. By losing the information about the time each load occurs, the durations of each particular load level is displayed. Hence, each level of load and especially peaks can be assessed duration-wise.

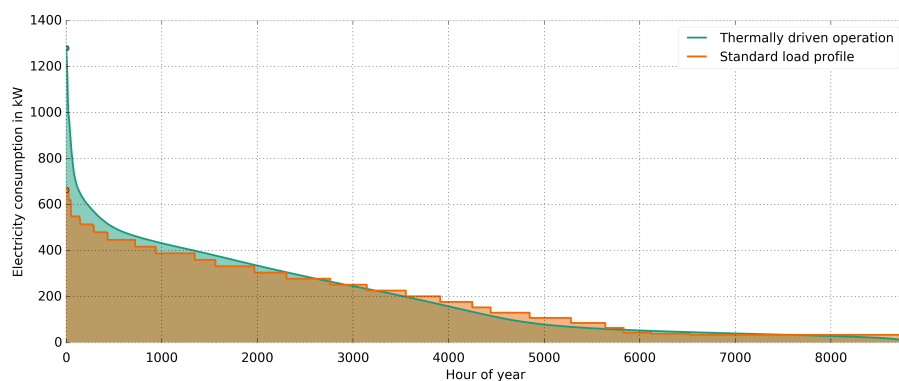


Figure 4.6: Annual duration curves of the electricity consumption of the heat pump pool for the thermally driven operation and for the standard load profile.

Figure 4.6 highlights, that the thermally driven operations shows high electricity consumption values for a short time of the year. These values reflect the peak consumption during the coldest days of the year. Moreover, the duration curve of the thermally driven operation is continuously descending. One third of the year is represented by a load lower

than 100 kW. In contrast, the annual duration curve of the SLP operation is illustrated by descending steps. These steps represent the various levels of the HP pool load as determined by the load profile set of curves used for the calculation of the SLP (for the calculation of the SLP see Section 4.2.1). Again, around one third of the year has a load below 100 kW. The comparison between the annual duration curves of the thermally driven and the SLP operation shows, that the peak loads in the thermally driven operation are higher. Thus, the highest loads observed in the thermally driven operation are not reproduced by the SLP. Moreover, the annual duration curve of the SLP shows higher durations of moderate HP pool loads compared to the thermally driven operation's annual duration curve. Hence, the SLP does not reflect the highest loads, while compensating this lower electricity consumption by increasing the times of moderate loads over the course of the year. This observation is supported by Figure 4.7, which is presenting the difference between the SLP and the thermally driven operation.

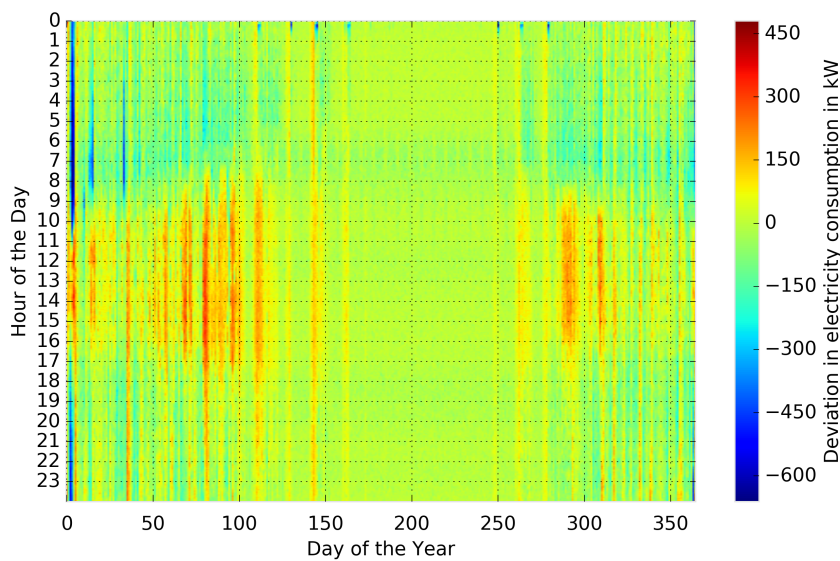


Figure 4.7: Deviation of the thermally driven operation from the standard load profile illustrated by the deviation of the heat pump pool's electricity consumption.

In times, where the SLP operation has a higher electricity consumption compared to the thermally driven operation, Figure 4.7 shows positive values. It can be seen, that the SLP suggests higher loads during midday in the changing season. These times cause the higher durations of moderate loads as presented in Figure 4.6. Figure 4.7 illustrates, that the highest peak loads, which are not represented by the SLP, are occurring during the coldest days of the year in January and February. Figure 4.8 presents the typical operations over the course of the day for the SLP and the thermally driven operation. The mean thermally driven operation is illustrated by the yellow line, while the petrol-green shapes indicate the quantiles obtained. The grey line in Figure 4.7 represents the mean SLP operation and the orange shapes indicate the associated quantiles. It can be seen, that the SLP operation is steady, while the thermally driven operation usually peaks in the morning, while being lower during midday compared to the rest of the day. The quantiles for the SLP and the thermally driven operation are representing the same patterns as their means.

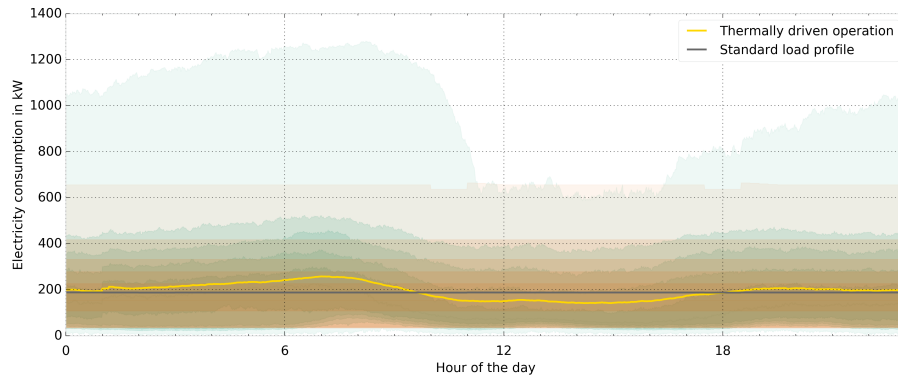


Figure 4.8: Average electricity consumption of the heat pump pool for the thermally driven operation and the for standard load profile operation for the whole year. The mean progress over the day is represented by the yellow (thermally driven operation) and grey (standard load profile) lines. The petrol-green (thermally driven operation) and orange (standard load profile) shapes indicate ranges of the quantiles within the mean day (q0-q100, q10-q90, q20-q80, q30-q70, q40-q60).

The results presented within this section show, that the thermally driven operation is deviating significantly from the SLP when analysing the intra-day operation. A larger pool of HPs to be considered in this work would smooth out the fluctuations over a short period of time as presented in Figure 4.2. However, the average daily pattern of the operation as being illustrated by the mean line of the thermally driven operation in Figure 4.7 is expected to be still present for a larger pool of HPs. Additionally, the SLP is not able to depict change in the intra-day HP pool operation, but is reflecting the mean operation of the day.

## 4.4 Costs of operation

In this master's thesis, the electricity costs are analysed based on the day-ahead spot market prices for the case of Germany. In this context, the *EPEX* day-ahead spot market prices for electricity for Germany are used as they can be found on the *EPEX* website (<http://www.epexspot.com/en/>). The data analysed is taken from the year 2015. This Section gives an analysis of the day-ahead electricity prices. Moreover, the costs of electricity consumption associated to these prices are presented here as well.

When analysing the day-ahead electricity prices in 2015, a wide range of values is observed. Figure 4.9 presents the prices over the course of the year and days. It can be seen, that the prices range from around -70 Euro/MWh to around 90 Euro/MWh. Moreover, the price is the highest in the morning and evening. Over the course of the year, this pattern remains. In the changing season, negative electricity prices occur, while they are positive most of the time.

Figure 4.10 presents the mean course of the day-ahead price for the whole year. This figure further illustrates the daily pattern with high prices in the morning and evening. Moreover, it can be seen, that 80 % of the days have a electricity price similar to the mean price. This mean price ranges from around 20 Euro/MWh to 40 Euro/MWh over

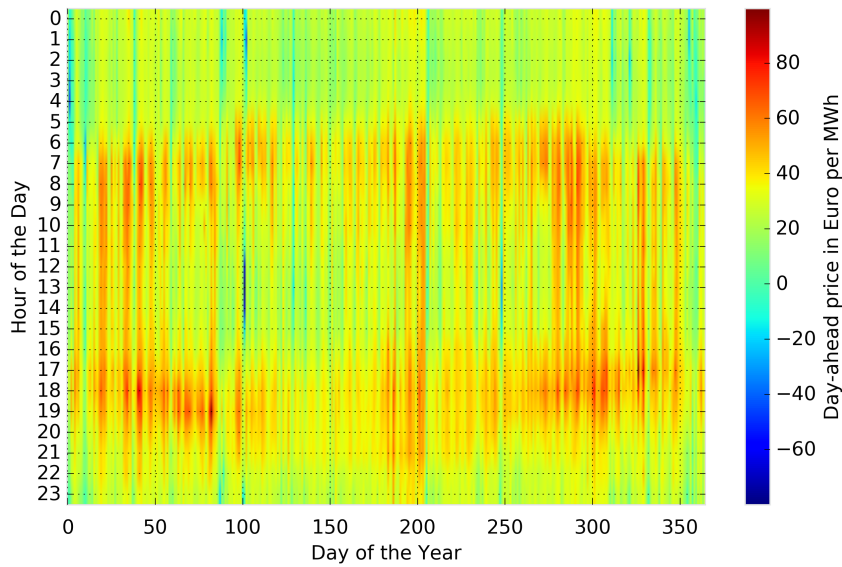


Figure 4.9: Day-ahead *EPEX* spot market price for electricity in 2015.

the course of the day. Only the quantile range q0-q100, which includes all days, shows negative prices. Thus, as illustrated by Figure 4.9, negative electricity prices occur rarely. However, in times when prices are negative, they reach high negative values.

As described in Section 1.2, this thesis uses the electricity consumption costs obtained by using the SLP as one of the reference costs for all further analyses. Moreover, the costs associated with the thermally driven operation form the second reference. Thus, the costs are calculated by matching the SLP/thermally driven operation load of the respective minute with the associated day-ahead spot market price. In the following the electricity costs of operation are analysed and the differences between thermally driven and SLP operation are highlighted.

When calculating the electricity consumption costs for both operations as described above, the annual electricity consumption costs for the thermally driven operation are higher. The

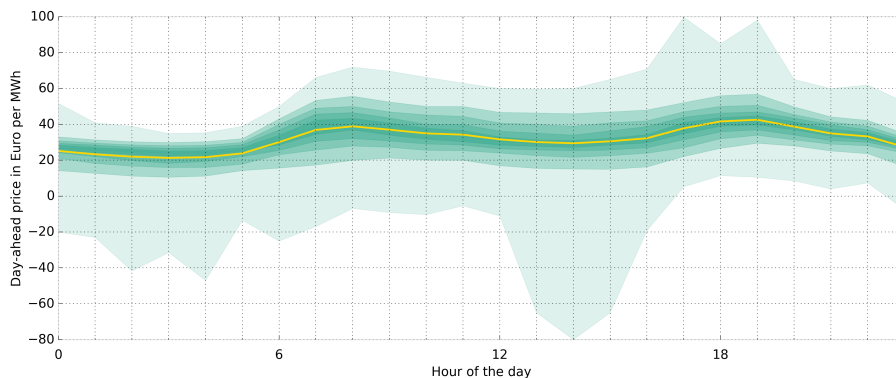


Figure 4.10: Average *EPEX* day-ahead spot market price for electricity in Germany for the whole year. The mean progress over the day is represented by the yellow line. The petrol-green shapes indicate ranges of the quantiles within the mean day (q0-q100, q10-q90, q20-q80, q30-q70, q40-q60).

annual electricity costs for the thermally driven operation amount to around 53522.3 Euro and the electricity costs for the SLP sum up to around 51806.4 Euro for the operation over the course of the whole year. The difference between the costs of the thermally driven and the SLP operation is caused by the correlation between high prices and electricity consumption in the morning hours (compare Figure 4.10 and 4.8). Hence, days with a high variety of load in the thermally driven operation lead to high deviations from the electricity costs of the SLP, when daily electricity consumption patterns are correlating well with the respective daily pattern of the day-ahead electricity price. This relation is illustrated by Figure 4.11, which shows the calculated electricity consumption costs in Euro per hour. Here, the mean costs of the thermally driven operation (yellow line) are higher in the morning hours and lower during midday compared to the mean SLP operation (grey line). Moreover, the ranges of the thermally driven operational electricity costs are peaking in the morning and evening as presented by the quantiles in Figure 4.11 (petrol-green shapes). In comparison, the SLP operational electricity costs are steady in a high level during day, when analysing the q0-q100 quantile range (light orange shape). The comparison of the narrower quantiles of the thermally driven and the SLP operation show, that the costs of electricity consumption are higher in the morning and lower during midday for the case of the thermally driven operation. When now considering the peaks of the day-ahead electricity price as presented in Figure 4.10, the cause of the deviation in electricity consumption costs is identified.

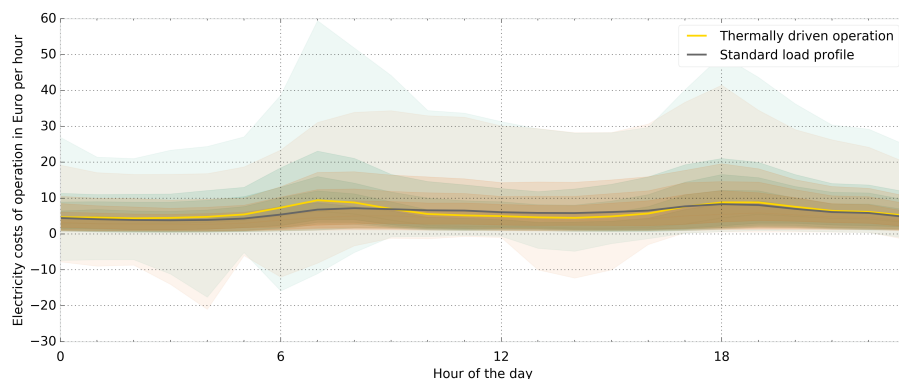


Figure 4.11: Average electricity consumption costs of the heat pump pool for the thermally driven operation and for the standard load profile operation for the whole year. The values are shown as costs in Euro per hour. The mean progress over the day is represented by the yellow (thermally driven operation) and grey (standard load profile) lines. The petrol-green (thermally driven operation) and orange (standard load profile) shapes indicate ranges of the quantiles within the mean day (q0-q100, q10-q90, q20-q80, q30-q70, q40-q60).

Figure 4.12 presents the cumulated costs of electricity consumption for both operations over the course of the year. The electricity costs of operation are low during summer and the highest in the coldest months, as depicted by the slopes in Figure 4.12. Moreover, the thermally driven operation yields higher costs in mid-February, which are afterwards compensated by the SLP operation in April. In the mid-November and the whole December, the thermally driven operation leads to higher electricity consumption costs, which cause the difference in the annual costs.

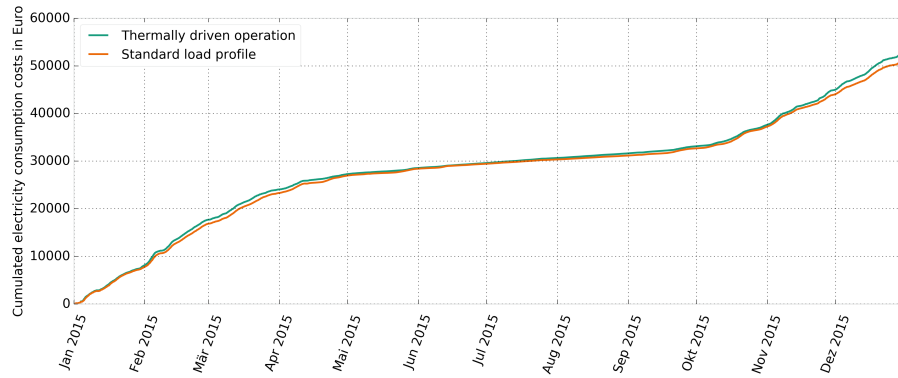


Figure 4.12: Cumulated costs of electricity consumption for the thermally driven and the standard load profile operation.

Figure 4.13 presents the deviation in the electricity costs of operation in detail. By analysing this figure, the reasons for the deviation in the cumulated costs becomes visible. In mid-February, Figure 4.13 shows highly negative values in the morning, which means that the electricity costs of the thermally driven operation in this time are much higher than the ones of the SLP operation. This is caused, by a high load in the thermally driven operation in the morning hours (see Figure 4.7) combined with high electricity prices in the morning (see Figure 4.9). In April, the relatively higher load of the SLP operation during midday is not compensated in the morning (see Figure 4.7). Consequently, the deviation in the cumulated electricity consumption costs between both operations is nearly balanced at the end of April. From mid-November over the whole December, the thermally driven operation is having a higher load over the course of the day than the SLP operation, since the higher load in the morning is not compensated in the midday (see Figure 4.7). Thus, Figure 4.13 shows dominantly negative values for this timespan and hereby explains the deviation in the annual electricity consumption costs between both operations.

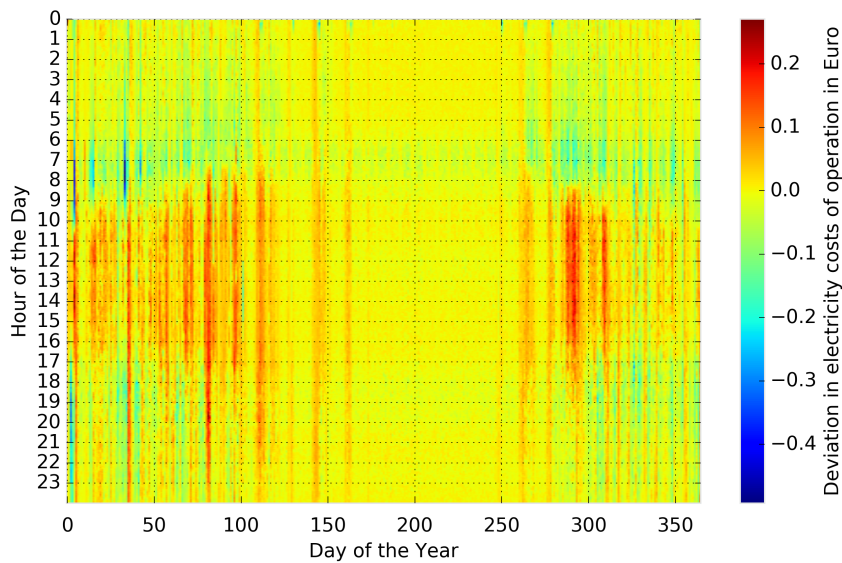


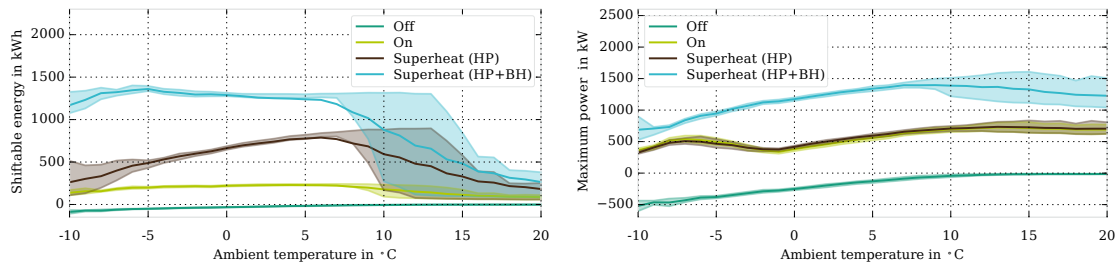
Figure 4.13: Electricity consumption costs for the deviation between the thermally driven and the SLP operation. Note, that the values represents the deviation in costs per minute.

The results presented suggest, that it is beneficial for the pool aggregator to operate the HP pool according to the SLP compared to the normal thermally driven operation. However, it should be noted, that this thesis is not investigating the tariff structures behind the SLP operation. Thus, the formation of the SLP oriented tariffs offered and how they are benefiting from the electricity consumption costs presented, are not treated here. Consequently, the following consideration of this thesis are using the electricity consumption costs of both, the thermally driven operation and the SLP operation. Moreover, as it is presented by Figure 4.11, every economic optimisation of the HP pool operation should aim to shift the high peak loads in the morning hours towards the midday or night hours. Moreover, the high electricity consumption in the evening is worth to be considered to be shifted as well. Furthermore, savings for the electricity consumption costs can also be generated throughout the whole day, since a variability of the costs is given. Consequently, the optimisation of the electricity consumption costs should take into account to conduct load shifting throughout the whole day.

## 4.5 Load shifting potential

When analysing the operation of the HP pool, the load shifting potential plays an important role. This potential represents the ability of the HP pool to shift its electricity consumption time-wise. Thus, the so-called flexibility, which the load shifting potential is being part of, is determining to which extent the HP pool can be used for DSM. For the quantification of the flexibility, the results of the investigations conducted and presented in *Fischer et al. [2016b]* and *Fischer et al. [2017]* are used within this work. The values of these studies can be used to quantify the flexibility of the HP pool of this work, since the same composition of houses is used and the share of ASHP/GSHP is the same. Thus, the overall operation and behaviour of the pool in *Fischer et al. [2016b]* and *Fischer et al. [2017]* is similar to the one in this thesis. The results of *Fischer et al. [2016b]* and *Fischer et al. [2017]* are used in this work in order to predict the flexibility of the HP pool (see Section 5). In the following, the findings of this study are presented. Since it is given in the source, their analysis and detailed interpretation is spared here.

In *Fischer et al. [2016b]*, the flexibility of the HP pool was investigated by triggering the pool with *SG-Ready* signals. Based on the trigger signal, the operations of the HPs were altered, until the individual thermal storages reached their temperature boundaries [Fischer et al., 2016b, pp. 858-859]. After that, the individual HP went back to normal non-triggered operation [Fischer et al., 2016b, pp. 858-859]. The implementation of the *SG-Ready* signals was similar to the one used within this work (compare Section 2.9 and Table 4 in *Fischer et al. [2016b, p. 859]*). In *Fischer et al. [2017]*, the HP pool was triggered over longer timespans. The implementation of the *SG-Ready* signals is the same as in this thesis. The energy consumed by the pool was compared for triggered and non-triggered (thermally driven) operation. The deviation in energy consumption represents the flexible energy (load shifting potential), which is referred to as shiftable energy [Fischer et al., 2016b, pp. 861]. *Fischer et al. [2016b]* grouped the results of the analyses by the ambient temperature. These results for the shiftable energy are presented in Figure 4.14a. Moreover, the maximum power of the pool, presenting the additional load when being triggered, is presented in Figure 4.14b [Fischer et al., 2016b, pp. 861].



(a) Shiftable energy versus ambient temperature. (b) Regeneration versus ambient temperature.

Figure 4.14: Available flexible energy and maximum power versus ambient temperature for the different *SG-Ready* signals. Mean values are indicated by a thick line, while the shapes represent the q25-q75 quartile range. Source: [Fischer et al., 2016b, p. 861].

It can be seen in Figure 4.14a, that the amount of flexibility is highly dependent on the ambient temperature. Activation signals accompanied by a higher increase in the storage temperatures ("Superheat (HP)" & "Superheat (HP+BH)") show higher values for the flexible energy compared to activation signals with smaller increases in the storage temperatures ("On"). The usage of the BH ("Superheat (HP+BH)") further increases the amount of flexible energy. The "Off" signal does not yield high values for the flexible energy compared to the other trigger signals. It can be seen, that the HP pool consists of various HPs being installed in buildings with various levels of refurbishment. Hence, the quartiles in Figure 4.14a show a wide range in moderate temperatures, since some of the buildings are still requiring SH, while other HPs only have to provide DHW [Fischer et al., 2016b, p. 861]. Thus, the shiftable energy is remarkably varying throughout the pool for temperatures about 7°C [Fischer et al., 2016b, p. 861]. Regarding the maximum power, the usage of the "On" signal shows similar peaks in power as the "Superheat (HP)" signal. Only the further usage of the BH increases the maximum power. The maximum power increases with ambient temperature, because more HPs are already active at lower ambient temperatures. When triggering the pool, its operation shows a characteristic response, which can be divided into "Duration" and "Regeneration" as presented in Figure 4.15 for short trigger signals [Fischer et al., 2016b, pp. 860-863]. This characteristic is obtained by comparing the triggered to the non-triggered operation.

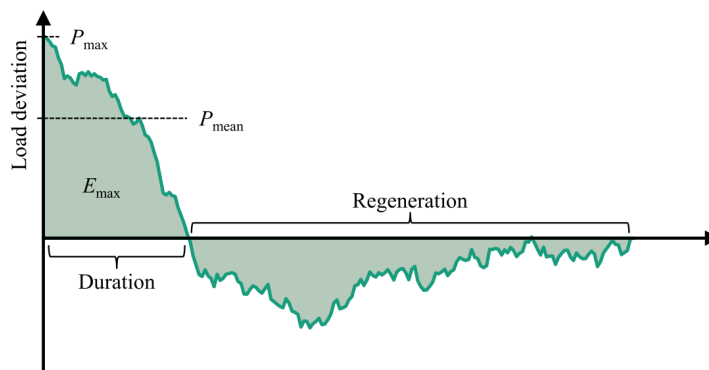
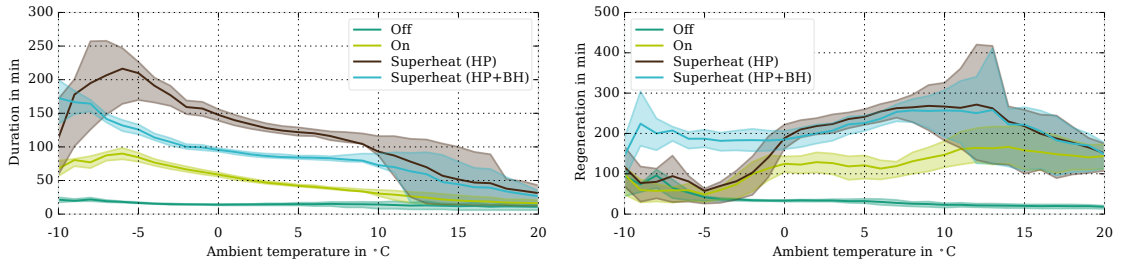


Figure 4.15: Characteristic response of a heat pump pool's electricity consumption to a short activation trigger signal. Source: [Fischer et al., 2016b, p. 860] (figure edited).

The duration represents the time it takes for an activation signal, until the HP pool's load is falling below the level of the standard non-triggered operation [Fischer et al., 2016b, p. 861]. The regeneration is the time it takes additionally to the duration time, until the HP pool is operating on the standard electricity consumption level again [Fischer et al., 2016b, p. 861]. During regeneration, the pool consumes less electricity compared to normal operation due to discharging the thermal storages [Fischer et al., 2016b, p. 861]. The found values for the duration and regeneration versus the ambient temperature are presented in Figure 4.16 for the various *SG-Ready* signals. Figure 4.16a presents, that the duration times are decreasing with increasing ambient temperatures. Thus, the HP pool can be charged for a shorter period with increasing temperatures. The regeneration times as presented in Figure 4.16b is acting vice-versa. Higher ambient temperatures are increasing the time it takes the HP pool to recover from the trigger signal. This is caused by the fact, that the thermal load is lower at higher ambient temperatures and therefore it takes more time to discharge the thermal storages [Fischer et al., 2016b, pp. 862].



(a) Duration versus ambient temperature. (b) Regeneration versus ambient temperature.

Figure 4.16: Times of duration and regeneration versus ambient temperature for the different *SG-Ready* signals. Mean values are indicated by a thick line, while the shapes represent the q25-q75 quartile range. Source: [Fischer et al., 2016b, p. 862].

Figure 4.17 shows the characteristic response of the pool to longer trigger signals. Here, the duration time is substituted by a charging phase having a high additional electricity consumption and a steady state phase with a relatively lower additional electricity consumption of the pool. For longer trigger signals, the additional electricity consumption of the pool decreases after a certain time, when the thermal storages have reached their higher temperature levels of the respective activation signal. [Fischer et al., 2017]

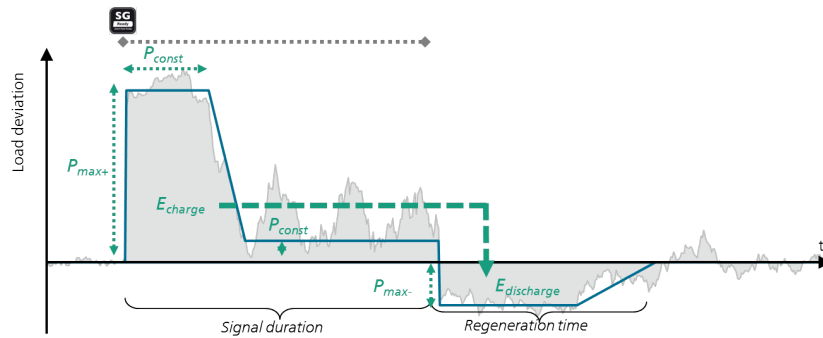


Figure 4.17: Characteristic response of a heat pump pool's electricity consumption to a long activation trigger signal. Source: [Fischer et al., 2017] (figure edited).



## 5 Optimisation of the heat pump pool operation

The section deals with the optimisation of the operation of the HP pool. With the aid of this optimisation, the costs of electricity consumption for the operation of the HP pool shall be minimised. The result of the optimisation is a schedule determining the electricity consumption of the pool over the course of time. According to this operation schedule obtained, the corresponding electricity consumption would be purchased on the *EPEX* day-ahead spot market. Then, the pool controller has to influence the HP pool operation in order to match the HP pool consumption with the one purchased (see Section 6).

### 5.1 Methodology of the optimisation

The aim of the optimisation is to minimise the overall electricity consumption costs. Thus, the scheduled electricity consumption is optimised with regard to the electricity prices. In times with high prices, the consumption should be lowered and increased in times with low prices. The operation cannot be optimised without constraints and therefore, the optimisation is limited by various flexibility parameters for the respective day. The optimisation is carried out for each day of the considered year 2015 with a resolution of one minute. The scenario considered in this work is assuming, that the optimised pool operation is determined day-ahead. For this optimisation, the predicted day-ahead spot market prices are used in order to calculate the costs of electricity consumption. Based on the obtained optimised electricity consumption trajectory, the electricity consumption would be purchased. The optimisation problem is presented and explained in the following.

For the formulation of the optimisation problem, a storage model representing the flexibility of the pool of HPs has been developed. Since every individual HP is equipped with two storages, the usage of a storage model for the optimisation is considered to be adequate. The model is presented in Figure 5.1. It is assumed, that the flexibility of the HP pool can be represented by a single storage for the whole pool. The storage is modelled with the parameters found in the flexibility study of *Fischer et al. [2016b]*. Since the parameters presented in *Fischer et al. [2016b]* are obtained by the analysis and assessment of a pool consisting of individual HPs, the attention to detail of this thesis is adequately maintained by representing the whole HP pool by a single storage model.

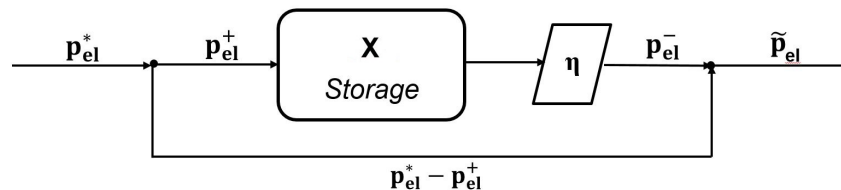


Figure 5.1: Model developed for and used in the optimisation.

As presented in Figure 5.1, the storage and the energy stored inside are represented by  $x$ , while the load of the pool, which is optimised, is  $p_{\text{el}}^*$ . In times, the optimised pool consumption is higher as the predicted consumption of the uninfluenced thermally driven operation  $\tilde{p}_{\text{el}}$ , the storage is charged with  $p_{\text{el}}^+$ . In times the HP pool is determined to consumes less energy as predicted for an uninfluenced thermally driven operation, the storage gets discharged. The discharging is associated with a load shifting efficiency  $\eta$ , which is accounting for losses due to the shift of energy and the heating of the HPs' thermal storages to higher temperature levels when being triggered (see Section 2.9). The power coming from the storage in order to balance  $p_{\text{el}}^*$  and  $\tilde{p}_{\text{el}}$  is called  $p_{\text{el}}^-$ , while the storage itself is discharged with  $p_{\text{el}}^-/\eta$ .

For each day, the mean ambient temperature  $\tilde{T}_{\text{amb}}$  is predicted. Within this thesis, a perfect prognosis of  $\tilde{T}_{\text{amb}}$  is assumed. Thus, the actual mean temperature of the respective day in 2015 is used (note, that these temperatures are the same as they have been presented in Figure 3.2 and have been used for the generation of the thermal load profiles of the respective houses). With this mean ambient temperature of the day, the flexibility parameters of the pool are defined based on the results of *Fischer et al. [2016b]*. Thus, the storage has a capacity equal to the shiftable energy for this ambient temperature and the maximum power for charging and discharging is constrained by the maximum power as presented in *Fischer et al. [2016b]* and in Figure 4.15. Moreover, the duration and the regeneration as shown in Figure 4.16 are obtained for the respective day from the results of *Fischer et al. [2016b]* as well. All these parameters are using the values for the "On" signal of *SG-Ready*. This signal is chosen, since its increase in storage temperatures is moderate and therefore not associated with high efficiency losses. Since the implementation of the "On" signal in *Fischer et al. [2016b, p. 859]* is having a lower increase in the storage temperatures compared to this study (see Table 2.1), the obtained parameters lead to a conservative optimisation. Consequently, the degree of freedom for the optimisation could be increased by using the flexibility parameters of one of the two "Superheat" signals. However, as presented in *Fischer et al. [2017]*, the usage of the "Superheat" signals is accompanied with high efficiency losses. Moreover, by using the "On" signal, the purchased trajectory of operation should be easier to be realised by the pool controller. Consequently, the "On" signal is the medium of choice within this thesis.

With these flexibility parameters, the behaviour of the storage as presented in Figure 5.1 is modelled. For the efficiency  $\eta$ , a value of 0.99 is assumed. This value is similar to the load shifting efficiency for unrepeatd "On" signals with a duration of 1 min as presented in *Fischer et al. [2017]*. In *Fischer et al. [2016b]*, the HPs were only following the *SG-Ready* triggering signal, until they have reached their respective storage temperature boundaries [Fischer et al., 2016b, p. 858-859]. Thus, the trigger signal could be seen as an impulse. Due to this fact, the load shifting efficiency for very short signals has to be used.

Moreover, the optimisation problem uses the prediction of the *EPEX* day-ahead spot market prices  $\tilde{c}$ . Here, a perfect prognosis is assumed, thus the actual *EPEX* day-ahead spot market prices from 2015 for Germany are used as the are available by *EPEX* (see the *EPEX* website <http://www.epexspot.com/en/>). For the predicted load of the thermally driven operation  $\tilde{p}_{\text{el}}$ , a perfect prognosis is assumed as well. Thus, the values are taken from the actual thermally driven operation as it has been presented in Section 4.1. Moreover,

the maximum power of the pool  $P_{\max,\text{std}}$  is calculated as the maximum load off the pool found for the uninfluenced thermally driven operation. The parameters of the optimisation are presented in the following.

$$\begin{aligned} \vec{p}_{\text{el}}^* &= \{p_{\text{el},0}^*, \dots, p_{\text{el},N-1}^*\}; & \vec{p}_{\text{el}}^+ &= \{p_{\text{el},0}^+, \dots, p_{\text{el},N-1}^+\}; & \vec{p}_{\text{el}}^- &= \{p_{\text{el},0}^-, \dots, p_{\text{el},N-1}^-\} \\ \vec{x} &= \{x_0, \dots, x_{N-1}\}; & \vec{\tilde{p}}_{\text{el}} &= \{\tilde{p}_{\text{el},0}, \dots, \tilde{p}_{\text{el},N-1}\}; & \vec{\tilde{c}} &= \{\tilde{c}_0, \dots, \tilde{c}_{N-1}\} \\ E_{\text{flex}} &= E_{\text{shiftable energy}}(\tilde{T}_{\text{amb}}); & P_{\max} &= P_{\max}(\tilde{T}_{\text{amb}}); & P_{\max,\text{std}} &= \max(P_{\text{th. op.}}) \\ \alpha &= \text{duration}(\tilde{T}_{\text{amb}}); & \beta &= \text{regeneration}(\tilde{T}_{\text{amb}}); & \eta &= 0.99; & \Delta t &= 60 \text{ sec} \\ N &= \begin{cases} 1380, & \text{if day} = 29^{\text{th}} \text{ of March 2015} \\ 1500, & \text{if day} = 25^{\text{th}} \text{ of October 2015} \\ 1440, & \text{otherwise} \end{cases} \end{aligned}$$

With these parameters, the optimisation is conducted. The target is to minimise the costs of electricity consumption of the pool of HPs being subject to the flexibility parameters. The constraints are explained in the following, after they have been presented in the optimisation problem.

$$\begin{aligned} \text{minimise:} & & J^* &= \sum_{k=0}^{N-1} (p_{\text{el},k}^* \cdot \tilde{c}_k) & (5.2a) \\ \{\vec{p}_{\text{el}}^*, \vec{p}_{\text{el}}^+, \vec{p}_{\text{el}}^-, \vec{x}\} & & & & \end{aligned}$$

$$\text{subject to: } 0 \leq p_{\text{el},k}^* \leq P_{\max,\text{std}}, \quad k \in [0, N-1] \quad (5.2b)$$

$$p_{\text{el},0}^* = \tilde{p}_{\text{el},0} \quad (5.2c)$$

$$p_{\text{el},N-1}^* = \tilde{p}_{\text{el},N-1} \quad (5.2d)$$

$$0 \leq x_k \leq E_{\text{flex}}, \quad k \in [0, N-1] \quad (5.2e)$$

$$x_0 = 0 \quad (5.2f)$$

$$x_{N-1} = 0 \quad (5.2g)$$

$$0 \leq p_{\text{el},k}^- \leq P_{\max}, \quad k \in [0, N-1] \quad (5.2h)$$

$$p_{\text{el},0}^- = 0 \quad (5.2i)$$

$$p_{\text{el},N-1}^- = 0 \quad (5.2j)$$

$$0 \leq p_{\text{el},k}^+, \quad k \in [0, N-1] \quad (5.2k)$$

$$p_{\text{el},k}^+ + P_{\max} \cdot \frac{x_k}{E_{\text{flex}}} \leq P_{\max}, \quad k \in [0, N-1] \quad (5.2l)$$

$$p_{\text{el},0}^+ = 0 \quad (5.2m)$$

$$p_{\text{el},N-1}^+ = 0 \quad (5.2n)$$

$$x_k - x_{k-1} - p_{\text{el},k}^+ \cdot \Delta t + \frac{p_{\text{el},k}^-}{\eta} \cdot \Delta t = 0, \quad k \in [1, N-1] \quad (5.2o)$$

$$p_{\text{el},k}^* - \tilde{p}_{\text{el},k} - p_{\text{el},k}^+ + p_{\text{el},k}^- = 0, \quad k \in [0, N-1] \quad (5.2p)$$

$$\sum_{k=i}^{i+\alpha+\beta} p_{\text{el},k}^+ - \frac{1}{\eta} \sum_{k=i}^{i+\alpha+\beta} p_{\text{el},k}^- = 0, \quad i \in [0, N-\alpha-\beta-1] \quad (5.2q)$$

- The target of the optimisation as presented in the Cost Function 5.2a is to minimise the costs for electricity consumption. These costs are represented by the sum of the product of the optimised load of the pool and the day-ahead prices in each minute/timestep  $k$  throughout the day. The optimisation is also considering the variables  $p_{\text{el}}^+$ ,  $p_{\text{el}}^-$  and  $x$  as they are representing the power charging/discharging the storage and the energy stored in the storage.
- The Constraint 5.2d is determining, that the optimised load of the pool has to be larger than zero and below the maximum power found for the thermally driven operation (1280.69 kW). Moreover, the optimised load of the HP pool has to be equal to the predicted load of the thermally driven operation in the first and in the last timestep of the day as determined by the Constraints 5.2b and 5.2c.
- The storage  $x$  is defined by the Constraints 5.2e, 5.2f and 5.2g. Here, the storage cannot have a negative amount of energy stored inside and the maximum capacity of the storage is constrained to the maximum available shiftable energy  $E_{\text{flex}}$  for this day. Furthermore, the storage has to be empty at the beginning and at the end of each day.
- The Constraints 5.2h, 5.2i and 5.2j are dealing with the power  $p_{\text{el}}^-$  originating from the storage after the efficiency losses, when discharging the storage. This power has to be at least zero. Moreover, it is assumed, that this power cannot exceed the power found in *Fischer et al. [2016b]* for the maximum peak in power, when triggering the HP pool with the "On" signal. Furthermore, in the first and in the last timestep of the day, the storage must not be discharged.
- The charging of the storage is treated by the Constraints 5.2k, 5.2l, 5.2m and 5.2n. Here, the power charging the storage has to be at least zero. Additionally, when charging the storage, the maximum load charging the storage decreases. Constraint 5.2l determines, that the maximum charging power is linearly decreasing with the amount of energy stored inside the storage. Hence, this constraint is dynamic. By this, the characteristic response of the HP pool when charging the storage as presented in Figure 4.15 is modelled. For increasing SOC of the storage, the power to load the storage decreases in the form of an idealised triangle. The Constraints 5.2m and 5.2n exclude the possibility to charge the storage in the first and in the last timestep of the day.
- The Constraint 5.2o is representing the change of the state of the storage. The time-wise derivative of  $x$  is represented by the backwards differential quotient of the state of the storage in the timesteps  $k$  and  $k-1$ . The change in the state of the storage is balanced by the input energy originating from the charging power  $p_{\text{el}}^+$  and the output energy originating from the discharging power  $p_{\text{el}}^-$  divided by  $\eta$ . Note, that  $p_{\text{el}}^-/\eta$  is exiting the storage, since every charging and subsequent discharging of the storage is accompanied by the load shifting efficiency  $\eta$ . Thus, the amount of energy discharging the storage is lower as the one, that has been expended for the charging the storage. Moreover, the powers  $p_{\text{el}}^+$  and  $p_{\text{el}}^-$  are multiplied with the stepwidth of the optimisation, which originates from the backwards differential quotient describing the change in the amount of energy in the storage  $\dot{x}$ .
- Constraint 5.2p is the balancing equation for the node after the storage in Figure 5.1. Here, the sum of all power has to be equal to zero.
- In order to guarantee, that HP pool is acting as it has been found as the characteristic response of the HP pool when being triggered (see Figure 4.15), Constraint 5.2q is

introduced. This constraint determines, that the amount of energy charging the storage is equal to the amount of energy discharging the storage (with respect to the load shifting efficiency) in a certain timespan. This comparison has to apply over a timespan with the size of the sum of the duration time  $\alpha$  and the regeneration time  $\beta$ . In order not to force the algorithm to conduct load shifting at specific times, these sums are calculated over the course of the whole day. Thus, the sums can be seen as a moving window, forcing the algorithm to balance energy input and energy output of the storage within a certain period of time. Consequently, the interaction of Constraint 5.2q with the Constraints 5.2f and 5.2g guarantees, that the storage is having completed a charging and discharging cycle within each timespan of the size  $\alpha + \beta$  to be found within the respective day. Where exactly the charging and subsequent discharging of the storage happens is up to the optimisation solver. Thus, the times of charging and discharging remain dynamic, although a charging and discharging pattern is demanded.

The optimisation procedure is conducted for all days in the considered year 2015. The resolution of the timesteps is one minute. Data with different resolution (*e.g.* day-ahead prices) is resampled to the resolution of one minute. Different resolutions of parameters are adjusted and scaled in the optimisation framework, in order that the units of parameters representing load ( $p_{el}$ ) are matching with parameters representing energy.

The obtained optimisation problem is a *Linear Programming (LP)* problem, due to the fact, that all constraints are linear. The obtained LP problem is solved by using the *PuLP* library in *Python* together with the *CBC\_CMD* solver. Since all the work within this thesis is carried out in *Python*, the free and open-source software *PuLP (Python Linear Programming)* is chosen for the environment for the implementation of the *LP* problem. The *PuLP* library uses the open-source solver *CBC\_CMD*, which is *LP* based and developed by the *COIN-OR (Computational Infrastructure for Operations Research)* project (see <https://www.coin-or.org/>). This solver was chosen, because of its availability. Moreover, the *PuLP* library and the solver *CBC\_CMD* have already been used by staff of the department of the *Fraunhofer ISE*, where this thesis has taken place. Hence, choosing this combination of optimisation framework and solver is the obvious choice.

## 5.2 Analysis of the optimised operation trajectory

This section analyses the results obtained by the optimisation as described in Section 5.1. All the results yielded by solving the *LP* problem are optimal and unique for each day. Moreover, the results obtained are aligned with the constraints defined in the optimisation problem. Figure 7.1 exemplary presents the results calculated for the 1<sup>st</sup> of February. The day-ahead electricity price is represented by the dark-brown line, whose values are given by the right y-axis. The petrol-green line shows the optimised electricity consumption of the HP pool, while the blue line presents the predicted operation of the pool. Both lines are associated with the left y-axis, which represents the electricity load. Since calculating with a perfect prognosis, the blue line of the predicted pool operation represents the thermally driven operation too. In times the optimised operation consumes more electricity than the predicted operation, the difference is highlighted by a red shape. A lower consumption of the optimised operation is highlighted by a green shape.

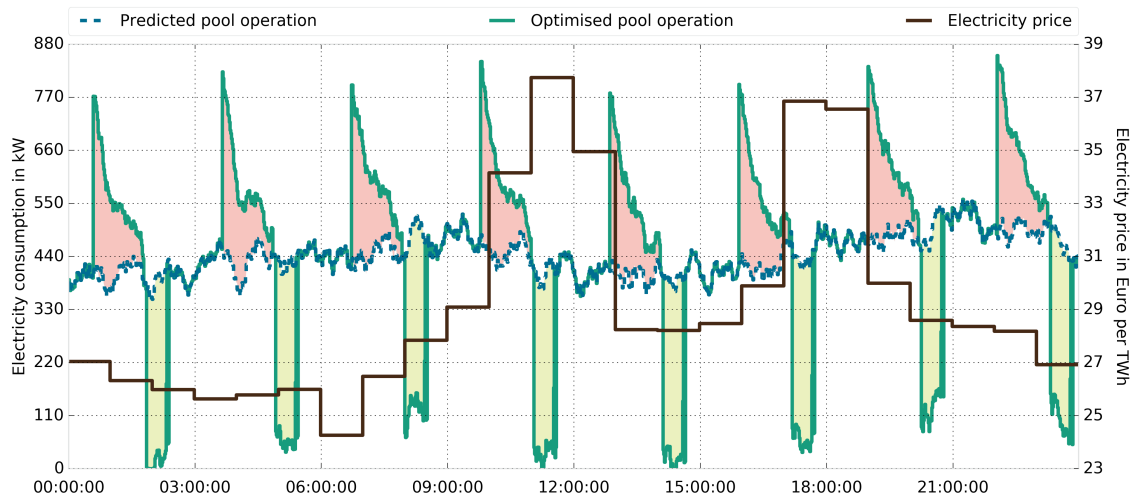


Figure 5.2: Results of the  $LP$  optimisation obtained for the 1<sup>st</sup> of February.

Figure 7.1 shows, that the optimised pool operation is saving electricity in times of the highest electricity prices (from 11 to 12 o'clock and from 17 to 19 o'clock). It can be seen, that the regeneration of the HP pool is directly following after having charged the storage. Moreover, the times in which one cycle of charging and discharging the storage has to be conducted are clearly indicated by the charging (red shapes) and discharging (green shapes) times. The optimisation fulfils the demand to charge and discharge the storage within one cycle of the length of the duration time plus the regeneration time of the respective day (see Constraint 5.2q). Furthermore, the regeneration time of the optimised HP pool operation is mostly followed by a timespan, in which the optimised pool's electricity consumption is equal to the predicted thermally driven operation. At the 1<sup>st</sup> of February the sum of duration time and regeneration time accounts for around three hours. This available time to conduct one charging and discharging cycle is not completely utilised by the optimisation.

The Constraint 5.2h is applied by limiting the possible discharging rates of the storage at the 1<sup>st</sup> of February. The charging is conducted at the lowest prices possible. The subsequent discharging is usually conducted in times of high electricity prices. The deviation of charging and discharging times from the times with most favourable electricity prices is based on the fact, that the charging and subsequent discharging are forced to be conducted within a certain timespan with the length of duration time plus regeneration time. Since the optimiser sets the times of discharging to the times with highest electricity prices (from around 11 to around 12 o'clock and from around 17 to around 19 o'clock), the charging of the storage is restricted to take place close to these times. However, the optimisation achieves to avoid most of the charging on the time from 12 o'clock to 13 o'clock, where relatively high electricity prices occur. Here, the advantages of the dynamic Constraint 5.2q become obvious. As a consequence, the energy consumption of the pool is lowered as much as possible in times of high prices. The associated compromise is to charge the storage in adjacent times, which are still having relatively high electricity prices. Nevertheless, this is carried out by the optimisation, since it is advantageous in terms of electricity consumption costs. However, all charging and discharging times of the whole day are dependent on each other, since the Constraints 5.2f and 5.2g are determining,

that the pool's storage has to be empty at the beginning of the day and the end of the day and no charging and discharging can happen in the first and last timestep of the day (see the Constraints 5.2i, 5.2j, 5.2m and 5.2n).

Additionally, at the 1<sup>st</sup> of February at around 2 o'clock, the optimised pool operation yields, that the pool should not consume any electricity. This means, that all HPs will have to be deactivated by the pool controller in order to match the actual operation with this optimised trajectory. Figure 7.1 presents, that when charging the storage, the maximum power to charge the storage is decreasing with increasing SOC as it is demanded by Constraint 5.2l. The overall obtained characteristic of the load shifting is similar to the one presented in Figure 4.15 and 4.17 and also in the findings of *Fischer et al. [2016b]* and *Fischer et al. [2017]*. Furthermore, when comparing the optimised operation with the thermally driven operation, the increase in the electricity consumption of the pool (meaning charging of the storage,  $p_{el}^+ > 0$ ) is mostly not decreasing to 0 before the regeneration phase of the pool starts. This suggests, that the storage capacity and therefore the available load shifting potential per cycle  $E_{flex}$  is not completely used within all load shifting cycles scheduled for the 1<sup>st</sup> of February.

The available daily load shifting potential and the maximum power to charge/discharge the storage are dependent on the ambient temperature. This is illustrated by the comparison of the sizes and shapes of the red shapes and the green shapes in Figure 7.1 with the ones depicted in Figure 5.3. Figure 5.3 presents the optimisation results for the 26<sup>th</sup> of December. On the 26<sup>th</sup> of December, negative electricity prices occur. Thus, the optimisation algorithm tries to shift as much electricity consumption as possible to these times, because there, electricity consumption is associated with monetary gains instead of losses. Thus, charging of the storage is scheduled to take place as much as possible between 2 o'clock and 7 o'clock. At this day, the sum of the duration times plus the regeneration time is not large enough in order to only conduct one charging and discharging cycle within this timespan of five hours. Consequently, several load shifts occur within this timespan as it is also seen for the whole day. Moreover, it can be seen, that some load shifts are using more storage capacity (for instance from around 5:30 o'clock to around

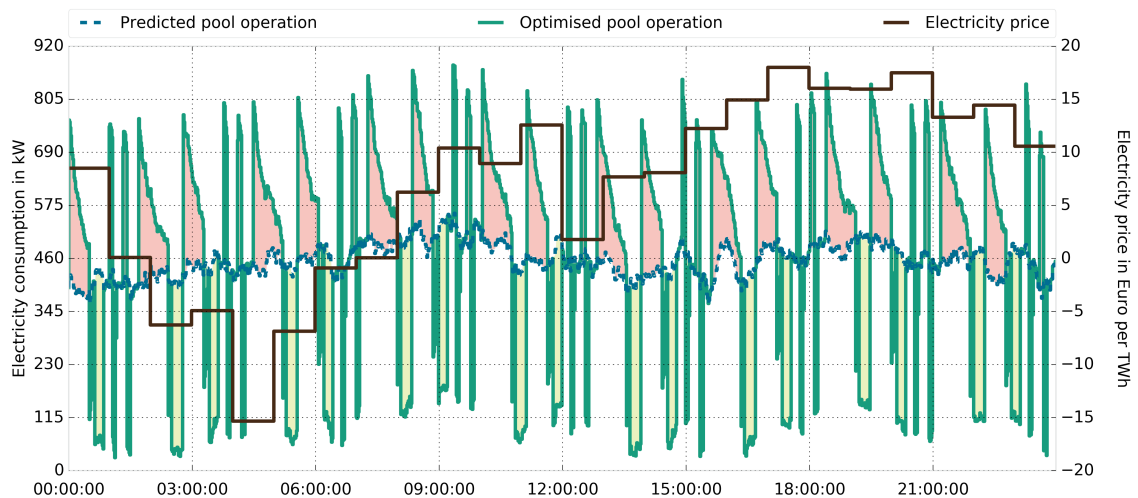


Figure 5.3: Results of the *LP* optimisation obtained for the 26<sup>th</sup> of December.

6:30 o'clock) than others (for instance from around 6:30 o'clock to around 6:45 o'clock). Thus, the optimisation is not using the whole storage capacity in every load shift. The optimiser has found, that it is advantageous to have the main load shifting at certain times and to conduct load shiftings with smaller amount of energy at the times between them. When conducting these load shifts with a lower energy turnover, a high power is observed and the opportunity to balance the storage within a certain timespan as demanded by Constraint 5.2q is given. However, every load shift is associated with a loss of energy, since the storage is discharging with the load shifting efficiency  $\eta$ . Nevertheless, the abundance of load shifting potential is used in order to utilise the negative electricity prices. As a result, the obtained optimised consumption for this exemplary day with negative prices does not reflect the most energy-efficient operation, but illustrates the possibility to monetarily benefit by using the flexibility of the HP pool. Thus, load shifting is scheduled by the optimisation as long as monetary benefits can be achieved for the respective day and the available load shifting potential is used to such an extent as it is beneficial for the electricity consumption cost of the whole day.

When comparing the optimised operation with the predicted operation, the patterns as presented in Figure 5.4 are observed. High values (red) represent a relatively higher load of the optimised operation. It can be seen, that the charging and discharging of the storage and thus duration times and regeneration times of the HP pool are directly adjacent to each other. Moreover, the majority of the load shifting occurs in winter. Hence, the times in which the load shifting is conducted are shorter in summer with lower amounts of energy accompanied, although similarly high powers are achieved in summer and in winter. The reason for this is the higher predicted mean ambient temperature of the day in summer, which is associated with altering flexibility parameters, that determine a lower load shifting potential for warmer temperatures (this has been presented in Figure 4.16 and 4.14).

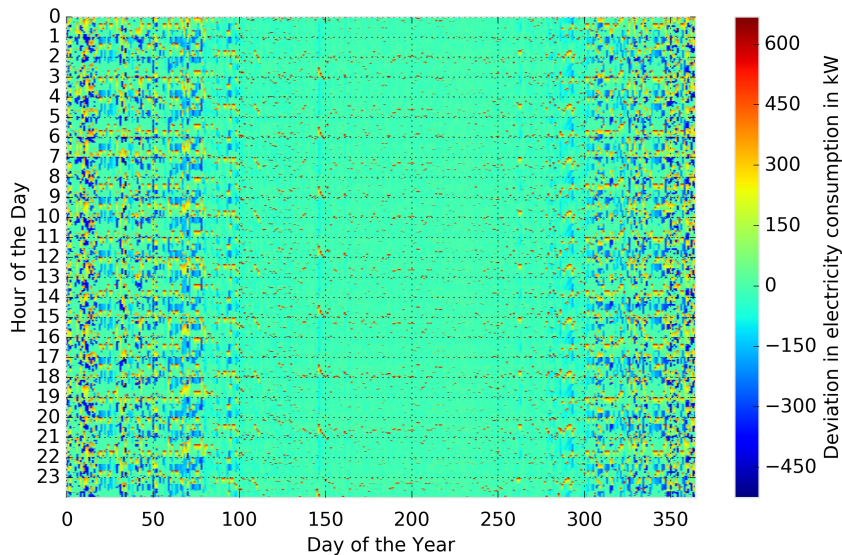


Figure 5.4: Difference between the optimised pool operation and the predicted pool operation.

Furthermore, Figure 5.4 shows, that the load shifting is rather scheduled to take place throughout the whole year and over the course of each day, instead of only using several times of the year. Since the allowed timespan for a full cycle of the storage is as little as it is shown in Figure 4.16, the variability of the day-ahead spot market prices for electricity cannot be utilised as much as desired for high electricity consumption cost savings. This is presented in Figure 5.5, which shows the cumulated costs of electricity consumption of the pool over the course of the year. Here, the thermally driven operation amounts to total electricity consumption costs of around 53522.3 Euro, while the SLP operation generates costs of around 51806.4 Euro and the costs of electricity consumption for the optimised pool operation sum up to around 53271.9 Euro. Hence, the optimisation achieves savings of around 0.47 % compared to the thermally driven operation. The SLP operation's cost of electricity consumption represent the other reference costs for the considerations made within this thesis. Thus, the optimised operation should also generate savings compared to the SLP operation. For this purpose, the savings have to be high enough to compensate the higher electricity consumption costs of the thermally driven operation. Unfortunately, this is not the case for the results of the optimisation obtained. The optimised operation of the HP pool would create losses of around 2.83 % compared to the SLP operation. However, the deviation between the electricity consumption costs of the thermally driven and the SLP operation has been discussed at the end of Section 4.4. Consequently, the thermally driven operation should be considered as the baseline case for all further optimisation of the electricity consumption costs, in order that the optimised operation is beneficial for the aggregator.

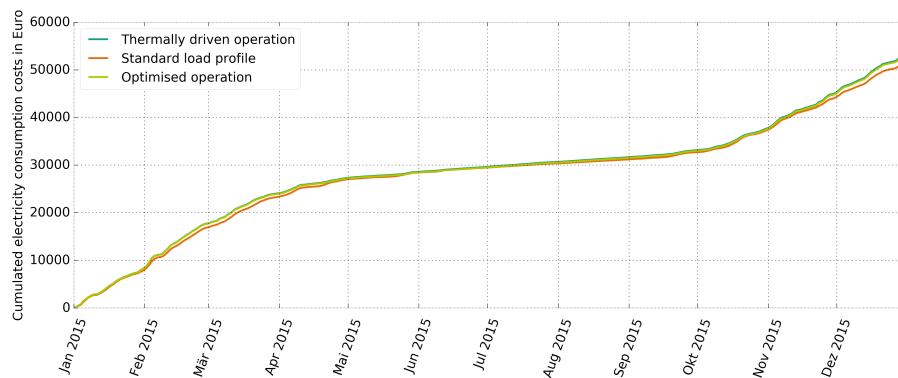


Figure 5.5: Cumulated costs of electricity consumption for the thermally driven operation, the standard load profile operation and the optimised operation.

Moreover, Figure 5.6 illustrates, when these respective savings and losses are generated. The values presented in the figure represent the daily savings and losses when comparing the optimised operation to the thermally driven operation and to the SLP operation. In general, the savings compared to the thermally driven operation (petrol-green line) are low and are mostly generated in the winter month, where a relatively high load shifting potential is available. The savings and losses of the optimised operation compared to the SLP operation are illustrated by the orange line in Figure 5.6. It can be seen, that the savings and losses compared to the SLP operation are remarkably changing throughout the year. Thus, at some days, savings of around 100 Euro would be achieved by the optimised pool operation, while other days would generate losses of around 150 Euro. The highest

fluctuations of the savings and losses is observed in the winter, which has the highest load shifting potential. The large difference in the daily savings when comparing both operations are caused by the fact, that the SLP operation is steady throughout the days as it is presented in Section 4.2.2 and 4.4.

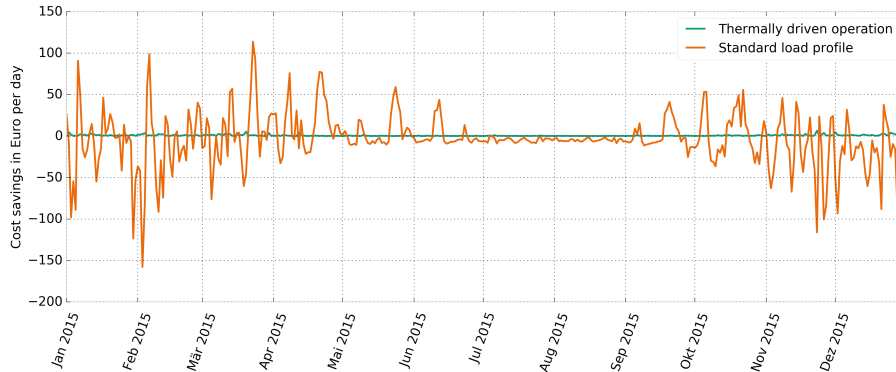


Figure 5.6: Daily savings in electricity consumption costs for the optimised operation compared to the thermally driven operation and to the standard load profile.

The savings obtained by the day-ahead optimisation of this work are lower than the ones yielded by *Biegel et al. [2013]*. However, it is expected that a well-tuned pool controller is able to operate the pool according to the optimised electricity consumption trajectory obtained in this work. When comparing the scenarios used directly, the optimisation of this work achieves savings of around 0.47 %, while *Biegel et al. [2013]* showed around 18 %. The lower savings within this thesis are mainly caused by three facts: First, *Biegel et al. [2013]* was using a lumped model with a lumped thermal capacity of the whole pool originating from the thermal capacities of the single houses. The results of *Biegel et al. [2013]* show, that the load has to be shifted over timespans longer than allowed in this thesis (see Figures 1.4 and 1.5). For its implementation, the approach of *Biegel et al. [2013]* would require larger thermal storages for the individual HPs, in order to account for simultaneousness, which complicate the implementation of the results of a lumped model by a pool controller. Secondly, the charging and discharging cycles within this thesis have to be conducted within the timespans having the size of the duration times plus the regeneration times. These two timespans are found for the respective day by using the findings of *Fischer et al. [2016b]* for the respective predicted mean ambient temperature. These timespans are usually too short in order to allow the optimisation to benefit from high variabilities in the electricity price. The third main cause for the level of the saving rate is the fact, that due to the size of the load shifting timespans, the amount of energy shifted is relatively small. Therefore, the associated saved consumption costs remain small as well. Thus, future work should investigate the effects on the savings, when increasing the timespans for the conduction of one charging and discharging cycle. For this purpose, the change in the flexibility parameters associated with longer trigger signals should be investigated. This has been carried out by *Fischer et al. [2017]* with a focus on the shiftable energy. Further studies quantifying the charging and discharging times of the HP pool and the quantifying the characteristic response of a HP pool to long-time triggering with respect to the thermal load/ambient temperature should be conducted. The results of these studies could be used for further improvements of the optimisation framework.

Moreover, the load shifting efficiency  $\eta$  should account for the respective load shifting time and therefore be automatically adjusted, when increasing the allowed load shifting periods. This should be focus of further modifications of the optimisation problem, since the closeness of reality is only taken into account sufficiently, when the load shifting efficiency is changing with the duration of the load shift. Additionally, further Constraints should be implemented into the optimisation problem, guaranteeing, that the regeneration phase is not only inside the allowed timespan (duration time plus regeneration time), but also directly adjacent to the respective charging phase. Moreover, additional constraints should be implemented in order to allow continuous charging/discharging only over a maximum timespan determined by the duration/regeneration time. When additionally allowing to conduct partial load shifting cycles together with dynamically changing the timespans in which a charging and discharging cycle has to be conducted to the lengths used by the partial load shift, the reality could be depicted by the optimisation results further. So far, only the flexibility associated with the usage of the "On" signal has been used. As a consequence, the obtained optimisation results are conservative. Furthermore, the usage of the other *SG-Ready* signals should be taken into account. For this purpose a multiple storage model could be used, with each storage representing one of the *SG-Ready* modes. In such a model, the more powerful *SG-Ready* activation signals could be engaged, when the load shifting potential of the current *SG-Ready* mode is depleted. Here, the load shifting efficiency should be changed dynamically for each respective storage/*SG-Ready* mode used. The obtained optimisation problem when using such a multiple storage model would be more complex as the one presented within this work in Section 5.1. However, the monetary gains evolved by the optimisation would probably increase. Moreover, the usage of the "Superheat (HP+BH)" mode would be additionally beneficial in times of negative prices, although the (load shifting) efficiency would decrease.

In general, it is expected, that the implementation of a model predictive control (MPC) approach into the optimisation problem would lead to the best results in terms of level of reality depicted and monetary gains achieved. However, in order to realise a MPC approach, models of the buildings, user behaviour, the HP and the thermal storages would be required for each individual house. Moreover, the response of these models to triggering and the impacts on the flexibility parameters would have to be implemented as well, together with a model of the behaviour of the pool controller. With these models, the optimisation could treat the calculation of an optimised operation trajectory and the subsequent operation of the pool accordingly as a closed loop. However, it is expected, that the implementation of such a holistic approach would be associated with big efforts.

The results obtained for the electricity consumption cost-wise optimisation of the HP pool operation are used by the pool controller (see Section 6). For this purpose, the yielded trajectory with a resolution of one min is resampled to a resolution of one hour by calculating the mean of the electricity consumption in each hour. In the scenario drawn and investigated in this work, this hourly changing steps are purchased on the *EPEX* day-ahead spot market and the associated optimised operation has to be matched by the actual operation of the HP pool. This has to be achieved by the pool controller through influencing the individual HPs by *SG-Ready* trigger signals.



# 6 Controlling the heat pump pool operation

This section deals with the pool controller, which shall accomplish the operation according to an operational setpoint. In general, the setpoint is represented by the electricity consumption trajectory, which was obtained as presented in Section 5. The pool controller then tries to match the actual electricity consumption of the pool with the one determined by the setpoint. Section 6.1 introduces the framework developed and implemented for this purpose. It is aimed to keep the complexity of the approaches used as low as possible, while still fulfilling the operational goals. Thus, only the electricity consumption of the units in the pool is used for the pool controller (approaches with higher complexity could further use the current respective thermal load, the respective ambient temperature, the respective SOC of the storages, *etc.*). Section 6.2 shows, how the pool controller is acting and analyses the behaviour of the pool controller for setpoints being relative steps. Moreover, Section 6.3 evaluates the accuracy of trajectory, when the pool controller is deployed in order to achieve the operational setpoints obtained by the optimisation. All the evaluation of the behaviour of the pool controller is conducted by the aid of simulations.

## 6.1 Framework of the pool controller

When designing a controller in order to influence the operation of a pool towards a more favourable state, several approaches may be taken. Within this thesis, the operation should be determined by a central aggregator, which is only getting the information about the electricity consumption monitored by smart-meters (see Section 1.2 and 1.4. By this, privacy issues and costs are minimised, since the amount of information transmitted is kept low. Moreover, the aggregator uses the market-available *SG-Ready* interface for the triggering of the units. The five different trigger modes of *SG-Ready* ("Off", "Normal", "On", "Superheat (HP)", "Superheat (HP+BH)") are specifying the change in operation of the respective HP (for more details about the implementation of *SG-Ready* see Section 2.9). In order to affect the operation of the individual HPs in the pool, two different general approaches can be taken:

- "Broadcast": Sending out a signal to all units. The units interpret this signal by themselves and convert it into the required alteration of their operation. The interpretation of the signal is dependent on the implementation within the individual units, which may include controllers (*e.g.* PID-controller, *lazy-switch* (delayed reaction to signal), *etc.*) that are manipulating the broadcasted signal further. The central aggregator may change the broadcasted signal based on the reaction of the pool.
- "Directed": Each unit gets its own specific signal. Based on the reaction of the pool, the distribution and shape of signals sent may be changed. Since no decentralised

intelligence beside the *SG-Ready* implementation is interpreting the signals sent, the degree of freedom of the operation of the single unit is easier to limit compared to the "Broadcast" approach.

Since this thesis is considering an approach, where a centrally acting aggregator has the responsibility for the determination and alteration of the pool operation, it is chosen to use the "*Directed*" approach. This approach allows a better predictability of the pool operation. Moreover, the costs are lower, since no decentralised intelligence is required beside *SG-Ready* interface. In order to give an overview about the control framework developed and used within this thesis, Figure 6.1 is given, which illustrates how the pool is operated and controlled.

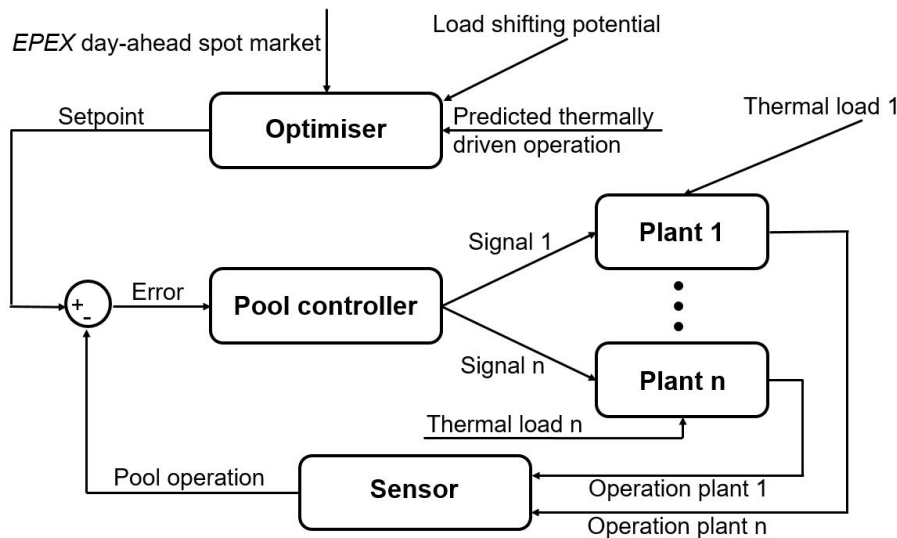


Figure 6.1: Schematic depiction of the pool operation and how the operation of the individual unit is influenced by the pool controller.

In Figure 6.1, the optimiser obtains the setpoint for the pool operation through optimisation by using the predicted *EPEX* day-ahead spot market prices, information about the load shifting potential of the pool and the predicted thermally driven operation (for further information about the optimisation, see Section 5). Each plant/unit in the pool is operating according to its respective thermal load. The sensor gathers the electricity

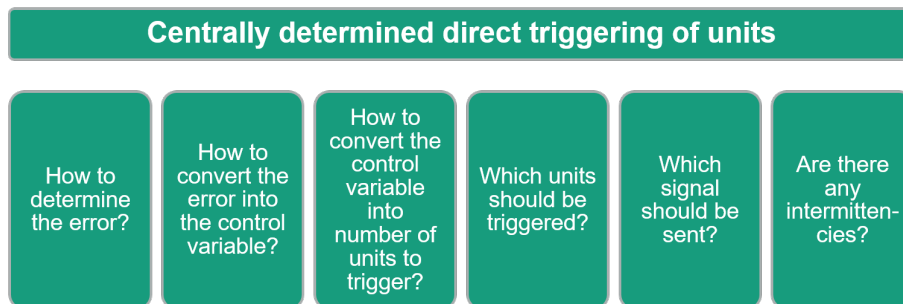


Figure 6.2: Degrees of freedom for the conversion of the error into direct load control signals for a centrally acting aggregator, which is triggering the units in the pool directly.

consumption of each plant in the pool for each timestep. The individual electricity consumption is aggregated to the consumption of the whole pool. The error is obtained by subtracting the actual pool operation from the one determined by the setpoint. This error representing the deviation of the actual pool operation from the targeted one is given to the pool controller. The pool controller interprets the error of the current timestep. The error may be manipulated by, for instance, a PID-controller. By this, the pool controller converts the error into the control variable. Based on this control variable, signals have to be derived to be sent to each unit. These signals are representing the *SG-Ready* signals, being specified for each unit. The individual unit interprets its *SG-Ready* signal and acts in order to fulfil the thermal demand with respect to the current *SG-Ready* signal applied (see Section 2.9 for information about the detailed implementation of and reaction to *SG-Ready* within the simulations carried out). The calculated error between setpoint and actual operation has to be converted into the *SG-Ready* signals to be sent to specific units in the pool. This conversion has different degrees of freedom as illustrated in Figure 6.2.

When considering how to calculate the error, the error can be determined for the current timestep. Moreover, predictions of the error can be used as well, or the error may be calculated by comparing the current pool operation with the setpoint of the next timestep. Within this thesis, the error is obtained by subtracting the electricity consumption of the actual pool operation for the current timestep from the setpoint of the current timestep. The control variable can be equal to the error calculated, or be formed by manipulating the error through, for instance, a PID-controller. This work is considering several approaches here (information is given in the following Section 6.2). In order to convert the control variable into the number of units that have to be triggered, Equation 6.1 is introduced.

$$\text{number of units to trigger} = |\omega| = \text{ceiling} \left( \left| \frac{\text{control variable}}{\left( \frac{\text{electricity consumption of the pool}}{\text{number of active units}} \right)} \right| \right) \quad (6.1)$$

This equation determines, how many units  $|\omega|$  have to be triggered (based on the error/control variable), in order to compensate the deviation between setpoint and actual pool operation. In the denominator of Equation 6.1, the mean electricity consumption of all active units is calculated. It is assumed, that the activation of a further unit will result in an increase of the pool's electricity consumption by the amount of this value. In case that no units are active, the denominator is calculated by dividing the maximum consumption of the thermally driven operation (see Section 4.1) by the number of units in the pool (1280.7 kW/284). Then, the control variable is divided by this mean electricity consumption of active units in order to determine the number of units to be activated/deactivated. The absolute of this number is taken, since it is impossible to trigger a negative number of units. After that, the obtained number of units to be triggered is rounded up to the closest integer. This guarantees, that the number of units triggered is at least as high as the number calculated to be required. If a further increase in the number of units to trigger would be required in order to match the actual operation of the pool with the setpoint, for instance a P-controller might increase the control variable and thereby weight the error further.

Two further points to be treated for by the pool controller as illustrated in Figure 6.2 are: Which units have to be triggered and which signals have to be sent. These two points are treated together by the pool controller as described in the following. In order to determine, which units have to be triggered, it is important to consider the current states of the units and how the triggering of them would affect the behaviour of the whole pool. For this purpose, two cases are defined: "specific triggering of units" and "random triggering of units". In general, the "specific triggering of units" approach is sorting the units by their runtime and makes the decision about the units to be triggered based on this sorted list. The idea behind this algorithm is, that units, that have been off/on for a long time, are more likely to be activated/deactivated by a trigger signal. This approach neglects the possibility, that long run-/pause-times of the individual units might result in a change of its status in the near future. However, this approach is investigated here, since the pool controller does not know anything about the minimum run- and pause-times of the individual units and neither how the individual unit will cope with its thermal demand (Due to minimisation of information transmitted to the pool controller, the following exemplary questions, that would allow the further assessment of the current runtime of the units, cannot be answered by the pool controller: Is the unit under- or oversized? What is the level of refurbishment of the building? How many occupants are in the building? *etc.*).

The list of units sorted by their runtime contains the number of timesteps the individual units was on or off. On-times result in positive values, off-times in negative values in the sorted runtime list. Based on the sorted runtime-list, the "specific triggering of units" approach derives the decisions about the respective *SG-Ready* signals to be sent to the respective units for the next timestep. The algorithm used is presented in Figure 6.3. When the control variable is positive, the actual pool operation consumes more electricity than determined by the setpoint. Thus, units have to switch off. Hence, the required number of units taken from the runtime-list in descending order is receiving the *SG-Ready* "Off" signal. An example should be given: If five units have to be switched off, the five units in the pool with the longest run-time are taken. When less than five units are active in the pool, the missing number of units receiving the "Off" signal is taken from the non-active units with the shortest off-times. It is to add for consideration, whether the "Off" signal has an effect on already non-active units. In general, units with a short off-times are more likely to have a SOC of the thermal storages, which allows them to be non-active further. Since the pool controller does not know, when which unit will change its state from on to off or vice-versa, this approach is considered to be adequate in order to switch the right amount of units off.

For positive control variables, the pool controller sends the "On" signal to the required units. Here, the ascending ordered runtime-list is used. In times, the control variable and the corresponding number of units to be triggered determined by Equation 6.1 exceeds the number of units in the overall pool, the "Superheat (HP)" signal is sent to the units in the pool with the longest off-times. The other units in the pool still get the "On" signal. If the required number of units to be triggered exceeds the number of units in the overall pool more than twice, the "Superheat (HP+BH)" signal is used as well. Since the "Superheat" signals are corresponding to a higher increase in the storage temperatures compared to the "On" signal, the usage of "Superheat" signals are leading to higher electricity consumption of the units. The usage of the BH further increase the consumption. Using the activation

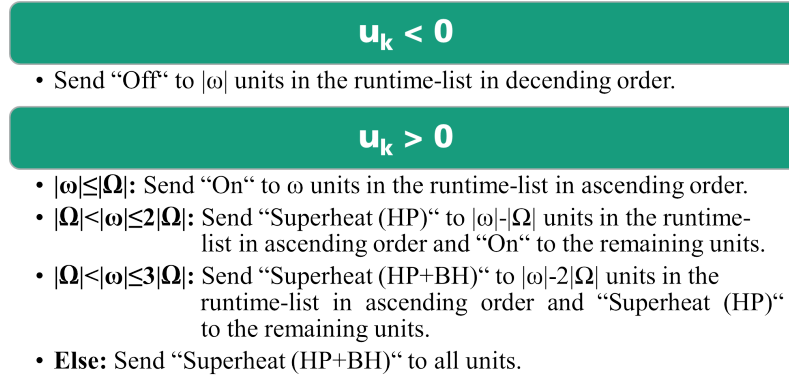


Figure 6.3: Algorithm for the "specific triggering of units" approach dependent on the control variable  $u$  in the timestep  $k$ . The algorithm transfers the number of units to trigger  $|\omega|$  into respective *SG-Ready* signals to be sent to specific units.  $\Omega$  represents the units in the pool and  $|\Omega|$  the size of the pool.

signals of *SG-Ready* can be seen as having three different and ascending levels of activation. Thus, the "On" signal is used first, before the "Superheat (HP)" signal is used. The usage of the "Superheat (HP+BH)" signal is seen as the last resort. The detailed algorithm is depicted in Figure 6.3.

The "random" triggering of units" approach acts similar to the "specific" triggering of units" approach, but uses randomised lists instead of the sorted runtime-list. It is illustrated in Figure 6.4. For the "random triggering of units" approach, the current states of the individual units (on/off) are used. The units are grouped by their status. In times,

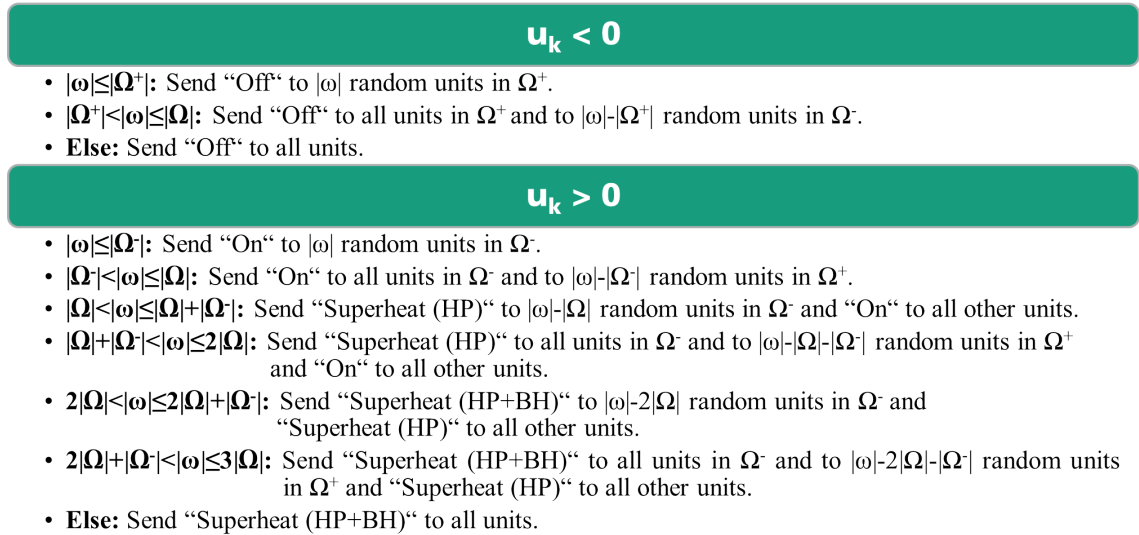


Figure 6.4: Algorithm for the "random triggering of units" approach dependent on the control variable  $u$  in the timestep  $k$ . The algorithm transfers the number of units to trigger  $|\omega|$  into respective *SG-Ready* signals to be sent to the units.  $\Omega$  represents the units in the pool and  $|\Omega|$  the size of the pool.  $\Omega^+$  are the active units in the pool,  $\Omega^-$  represent the non-active units in the pool and the respective norms stand for the sizes of the respective group.

where less consumption of the pool is required (negative control variable), the "Off" signal is sent to the respective number of units to be triggered in the group of currently active units. Within this group, the units to be triggered are chosen randomly. The composition of the randomly chosen units to be triggered is refreshed at every timestep. In times, the number of units to be triggered exceeds the number of active units in the overall pool, all active units get the "Off" signal, while the still missing number of units to be triggered is chosen randomly from the list of non-active units. By this, it is more likely, that the already non-active units will stay off in the next timestep.

For positive control variables, the algorithm as presented in Figure 6.4 is depending on the relation of number of units to be triggered to the number of units in the pool as well. Here, the same consideration for the usage of the different *SG-Ready* activation signals as being presented above applies, while choosing the units randomly from the on-list and off-list. In general for the "random triggering of units" approach, the *SG-Ready* signals are sent to random units in the off-list. If the number of non-active units is not sufficient, units are chosen randomly from the on-list as well. If the number of units to be triggered exceeds the number of units in the pool, the "Superheat (HP)" signal is used for non-active units first, before being sent to active-units as well. Active units, which are not receiving the "Superheat (HP)" are still receiving the "On" signal. If this is still not sufficient in order to trigger enough units in the pool, the "Superheat (HP)" signal is replaced by the "Superheat (HP+BH)" signal and the "On" signals is replaced by the "Superheat (HP)" signal. A threefold or more exceeding of the size of the pool results in sending the "Superheat (HP+BH)" to all units in the pool.

As it can be seen, the activation of units with *SG-Ready* offers more degree of freedom than the deactivation of units with *SG-Ready*. This is caused by the fact, that activation signals are associated with an increase in the storage temperature as presented in Section 2.9, while deactivation can only switch the units off. Moreover, the pool controller is not knowing, whether the unit triggered will react to the signal or will ignore it due to its unfavourable storage states. Furthermore, due to privacy issues, the minimum run- and pause-times of the individual units are unknown to the pool controller. For both approaches presented above, the pool controller is not taking into account the minimum run- and pause-times for its decision about which unit has to be triggered. A further modification might reflect various run- and pause-times of the units combined with a probability distribution describing the likelihood of the unit to change from on to off or vice-versa.

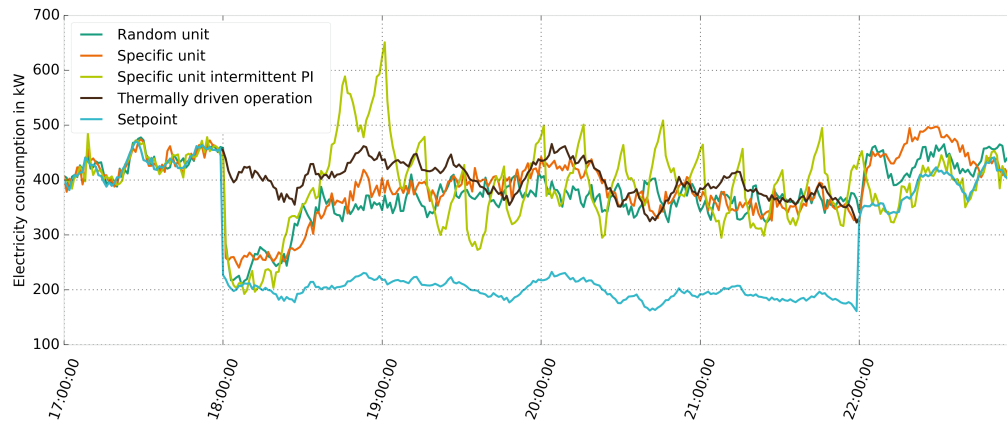
Within this thesis, the possibility to manipulate the error by using a PID-controller is implemented. The usage of a PID-controller offers the possibility to account for units not reacting to the signals sent by setting the  $P$  value above 1. Additionally, abrupt changes in the error can be considered ( $D$  value), as well as the summed error ( $I$  value). The integral part of the PID-controller allows to avoid steady-state errors by summing up the error and therefore penalising each deviation. Within the work presented here, the  $D$  value is always set to zero due to the discretised nature of the data treated. The last issue presented in Figure 6.2 to be treated by the pool controller is intermittencies. This encloses possible changes in the behaviour of the pool controller due to changes of the boundary conditions (*e.g.* from winter to summer). The consideration of intermittencies is important for the pool controller in order to chose the right strategy to cope with errors

between actual pool operation and setpoint. Intermittencies are treated within this work by offering the possibility to reset the integral part of the PID-controller to zero every 15 min. This is motivated by the fact, that the balancing responsible party is responsible for scheduling the energy consumption in 15 min slots [Konstantin, 2013, p. 465]. Thus, the scheduled energy consumption has to be matched every 15 min. Another possible setting is, to reset the integral part of the PID-controller only every hour, corresponding to the hourly time slots to purchase the electricity consumption. The reset to zero of the summed error every 15 min is the only intermittencies considered within this work. Thus, when the pool controller does not achieve to fulfil the setpoint in a 15 min block, the following 15 min blocks are not affected by soaring integral values. Further considerations and implementations of intermittencies may come with big advantages for the performance of the pool controller, but are not treated within this work.

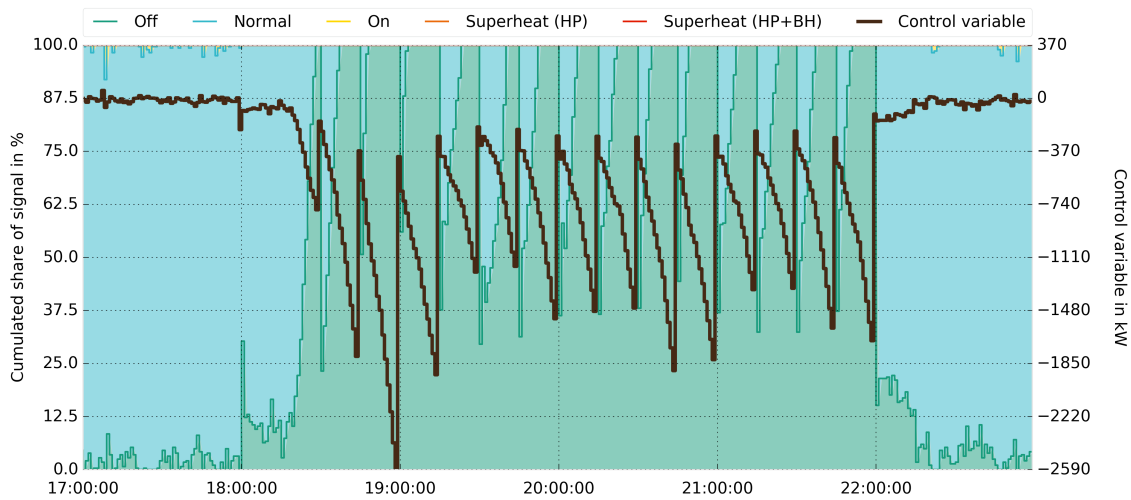
## 6.2 Proof of concept

This section analyses, the performance of the pool controller when having to change the pool's operation according to a setpoint. Thus, the pool controller framework as presented in Section 6.1 is tested here with different settings of the pool controller. The pool controller settings investigated are: "random triggering of units", "specific triggering of units" and "specific triggering of units" with PID-controller with enabled intermittency behaviour. The PID-controller configuration is:  $P=1.0$ ,  $I=1.0$ ,  $D=0.0$ . Due to the discretised nature of the simulation, the  $D$  value is chosen to be zero. By doing so, the controller manipulating the error is a PI-controller. The  $P$  and  $I$  values are chosen randomly and shall only highlight the operation of the HP pool, when the error is manipulated by a PI-controller. Moreover, the integral part of the PI-controller is reset to zero every 15 min. Therefore, the control variable, which is converted to the number of units to trigger afterwards, is fluctuating due to the intermittent integrated error between setpoint and actual pool operation. The setpoints investigated are relative steps of  $\pm 50\%$  of the current thermally driven operation. These steps are applied in the morning and evening hours, when a high thermal demand occurs (see Section 4.1). The steps are applied over a period of four hours. The results presented here represent exemplary chosen winter days.

First, the performance of the pool controller when having to achieve a step of  $-50\%$  of the current thermally driven operation is analysed. The results are presented in Figure 6.5a, which is illustrating the electricity consumption of various simulations with different pool controller settings for the 16<sup>th</sup> of February 2015. When the pool controller is not active, the operation is similar to the thermally driven operation in Figure 6.5a. From 18 to 22 o'clock, the step is applied, which is forming the setpoint. It can be seen, that all three investigated controllers can not follow the setpoint longer than 20 min. Moreover, the "random triggering of units" and the "specific triggering of units" are performing similarly. The PI-controller is able to follow the setpoint longer than the other two pool controller settings. Nevertheless, after around 20 min, the error between HP pool operation controlled by the PI-Controller is increasing. Moreover, the HP pool is consuming more energy than the thermally driven operation around 35 min after the step setpoint has been applied. After that, the PI-controller affected operation shows an electricity consumption oscillating around the thermally driven operation. The "random" and the "specific triggering of



(a) Operation of the pool controller with different settings at the 16<sup>th</sup> of February. The setpoint is a relative step of -50 % of the thermally driven operation.



(b) Operation of the pool controller affected by the intermittent PI-controller at the 16<sup>th</sup> of February. The cumulated share of signals sent by the pool controller is depicted together with the control variable.

Figure 6.5: Operation of the pool controller at the 16<sup>th</sup> of February.

units" approaches are achieving an electricity consumption closer to the setpoint as the PI-controller from around 20 min to around 80 min after the step setpoint has been begun.

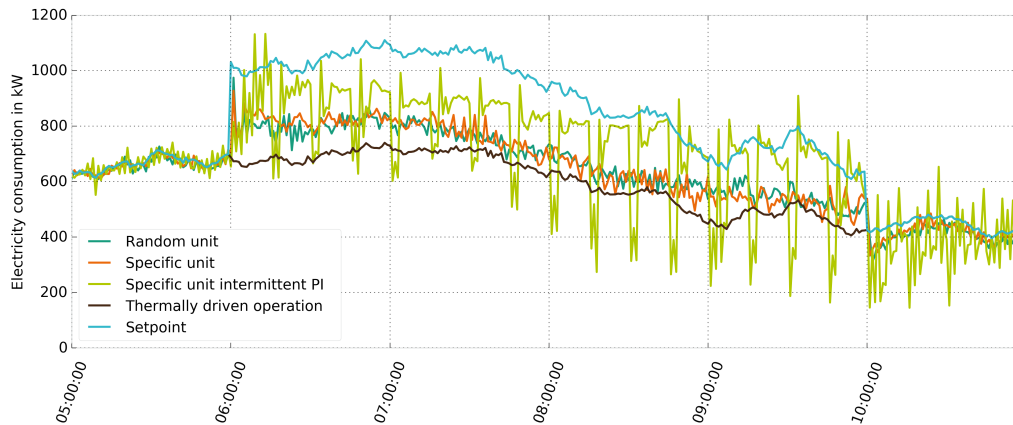
In the following, the behaviour of the pool controller itself shall be analysed. For this purpose, the control variable and the corresponding signals sent are investigated. This is presented for the PI-controller exemplary. The cumulated shares of signals being sent by the pool controller are illustrated by Figure 6.5b together with the control variable. It can be seen, that the pool controller is sending varying "Off" and "On" signals, before the step setpoint becomes active. Without action of the pool controller, all units would have the signal "Normal", representing the uninfluenced operation. With active step setpoint at 18 o'clock, the control variable drops and the number of units receiving the "Off" signal increases remarkably. Between 18:15 and 18:30 o'clock, the control variable decreases to a lower level, forcing the pool controller to send the "Off" signal to all units. However, the pool controller is not able to follow the setpoint. At 18:30 o'clock, the control variable leaps to a higher level as before. This is caused by the reset to zero of the integral part of

the PI-controller every 15 min. The same applies every 15 min, which causes the leaps in the control variable associated with the leaps in the number of units receiving the "Off" signal.

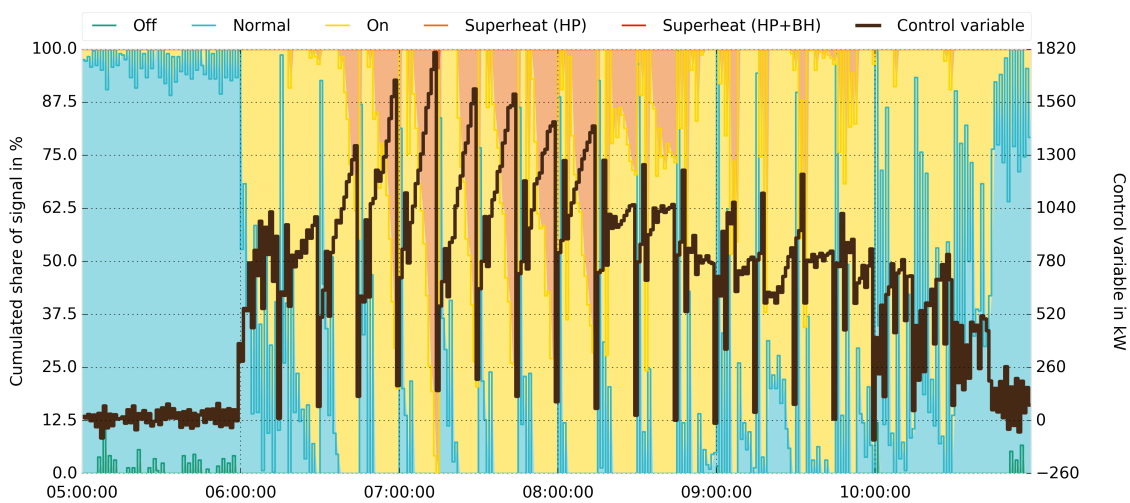
The integral value of the PI-controller is affecting the number of units receiving the "Off" signal remarkably, since the reset to zero of  $I$  results in a decrease in the number of units to be triggered with the "Off" signal. However, the sending of the "Off" signal to all units does not lead to a match between pool controller affected operation and setpoints. Even increasing the number of units to trigger would not improve the performance of the pool controller, since the HP pool has to regenerate from the triggering with the deactivation signal. Due to this regeneration, some of the HPs are ignoring the trigger signal and are operating their individual thermal storages within their respective boundaries and with regard to minimum run- and pause-times priority. Thus, long timespans with a setpoint lower than the electricity consumption of the thermally driven operation are hard to be realised by the pool controller. This is caused by the fact, that the deactivation with *SG-Ready* as it is implemented within this thesis is not accompanied by a decrease in the temperatures of the thermal storage. Thus, the available flexibility for the deactivation of the units is limited, since the HPs are already running in their energy efficient mode and deactivations only shift the times of the provision of the thermal demand. These observations, considerations and conclusions are well aligned with the findings of *Fischer et al. [2016b]*, *Wolf [2016]* and *Fischer et al. [2017]*, which were using the same pool of houses (while *Fischer et al. [2017]* has used the same implementation of the *SG-Ready* signals as well).

In the following, the performance of the pool controller is analysed for a step setpoint of +50 % relative to the current thermally driven operation. The presented day is the 12<sup>th</sup> of February. Figure 6.6a shows the operation of the pool with the same various pool controller settings as presented above. It can be seen, that the "random triggering of units" approach and the "specific triggering of units" approach perform similar again. Moreover, the operation affected by the PI-controller is able to follow the setpoint better than with the other two pool controller settings. However, the PI-controller affected operation is oscillating around the thermally driven operation with a period of 15 min. This is caused by the reset to zero of the  $I$  value every 15 min. Compared to the step of relatively -50 %, the pool controller is able to handle a step of relatively +50 % better. Thus, the error between setpoint and actual pool operation is not rising with increasing length of the step setpoint when using the intermittent PI-controller. Moreover, the pool operation sometimes matches with the setpoint even 3 hours after the step has begun.

Figure 6.6b is showing the signal distribution sent by the pool controller with intermittent PI-controller. Before resetting the  $I$  value to zero, the control variable reaches high values, especially around 7:15 o'clock. This is accompanied by the sending of the "Superheat (HP)" signal to the units with the longest off-time. At 7:15 o'clock, even the "Superheat (HP+BH)" signal is sent to a few HP units in the pool. Due to the reset of the  $I$  value every 15 min, the "Superheat" signals are not sent constantly. Thus, the pool operation affected by the PI-controller is converging towards the setpoint before resetting the integral value. Figure 6.6b shows, that the effect of the different activation levels of *SG-Ready* offer the possibility to shift load over a wide timespan. Moreover, it seems,



(a) Operation of the pool controller with different settings at the 12<sup>th</sup> of February. The setpoint is a relative step of +50 % of the thermally driven operation.



(b) Operation of the pool controller affected by the intermittent PI-controller at the 12<sup>th</sup> of February. The cumulated share of signals sent by the pool controller is depicted together with the control variable.

Figure 6.6: Operation of the pool controller at the 12<sup>th</sup> of February.

that most of the units triggered are following the trigger signals received, as the error in Figure 6.6a correlates well with the control variable depicted in Figure 6.6b. The findings for the setpoint of a relative step of +50 % are aligned with the findings of *Fischer et al. [2016b]*, *Wolf [2016]* and *Fischer et al. [2017]*, since by activating the pool, a remarkable load shifting potential can be unlocked.

The performance of the pool controller with intermittent PI-controller could further improve by modifying the resetting to zero and the associated impact of the error history on the control variable. Limiting the  $I$  value could be a possible solution, as well as the change of the reset times to higher values than 15 min, or the implementation of self-adjusting  $I$  values. Furthermore, the configuration of the PID-controller has to be fine-tuned. Moreover, the relation between current run-/pause-times and their respective minimum run-/pause-times could be considered as well. Additionally, the implementation of the relative current thermal demand into these considerations might lead to further improvements of the performance of the pool controller. Thus, units with high off-times

would not be preferred to be activated by the pool controller, since they are more likely to switch on by themselves due to the required provision of the respective thermal demand. These considerations explain the similarity in the pool operation, when using the "random units to be triggered" and the "specific units to be triggered" approaches.

### 6.3 Analysis of the controlled cost-efficient operation

This section evaluates the performance of the pool controller when influencing the pool in order to match the operation of the HP pool with the purchased operation trajectory. Here, the setpoint of the pool operation is the optimised pool operation trajectory obtained as described in Section 5. For the operation of the pool controller, the hourly means of the optimised operation are used. For the scenario considered within this thesis, this hourly consumption curve would be purchased on the *EPEX* day-ahead spot market and this purchased hourly blocks of energy would have to be matched by the actual pool operation (see Section 1.2 and 1.4). For this purpose, the pool controller is introduced in Section 6.1 and its general performance is analysed in Section 6.2. In the following, the same three configurations as they are presented in Section 6.2 are used in order to operate the pool of HPs according to the setpoint: "random triggering of units", "specific triggering of units" and "specific triggering of units" with PID-controller with enabled intermittency behaviour. Thus, for the latter, the integral value is reset to zero every 15 min. The proportional value  $P=1.0$ , and the weight of the integral error  $I=1.0$ .

Figure 6.7 presents the operation of the three different pool controller configurations from morning to noon at the 1<sup>st</sup> of February. The optimisation of the same day is presented in Figure 7.1. The electricity consumption obtained by the optimisation is resampled to a resolution of one hour in order to be purchased and used as the setpoint of the pool controller. Thus, the setpoint in Figure 7.1 has a resolution of one hour. Moreover, the thermally driven operation representing the HP pool operation when not being influenced externally and only providing the thermal demand of the respective houses is given as well.

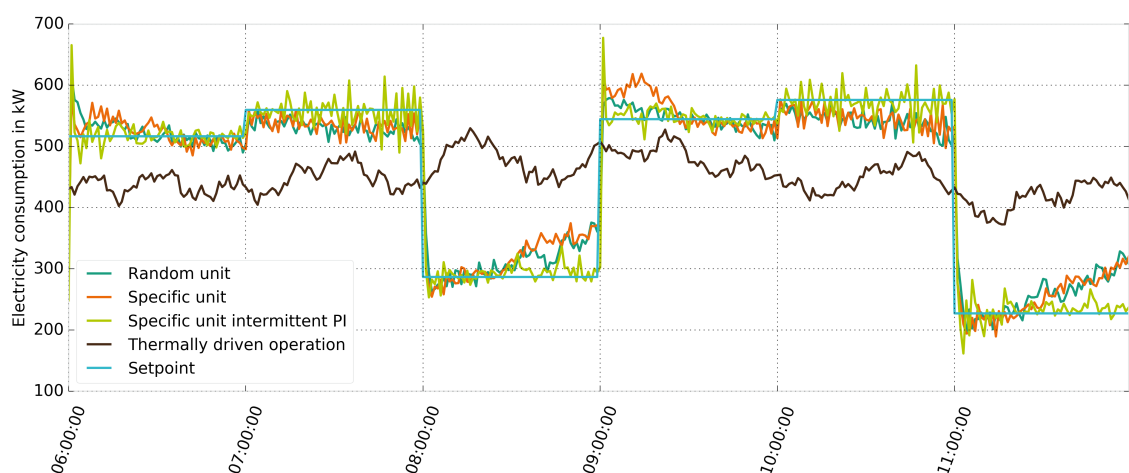


Figure 6.7: Operation of the heat pump pool at the 1<sup>st</sup> of February. The figure compares different configurations of the pool controller and their ability to operate the pool according to the setpoint. The setpoint is represented by the optimised operation trajectory purchased.

Figure 6.7 shows, that the three different configurations of the pool controller perform differently. The energy consumed is reflected by the integrals under the curves in Figure 6.7. As already seen in Section 6.2, the PI-controller configuration with enabled intermittency performs the best. When the pool has to consume more energy as determined by the thermally driven operation, the intermittent PI-controller is able to affect the operation of the HPs in a way, that the pool is following close to the setpoint. Thus, the pool controller with intermittent PI-controller is able to increase the electricity consumption of the pool from 6 o'clock to 8 o'clock and from 9 o'clock to 11 o'clock. Between 8 o'clock to 9 o'clock and between 11 o'clock to 12 o'clock, the pool controller has to initiate a partly regeneration of the HP pool and thereby decrease the energy consumption of the pool. Here, the advantages of the intermittent PI-controller manipulating the error between setpoint and actual pool operation become obvious: The other two pool controller configurations are not able to decrease the pool's electricity consumption sufficiently longer than over a timespan of around 30 min. In contrary, the intermittent PI-controller configuration is able to closely shift the operation to the setpoint even at the end of the respective hour. However, the reset of the integral value in the intermittent PI-controller is illustrated by the peaks in the error between setpoint and operation every 15 min.

In order to quantify the error of the operation influenced by the pool controller, the error values are investigated for every hour. Since the energy is purchased for the respective hour, the pool operation has to consume the respective amount of energy. Thus, the difference between energy consumed and purchased should be zero. For the assessment of the three different pool controller settings, these differences in energy consumed per hour are calculated. The results obtained for the configuration with intermittent PI-controller are presented in Figure 6.8. It can be seen, that the difference is higher in winter than in summer. Moreover, it can be seen, that the majority of the values is negative. This indicates, that the HP pool consumed more energy as determined by the setpoint.

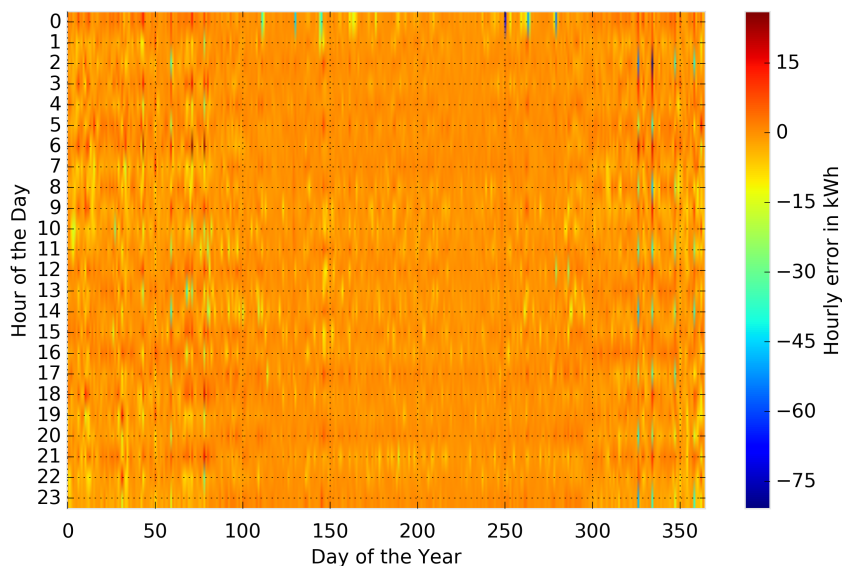


Figure 6.8: Hourly error of the operation influenced by the pool controller with intermittent PI-controller. The values represent the difference in the energy purchased and the energy consumed by the pool operation in the respective hour.

The accuracy of trajectory of the setpoint is analysed by calculating the absolute of the differences in energy purchased and energy consumed for every hour  $h$ . These absolute values are summed over the whole year and normed by the sum of energy purchased as described in Equation 6.2. The results show, that the pool controller performs the best by having the configuration with an intermittent PI-controller with a  $\gamma$  value of 1 %. The configuration with "specific triggering of units" yields a relative annual absolute error in the energy consumed of around 2.5 %. The "random triggering of units" approach performs the worst by having a  $\gamma$  of around 2.7 %. Here, it can be concluded, that in general, using the "specific triggering of units" is advantageous compared to using the "random triggering of units" approach. However, further studies should investigate, whether a larger pool of HPs with various minimum run- and pause-times reduce this advantage. Furthermore, it has to be stated, that these three pool controller configurations as they are presented here are not fine-tuned yet and have to be seen as a general assessment of the pool controller's performance rather than representing the optimal state and configuration of the pool controller.

$$\text{relative annual absolute error} = \gamma = \frac{\sum_{h=1}^{8760} |\text{error in energy consumption}(h)|}{\sum_{h=1}^{8760} \text{energy consumption of the setpoint}(h)} \quad (6.2)$$

In order to analyse, how the pool controller with intermittent PI-controller deals with various setpoints at various thermal loads in the houses, Figure 6.9 is given. Here, the relative error is calculated by dividing the differences between energy purchased and energy consumed for every hour by the energy consumed by the thermally driven operation at the respective hour. The relative setpoint is obtained similarly by dividing the energy purchased and determined by the setpoint at every hour by the energy consumed by the thermally driven operation at the respective hour. By this normalisation procedure, the influence of the thermal demand of the buildings and thereby the influence of the ambient temperature on the pool controller's performance is taken out of Figure 6.9. An explanatory example should be given: A relative error of -0.05 at a relative setpoint of 0.5 means, that the HP pool is exceeding the energy purchased by amount being equal to 5 % of the thermally driven energy consumption in this hour, when the setpoint demands a decrease in the energy consumption to half the level of the thermally driven operation. Note, that due to reasons of clarity, extreme values are cut of Figure 6.9 by adjusting the ranges of the axes presented.

It can be seen in Figure 6.9, that in general, the controlled HP pool tends to consume too much energy, when a decrease in consumption is demanded by the setpoint. Moreover, the controlled HP pool consumes too less energy, when an increase in consumption is required. This issue could be solved by increasing the  $P$  or the  $I$  value. Additionally, when only the provision of the thermal demand is required (relative setpoint equal to one), there is a visible trend, that the pool consumes too much energy. This is caused by a regeneration of the pool with an associated increase in electricity consumption. However, the majority of the 8760 hours analysed in Figure 6.9 is having parameters indicating that the setpoint is nearly fulfilled. Nevertheless, it becomes obvious, that the pool controller's configuration with the intermittent PI-controller needs further fine-tuning. Thus, the impact of adjusted  $P$  and  $I$  values on the performance should be investigated in further work. Moreover, the

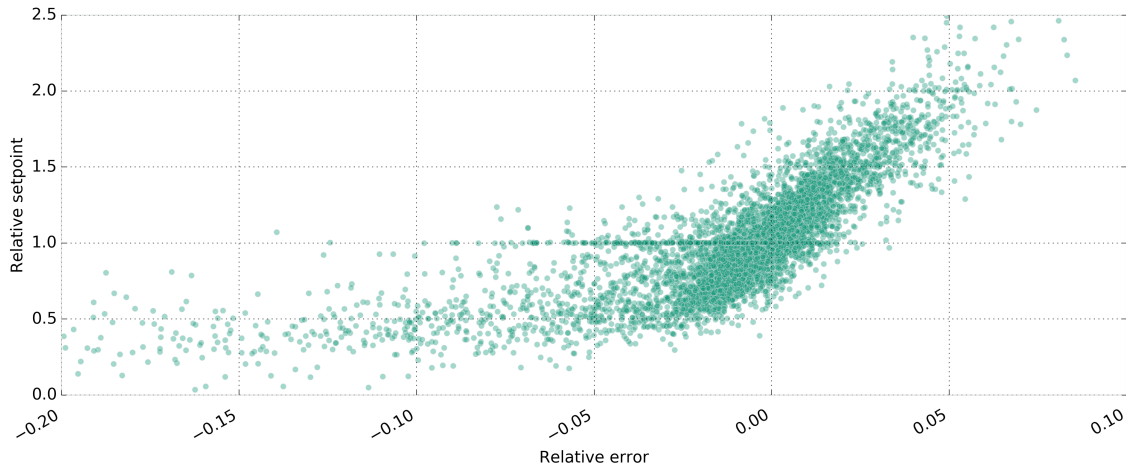


Figure 6.9: Relative error of the operation influenced by the pool controller with intermittent PI-controller versus relative setpoint. The relation is calculated with regard to the thermally driven operation at the respective hour.

resetting to zero of the  $I$  value could be revised to be only conducted every hour (although this might come with an increased tendency for an oscillating behaviour). The need for a fine-tuning is further supported by Figure 6.10, which is presenting the relative error in energy consumption being normalised to the setpoint over the whole year (Note, that the few amount of extreme values are limited to the bounds presented in Figure 6.10). This figure illustrates, that the fine-tuning of the intermittent PI-controller configuration should focus on the summer months, where the pool is repeatedly consuming too much energy. The implementation of a further intermittency by increasing the weight of the integral error  $I$  in summer, could be one possible solution in order to obtain a better performance of the pool controller here.

However, the general fine-tuning should be carried-out for the behaviour of the pool controller over the course of the whole year. This is represented by the fact, that the more progressive setpoint being the SLP operation as presented in Section 4.2.2 is yielding poorer results. The operation according to the SLP cannot be realised as good by the pool controller as the operation according to the optimised operation. Here, the best-performing configuration with intermittent PI-controller achieves a relative annual absolute error value  $\gamma$  of 16.3 %. The reason for this performance is, that the required load shiftings have a long duration and thereby are more than exceeding the available load shifting potential of the HP pool.

Furthermore, future studies should investigate, whether the increase of the amount of information available for the pool controller (*e.g.* SOC of the thermal storages of the individual HPs, indoor temperatures, *etc.*) would lead to any further improvements of the pool controller's performance. Nevertheless, the additional costs of monitoring and transmitting more information have to be taken into account, when deciding about the modification of the pool controller's algorithms.

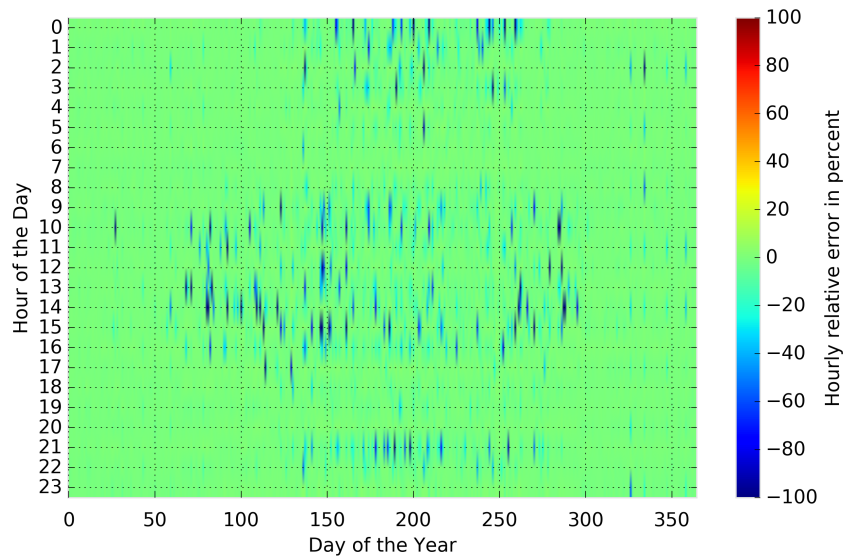


Figure 6.10: Hourly relative error of the operation influenced by the pool controller with intermittent PI-controller. The values represent the difference in the energy purchased and the energy consumed by the pool operation in the respective hour. The values are normalised to the setpoint in the respective hour.



# 7 Conclusion and perspectives

## 7.1 Conclusion

This master's thesis investigates with the aid of simulations, how the operation of a pool of heat pumps (HP) can be conducted more cost-efficiently. The demand for such an optimisation originates from the correlation between installation rates and electricity consumption costs and the need to install more HPs in residential buildings in order to achieve the German climate goals. Within this work, the scenario drawn comprises of a centrally acting aggregator, which is responsible for the operation of a pool of HPs. This aggregator calculates day-ahead the optimised pool operation in terms of electricity consumption costs and purchases the obtained optimised energy consumption trajectory on the *EPEX* day-ahead spot market. Then, a pool controller has to influence the pool's operation in order to match the actual electricity consumption with the one purchased. The HP pool used consists of 284 individually acting HPs, which are influenced through direct load control signals defined by the *SG-Ready* label. The individual HP follows the *SG-Ready* trigger signal, unless either the provision of space heating (SH) and domestic hot water (DHW) demand, or their minimum run-/pause-times would be affected negatively.

The analysis of the uninfluenced thermally driven operation of the HP pool shows, that SH is causing the highest peak in electricity consumption in winter. These peaks occur in the morning and evening. In summer, electricity consumption peaks originating from the DHW demand are observed in the morning. The peaks in electricity consumption correlate positively with high day-ahead prices in the same timespans. Consequently, a cost-efficient operation should aim, to shift the electricity consumption from the morning and evening hours to the midday and night. When evaluating the standard load profile (SLP) for this pool of HPs, it is found, that the local distribution system operator (DSO) assumes the electricity consumption to be steady throughout the day. Thereby, the DSO does not take into account the peak loads for its considerations.

The optimisation of the HP pool operation is based on a storage model representing the available flexibility of the HP pool. The optimisation algorithm predicts the day-ahead spot market prices for electricity, as well as the uninfluenced thermally driven operation. For the determination of the pool's flexibility parameters, the findings of *Fischer et al. [2016b]* and *Fischer et al. [2017]* are used. The obtained *Linear Programming* problem (*LP*) within this work is constrained by these flexibility parameters and uses perfect prognoses. In general, it is important to constrain the optimisation sufficiently, in order to enable the pool controller to subsequently operate the pool according to the optimised trajectory obtained. The optimised operation trajectory shows a load shifting pattern similar to the ones presented in the related research. However, a small saving rate in the electricity consumption costs of around 0.47 % is yielded. This is based on the constraint, that the load shifting has to be conducted and completed within a certain timespan defined by the pool's flexibility. This timespan is not large enough in order to utilise the existing

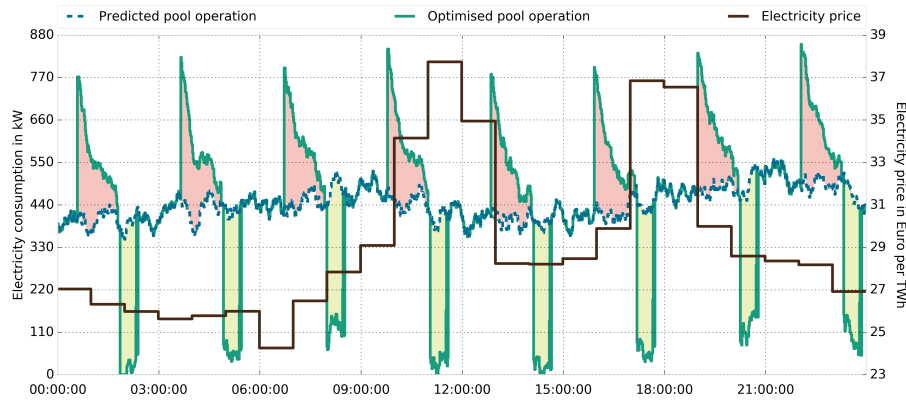


Figure 7.1: Results of the  $LP$  optimisation obtained for the 1<sup>st</sup> of February.

variability in the electricity prices and should be revised. Further modifications of the optimisation should comprise of a higher level of detail and complexity and are expected to yield higher rates of savings by extending the load shifting periods. By this, the requested shift of the pool's load in the morning and evening towards the midday and night could be achieved further.

In order to operate the HP pool according to the optimised electricity consumption trajectory purchased, a pool controller is introduced. This controller calculates the error between actual operation and the one purchased and converts this error into the control variable. Afterwards, the pool controller converts the control variable into the required number of units, that have to be triggered, and calculates, which signals have to be sent. Three different preliminary configurations of the pool controller are investigated: Random triggering of units, specific triggering of units, and specific triggering of units where the control variable is obtained by manipulating the error with a PI-controller. This PI-controller is implemented in a way, that the integral error is reset to zero every 15 min. An investigation of long-term load shifts shows, that the pool controller is able to decrease the pool's electricity consumption only for a limited period of time. Therefore, when decreasing the pool's load, an elaborated acting of the pool controller is required in order not to exceed the available flexibility and to allow the pool to restore its load shifting potential adequately. The pool controller shows good results when influencing the HP pool's operation in order to match the optimised trajectory purchased. The specific triggering of units with the intermittent PI-controller shows the best accuracy of trajectory having a relative annual absolute error in the energy consumption of around 1 %. This error, mostly occurs in winter when trying to decrease the pool's load. The three configurations of the pool controller presented and evaluated are preliminary and it is expected, that further fine-tuning of the pool controller will lead to remarkable improvements in the accuracy of trajectory.

**This work presents with the aid of simulations, that saving potential exists for the electricity consumption costs of a heat pump pool operated by a centrally acting aggregator. Moreover, this potential can be lifted by  $LP$ -optimisation with regard to the flexibility of the pool. Furthermore, the operation of the pool according to this optimised trajectory is possible with a good accuracy of trajectory when conducted by a centrally acting pool controller.**

## 7.2 Perspectives

This master's thesis has identified several fields, where future work could lead to useful further insights about the operation of a HP pool and its economic optimisation. For example, it should be investigated, whether the peaks in the electricity demand of the individual HPs smooth out by increasing the number of HPs in the pool. Note, that the individual HP should still be represented by underlying stochastic bottom-up models. If such a smoothing cannot be found, these further studies would support the necessity to shift the HP pool's load. Moreover, additional SLPs from other distribution system operators should be analysed with regard to their ability to reflect the peak consumptions.

In order to develop suitable business models for the implementation and action of a pool aggregator, it is essential to take a deep look into the structures forming the electricity tariffs, that are offered for the operation of HPs. By doing so, possible further obstacles and revenue streams could be revealed. Based on the findings, the operation of the aggregator and the pool controller should be adjusted accordingly. The implementation of the investment costs, operation costs and maintenance costs into the calculations should be considered as well in order to achieve a holistic economic assessment of the aggregator's role. Moreover, the impact of the actions of the aggregator on the composition of the prices and HP electricity tariffs could be assessed too. It should be noted, that the bidding of the aggregator on the day-ahead market is expected to influence the prices, which would affect the saving rates. Additionally, possible compensatory payments when the pool's energy consumption deviates from the one purchased should be considered.

For the optimisation and the subsequent influence of the HP pool's operation, sufficient knowledge about the pool's flexibility is essential. In order to cope with intra-day incalculables due to insufficient predictions, the implementation of intra-day purchase of energy could also be included into the role of the aggregator. Moreover, the optimisation should predict the input parameters, rather than using perfect predictions. In general, the load shifting should be allowed to cover longer timespans, in order to utilise the price variabilities further. For this purpose, a better knowledge about the pool's flexibility by exactly knowing the expectable load shifting characteristics at the respective ambient temperature would be useful. Additionally, negative electricity prices could be further utilised by superheating the HPs to the highest possible storage temperature levels in order to reduce the load in the subsequent timespan. Regarding the pool controller, it could be investigated, whether using more information besides the HPs' electricity consumption leads to a better accuracy of trajectory. This investigation should also consider the additional costs for installation and maintenance of the measurement infrastructure and the costs for processing of the additional information. By this, a suitable trade-off between amount of information transmitted and accuracy of trajectory achieved could be found.

In general, it should be considered to implement a model predictive framework into the optimisation and the action of the pool controller. By this, the interdependency between the optimisation and the pool controller could be taken into account sufficiently. Thereby, the optimum operation of the pool, which is still able to be realised by the pool controller and does not jeopardise the near-future flexibility and load shifting ability of the pool, could be found. However, it is expected that such a holistic model predictive approach would come with high efforts for the sufficient modelling of the various systems' behaviour.



# Bibliography

- Arbeitsgemeinschaft Energiebilanzen e.V. Anwendungsbilanzen für die Endenergiesektoren in Deutschland in den Jahren 2011 und 2012 mit Zeitreihen von 2008 bis 2012. (Projektnummer: 23/11):33, 2013. URL [http://www.ag-energiebilanzen.de/index.php?article\\_id=29&fileName=ageb\\_endbericht\\_anwendungsbilanzen\\_2011-2012\\_endg.pdf](http://www.ag-energiebilanzen.de/index.php?article_id=29&fileName=ageb_endbericht_anwendungsbilanzen_2011-2012_endg.pdf).
- B. Biegel, P. Andersen, T. S. Pedersen, K. M. Nielsen, J. Stoustrup, and L. H. Hansen. Electricity market optimization of heat pump portfolio. In *IEEE International Conference on Control Applications (CCA)*, pages 294–301, Hyderabad, 2013. ISBN 9781479915590. doi: 10.1109/CCA.2013.6662774.
- B. Biegel, M. Westenholz, L. Henrik, J. Stoustrup, P. Andersen, and S. Harbo. Integration of flexible consumers in the ancillary service markets. *Energy*, pages 1–11, 2014. ISSN 0360-5442. doi: 10.1016/j.energy.2014.01.073. URL <http://dx.doi.org/10.1016/j.energy.2014.01.073>.
- BMUB. Bundesministerium für Umwelt, Naturschutz, Bau und Reaktorsicherheit. Klimaschutzplan 2050. pages 1–96, 2016. ISSN 00308870. doi: 10.1016/j.aqpro.2013.07.003.
- Bundesamt für Bauwesen und Raumordnung (BBR) in Zusammenarbeit mit der Climate and Environment Consulting Potsdam GmbH und dem Deutschen Wetterdienst. Handbuch Testreferenzjahre von Deutschland für mittlere, extreme und zukünftige Witterungsverhältnisse. *Download 2014* [Http://Www.Bbsr-Energieeinsparung.De/](http://Www.Bbsr-Energieeinsparung.De/), Offenbach(last update: September 2014):75 pages, 2012. URL [http://www.bbsr-energieeinsparung.de/EnEVPortal/DE/Regelungen/Testreferenzjahre/Testreferenzjahre/TRY\\_Handbuch.pdf?\\_\\_blob=publicationFile&v=2](http://www.bbsr-energieeinsparung.de/EnEVPortal/DE/Regelungen/Testreferenzjahre/Testreferenzjahre/TRY_Handbuch.pdf?__blob=publicationFile&v=2).
- B. Burger and Fraunhofer Institute for Solar Energy Systems ISE. Electricity production and spot prices in March 2017, 2017, cited: 2017-04-20, 2017a. URL <https://energy-charts.de/price.htm>.
- B. Burger and Fraunhofer Institute for Solar Energy Systems ISE. Annual renewable shares of electricity production in Germany, 2017, cited: 2017-04-20, 2017b. URL [https://energy-charts.de/ren\\_share.htm](https://energy-charts.de/ren_share.htm).
- C. Carmo, N. Detlefsen, and M. Nielsen. Smart Grid Enabled Heat Pumps: An Empirical Platform for Investigating how Residential Heat Pumps can Support Large-scale Integration of Intermittent Renewables. *Energy Procedia*, 61:1695–1698, 2014. ISSN 18766102. doi: 10.1016/j.egypro.2014.12.194. URL <http://linkinghub.elsevier.com/retrieve/pii/S1876610214032238>.
- Y. A. Cengel, J. M. Cimbala, and R. H. Turner. *Fundamentals of Thermal-Fluid Sciences*. McGraw-Hill, second edition, 2003.

- Deutscher Bundestag. Verordnung über den Zugang zu Elektrizitätsversorgungsnetzen (Stromnetzzugangsverordnung - StromNZV). 2016.
- DIN EN ISO 13790. Berechnung des Energiebedarfs fuer Heizung und Kuehlung, 2008.
- J. Fink and R. P. V. Leeuwen. Earliest Deadline Control of a Group of Heat Pumps with a Single Energy Source. *Energies*, pages 1–16, 2016. doi: 10.3390/en9070552.
- D. Fischer and H. Madani. On heat pumps in smart grids: A review. *Renewable and Sustainable Energy Reviews*, 70:342–357, 2017. ISSN 13640321. doi: 10.1016/j.rser.2016.11.182.
- D. Fischer, T. Wolf, J. Scherer, and B. Wille-Haussmann. A stochastic bottom-up model for space heating and domestic hot water load profiles for German households. *Energy and Buildings*, 124:120–128, 2016a. ISSN 03787788. doi: 10.1016/j.enbuild.2016.04.069. URL <http://linkinghub.elsevier.com/retrieve/pii/S0378778816303358><http://www.sciencedirect.com/science/article/pii/S0378778816303358>.
- D. Fischer, T. Wolf, J. Wapler, and R. Hollinger. Model-based Flexibility Assessment of a Residential Heat Pump Pool. *Energy*, 118:853–864, 2016b. ISSN 03605442. doi: 10.1016/j.energy.2016.10.111. URL <http://dx.doi.org/10.1016/j.energy.2016.10.111>.
- D. Fischer, T. Wolf, and M.-A. Triebel. Flexibility of heat pump pools: The use of SG-Ready from an aggregator’s perspective. In *12th IEA Heat Pump Conference*, pages 1–12, Rotterdam, 2017. IEA Energy Technology Network.
- Fraunhofer IWES/IBP. Wärmewende 2030. Schlüsseltechnologien zur Erreichung der mittel- und langfristigen Klimaschutzziele im Gebäudesektor. Technical report, Agora Energiewende, Berlin, 2017. URL [https://www.agora-energiewende.de/fileadmin/Projekte/2016/Sektoruebergreifende\\_EW/Waermewende-2030\\_WEB.pdf](https://www.agora-energiewende.de/fileadmin/Projekte/2016/Sektoruebergreifende_EW/Waermewende-2030_WEB.pdf).
- V. Gorris and A. Jacob. BWP-Branchenstudie 2013: Szenarien und politische Handlungsempfehlungen. Technical report, Bundesverband Waermepumpe (BWP) e.V., Berlin, 2013.
- T. Hartmann, T. Mühlhaus, H. Neumann, H. Reuter, and H. Röschmann. Lastprofile für unterbrechbare Verbrauchseinrichtungen - LPuVe-Praxisleitfaden. *VWEW Energieverlag GmbH*, page 26, 2003.
- Intergovernmental Panel on Climate Change. *Climate Change 2014: Mitigation of Climate Change*. 2014. ISBN 9781107654815. doi: 10.1017/CBO9781107415416. URL <http://www.ipcc.ch/report/ar5/wg3/>.
- W. Kahlenborn and L. Brüning. *Climate Protection in Figures Facts - Trends and Incentives for German Policy*. Federal Ministry for the Environment, Nature Conservation, Building and Nuclear Safety (BMUB), 2014. URL [http://www.bmub.bund.de/fileadmin/Daten\\_BMU/Pool/Broschueren/klimaschutz\\_in\\_zahlen\\_2014\\_broschuere\\_en\\_bf.pdf](http://www.bmub.bund.de/fileadmin/Daten_BMU/Pool/Broschueren/klimaschutz_in_zahlen_2014_broschuere_en_bf.pdf).

- M. Koch. Regularium für das Label "SG Ready" für elektrische Heizungs- und Warmwasserwärmepumpen, 2013. URL [http://www.waermepumpe.de/fileadmin/user\\_upload/waermepumpe/02\\_Waermepumpe/Qualitaetssicherung/SG\\_Ready/2012-11-01\\_SG\\_Ready\\_Regularien\\_Version1.1.pdf](http://www.waermepumpe.de/fileadmin/user_upload/waermepumpe/02_Waermepumpe/Qualitaetssicherung/SG_Ready/2012-11-01_SG_Ready_Regularien_Version1.1.pdf).
- M. Koch, A. Sperr, H. Thamm, V. Weinmann, E. Tippelt, S. Höfener, and J. Rummen. BWP-Branchenstudie 2015 - Szenarien und politische Handlungsempfehlungen. Technical report, German Heat Pump Association, BWP, Berlin, 2015.
- P. Konstantin. *Praxisbuch Energiewirtschaft*. Springer Berlin Heidelberg, Berlin, Heidelberg, 2013. ISBN 978-3-642-37264-3. doi: 10.1007/978-3-642-37265-0. URL <http://link.springer.com/10.1007/978-3-642-37265-0>.
- T. Nowak and P. Westring. European Heat Pump Market and Statistics Report 2015. Technical report, The European Heat Pump Association AISBL (EHPA), Brussels, 2015.
- T. S. Pedersen, P. Andersen, and K. M. Nielsen. Central control of heat pumps for smart grid purposes tested on single family houses. In *2013 10th IEEE INTERNATIONAL CONFERENCE ON NETWORKING, SENSING AND CONTROL (ICNSC)*, pages 118–123. Ieee, apr 2013. ISBN 978-1-4673-5200-0. doi: 10.1109/ICNSC.2013.6548722. URL <http://ieeexplore.ieee.org/lpdocs/epic03/wrapper.htm?arnumber=6548722>.
- T. S. Pedersen, K. M. Nielsen, and P. Andersen. Maximizing Storage Flexibility in an Aggregated Heat Pump Portfolio. In *IEEE Conference on Control Applications*, pages 286–291, Antibes, France, 2014. ISBN 9781479974092. doi: 10.1109/CCA.2014.6981360.
- M. Platt, S. Exner, and R. Bracke. Analyse des deutschen Waermepumpenmarktes: Bestandsaufnahme und Trends. Technical report, GeothermieZentrum Bochum; Hochschule Bochum – Bochum University of Applied Sciences, Bochum, 2010.
- G. Rohbogner, S. Fey, U. Hahnel, P. Benoit, and B. Wille-Haussmann. What the term agent stands for in the Smart Grid definition of agents and multi-agent systems from an engineer’s perspective. In *Computer Science and Information Systems (FedCSIS), 2012 Federated Conference*, pages 1301–1305, 2012. ISBN 9788360810484.
- Stromnetz Berlin GmbH. Tagesparameterabhängiges Lastprofil Wärmepumpe ab 2013 (Berlin), 2016, cited 2017-04-25, 2016a. URL <https://www.govdata.de/daten/-/details/tagesparameterabhaengiges-lastprofil-waermepumpe-ab-2013-berlin>.
- Stromnetz Berlin GmbH. Tagesparameterabhängiges Lastprofil Wärmepumpe ab 2013 (Berlin), 2013, citetd 2017-04-25, 2016b. URL [www.stromnetz.berlin/de/file/TLP-Waermepumpe-B-ab-2013\\_22500816.xls](http://www.stromnetz.berlin/de/file/TLP-Waermepumpe-B-ab-2013_22500816.xls).
- Verband der Netzbetreiber. Step-by-step-Unterlagen (für Normierung auf die elektrische Arbeit und die dazugehörige Temperaturmaßzahl). *Praxisleitfaden*, pages 1–8, 2004. URL [https://www.bdew.de/bdew.nsf/id/DE\\_Lastprofile\\_unterbrechbare\\_Verbrauchseinrichtungen/\\$file/Step\\_by\\_Step.pdf](https://www.bdew.de/bdew.nsf/id/DE_Lastprofile_unterbrechbare_Verbrauchseinrichtungen/$file/Step_by_Step.pdf).

T. Wolf. Model-based Assessment of Heat Pump Flexibility. *Master thesis*, (MSc ET 16002), 2016.